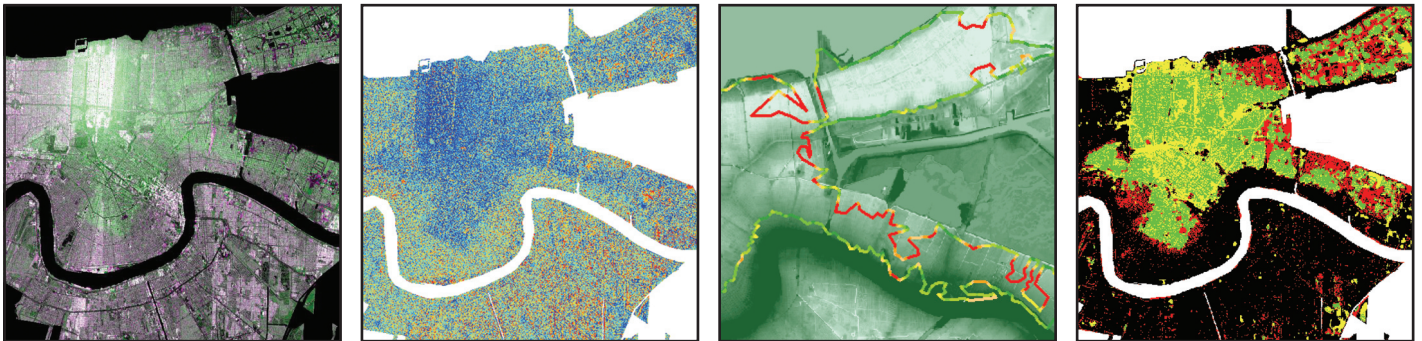


Remote Sensing for Resilient Multi-Hazard Disaster Response

Volume IV: A Study of Multi-Temporal and Multi-Resolution SAR Imagery for Post-Katrina Flood Monitoring in New Orleans

by
**Anneley McMillan, Jeremy G. Morley, Beverley J. Adams
and Simon Chesworth**



Technical Report MCEER-08-0023

November 17, 2008

NOTICE

This report was prepared by ImageCat, Ltd., University College London and MDA Geospatial Services, Inc. as a result of research sponsored by MCEER through a grant from the Earthquake Engineering Research Centers Program of the National Science Foundation under NSF award number EEC-9701471 and other sponsors. Neither MCEER, associates of MCEER, its sponsors, ImageCat, Ltd., University College London, MDA Geospatial Services, Inc., nor any person acting on their behalf:

- a. makes any warranty, express or implied, with respect to the use of any information, apparatus, method, or process disclosed in this report or that such use may not infringe upon privately owned rights; or
- b. assumes any liabilities of whatsoever kind with respect to the use of, or the damage resulting from the use of, any information, apparatus, method, or process disclosed in this report.

Any opinions, findings, and conclusions or recommendations expressed in this publication are those of the author(s) and do not necessarily reflect the views of MCEER, the National Science Foundation, or other sponsors.

Remote Sensing for Resilient Multi-Hazard Disaster Response

Volume IV: A Study of Multi-Temporal and Multi-Resolution SAR Imagery for Post-Katrina Flood Monitoring in New Orleans

by

Anneley McMillan,¹ Jeremy G. Morley,² Beverley J. Adams³ and Simon Chesworth⁴

Publication Date: November 17, 2008

Submittal Date: January 31, 2008

Technical Report MCEER-08-0023

Task Number 10.3.1

NSF Master Contract Number EEC 9701471

- 1 Research Scientist, ImageCat, Ltd.
- 2 Lecturer, Department of Civil, Environmental and Geomatic Engineering, University College London
- 3 Managing Director, ImageCat, Ltd.
- 4 European Sales Director, MDA Geospatial Services, Inc.

MCEER

University at Buffalo, State University of New York

Red Jacket Quadrangle, Buffalo, NY 14261

Phone: (716) 645-3391; Fax (716) 645-3399

E-mail: mceer@buffalo.edu; WWW Site: <http://mceer.buffalo.edu>

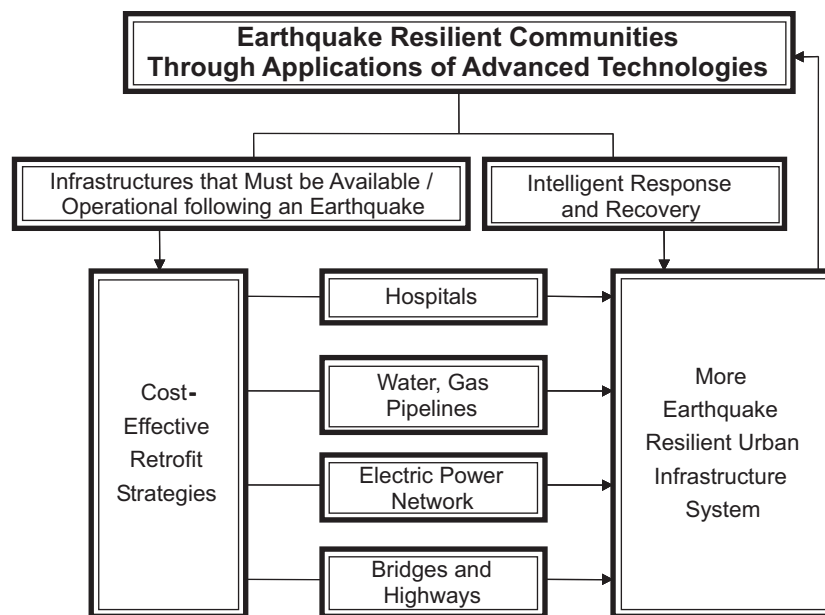
Preface

The Multidisciplinary Center for Earthquake Engineering Research (MCEER) is a national center of excellence in advanced technology applications that is dedicated to the reduction of earthquake losses nationwide. Headquartered at the University at Buffalo, State University of New York, the Center was originally established by the National Science Foundation in 1986, as the National Center for Earthquake Engineering Research (NCEER).

Comprising a consortium of researchers from numerous disciplines and institutions throughout the United States, the Center's mission is to reduce earthquake losses through research and the application of advanced technologies that improve engineering, pre-earthquake planning and post-earthquake recovery strategies. Toward this end, the Center coordinates a nationwide program of multidisciplinary team research, education and outreach activities.

MCEER's research is conducted under the sponsorship of two major federal agencies: the National Science Foundation (NSF) and the Federal Highway Administration (FHWA), and the State of New York. Significant support is derived from the Federal Emergency Management Agency (FEMA), other state governments, academic institutions, foreign governments and private industry.

MCEER's NSF-sponsored research objectives are twofold: to increase resilience by developing seismic evaluation and rehabilitation strategies for the post-disaster facilities and systems (hospitals, electrical and water lifelines, and bridges and highways) that society expects to be operational following an earthquake; and to further enhance resilience by developing improved emergency management capabilities to ensure an effective response and recovery following the earthquake (see the figure below).



A cross-program activity focuses on the establishment of an effective experimental and analytical network to facilitate the exchange of information between researchers located in various institutions across the country. These are complemented by, and integrated with, other MCEER activities in education, outreach, technology transfer, and industry partnerships.

This report investigates the use of cloud-penetrating radar to assess the extent of flooding throughout storm-ridden areas. Multi-resolution SAR data using fine-beam and standard-beam Radarsat-1 scenes was investigated through a case study of the New Orleans flood following Hurricane Katrina. Few prior studies have addressed urban flood detection using SAR, because of complicating double and triple bounce effects that commonly affect urban SAR response. In the case of New Orleans, initial exploratory assessments of Radarsat imagery acquired at the time of flooding indicated that the flooded urban area showed increased backscatter. This is Volume IV of a five part series of reports that investigate the use of remote sensing techniques for resilient multi-hazard disaster response.

PREFACE

This preface introduces a five-volume series, documenting scientific research conducted by MCEER researchers at ImageCat, Inc., investigating remote sensing techniques for resilient disaster response.

Volume I: INTRODUCTION TO DAMAGE ASSESSMENT METHODOLOGIES

Volume II: COUNTING THE NUMBER OF COLLAPSED BUILDINGS USING AN OBJECT-ORIENTED ANALYSIS: CASE STUDY OF THE 2003 BAM EARTHQUAKE

Volume III: MULTI-SENSOR IMAGE FUSION TECHNIQUES FOR ROBUST NEIGHBORHOOD-SCALE URBAN DAMAGE ASSESSMENT

Volume IV: A STUDY OF MULTI-TEMPORAL AND MULTI-RESOLUTION SAR IMAGERY FOR POST-KATRINA FLOOD MONITORING IN NEW ORLEANS

Volume V: INTEGRATION OF REMOTE-SENSING IMAGERY AND VIEWS™ FIELD DATA FOR POST-HURRICANE CHARLEY BUILDING DAMAGE ASSESSMENT

The report series embraces MCEER's stated mission of pursuing *the discovery and development of new knowledge, tools and technologies that equip communities to become more disaster resilient in the face of earthquakes and other extreme events*. Accordingly, the research documented here is multi-hazard in nature, spanning international earthquake, flood and hurricane events. In all cases, the research is undertaken with the underlying goal of improving resilience, in particular the *rapidity* and *resourcefulness* of disaster response activities. Further, it is aimed at meeting stated user needs in the immediate aftermath of disasters, such as a rapid estimate of the number of collapsed/damaged structures, and the delineation of flood inundation zones.

These volumes represent a significant milestone in post-disaster damage assessment, constituting the culmination of seven years' research activities. During this time, we have witnessed the 'Coming of Age' of remote sensing technologies and analytical techniques within the disaster response arena. *Technology push* in the form of new sources of high-resolution imagery and increasingly advanced and analytical techniques has driven the development of new capabilities attuned to meet the needs of responders. This has been coupled with heightened *User pull* from sectors including the re/insurance industry, and with the onset of recent catastrophes such as hurricane Katrina, opportunities for operational implementation.

Research collaborations established by ImageCat, Inc. with multi-hazard researchers from the US, Italy and UK, underpin this report series. Through sharing and exchanging a wealth of experience and expertise, the teams of scientists and engineers have advanced the knowledge boundaries of remote sensing damage detection. Particular highlights include:

- ✓ The ability to rapidly count the number of collapsed buildings, where a building is treated as an ‘object’ within the digital image, rather than a group of pixels (Volume II in collaboration with the University of Bologna)
- ✓ The fusion of pre- and post-disaster imagery captured by different high resolution sensors to facilitate flexible damage mapping irrespective of which sensor passes first over the disaster zone (Volume III)
- ✓ The use of cloud-penetrating to assess flooding extent throughout storm-ridden areas (Volume IV in collaboration with University College London)
- ✓ HAZUS-compatible post-hurricane damage assessment based on remote sensing imagery, when access to the disaster zone is precluded (Volume V in collaboration with Texas Tech University).

In June 2006, MCEER launched its Remote Sensing Institute (RSI), which will *serve as a platform for developing and operationally implementing innovative multi-hazard techniques, strategies and products for rapidly assessing post-disaster impacts, modeling and quantifying the built environment, and monitoring recovery*. The RSI will continue to embrace fundamental and applied research activities to develop innovative new approaches to short- and long-term disaster management. Commercial products and services developed by MCEER researchers and available through RSI include: near real-time flood, surge, hurricane, earthquake and tsunami damage assessment through remote sensing-based damage scales and advanced image analysis techniques; and forensic GPS-registered damage assessment using the in-field VIEWS™ data collection and visualization system.

ABSTRACT

The performance of multi-resolution SAR data for detecting urban flooding was investigated using fine-beam and standard-beam Radarsat-1 scenes. The flooding of New Orleans due to Hurricane Katrina was used as a case study. Few prior studies have addressed urban flood detection using SAR, because of complicating double and triple bounce effects commonly affecting urban SAR response. In the case of New Orleans, initial exploratory assessments of Radarsat imagery acquired at the time of flooding indicated that the flooded urban area showed increased backscatter.

To isolate changes in backscatter from the flooded urban environment, image differencing, high thresholding methods, and false color composites were explored. A comparison of high backscatter and flooded areas was undertaken, to investigate whether the signal could be utilized to map urban flooding. Two validation methods were implemented. A manual delineation of high backscatter areas from both beam mode data was compared with SPOT and Landsat derived flood boundary delineation using a buffering technique. The optimum results were gained from fine beam mode, demonstrating that 58% of the radar derived boundaries fell within 150m of the optically derived data, and 82% fell within 550m. A second analysis used an area-based contingency matrix method to compare radar classified flood with the validation layers. The most accurate result was obtained using fine beam mode imagery with large window size filtering. Results show user accuracies of 56% for flooded and 84% for non-flooded regions, and produced accuracies of 55% and 81% for flood and non-flood classes, respectively. It is a fair assumption that this relationship did not occur by chance, as a calculated kappa coefficient was recorded at 0.40. Empirically, the highest correlation between high backscatter signal and flooded area appeared to occur from high-density residential areas. Areas of non-agreement appear to be due to open areas in the urban environment, particular street orientation and building patterns and temporal differences between acquisition and validation layer dates.

ACKNOWLEDGMENTS

This research was conducted at ImageCat, and was supported in whole or in part by the Earthquake Engineering Research Centers Program of the US National Science Foundation under award number EEC-9701471 to MCEER. We would like to thank MCEER Thrust Area III leader Kathleen Tierney for her continued guidance and support for this research.

Additionally, we would like to acknowledge the following individuals for their contributions to the work documented in these five volumes:

Gabriele Bitelli, DISTART, University of Bologna

Shubharoop Ghosh, ImageCat, Inc.

Marjorie Greene, EERI

Charles K. Huyck, ImageCat, Inc.

Kishor Mehta, WISE Center, Texas Tech University

Keiko Saito, Cambridge University Centre for the Risk in the Built Environment (CURBE)

J. Arn Womble, WindForce Associates, Inc.

Thuy Vu, GTRC, Japan

TABLE OF CONTENTS

SECTION	TITLE	PAGE
1	INTRODUCTION	1
1.1	Importance of Flood Detection	1
1.2	Previous Literature on Radar Use for Flood Detection	2
1.2.1	Overview	2
1.2.2	Urban Orientation Effects on Radar Response	4
1.2.3	Surface Material Effects on Backscatter Response	6
1.2.4	Previous Methods of Flood Detection	7
1.3	Hurricane Katrina	9
1.4	Aims and Objectives	9
2	STUDY AREA	11
2.1	Area Description	11
2.2	Multi-mode Radarsat-1 Data	12
3	METHODOLOGY	17
4	RESULTS	23
4.1	Amplitude Images	23
4.2	False Color Composite	24
4.3	Difference Image	26
4.4	Statistical Analysis	29
4.4.1	Area A	30
4.4.2	Area B	30
4.4.3	Area C	32
4.4.4	Area D	33
4.4.5	Area E	33
4.4.6	Area F	33
4.4.7	Summary	34
5	VALIDATION	37
5.1	Boundary Intersection Analysis	37
5.2	Area Intersection Analysis	40
5.2.1	Fine Beam Mode	43
5.2.2	Standard Beam Mode	45
6	KEY FINDINGS AND FUTURE WORK	47
7	REFERENCES	51

LIST OF ILLUSTRATIONS

FIGURE	TITLE	PAGE
1-1	Types of Radar Scattering Encountered in Urban Areas	5
2-1	Study Area	11
2-2	Optical Derived Validation Data Sets from (a) SPOT from the 2 nd September 2005, and (b) Landsat from the 7 th September 2005	15
3-1	Methodology	17
3-2	Threshold Difference Images from (a) Fine Beam and (b) Standard Beam Modes	19
3-3	Effect of Median Filtering on Threshold Flood Signal	20
4-1	Raw Radarsat Imagery	24
4-2	Fine Beam Mode False Color Composite Where Red = 13 th April Pre-Flood, Green = 9 th September – Flood, and Blue = 13 th April Pre-Flood	25
4-3	Standard Beam Mode False Color Composite Where Red = 30 th April Pre-Flood, Green = 2 nd September Flood, and Blue = 30 th April Pre-Flood	26
4-4	Decibel Difference Images for a) Standard and b) Fine Beam Modes	27
4-5	Normalized Frequency of Db Difference for Fine and Standard Beam Modes, Clipped to 99%	28
4-6	Study Area Split into 6 Zones of Investigation, and Sample Areas for Statistical Analysis (Circles)	29
4-7	Area B Overlain with Tiger Lines™ Comparing Street Alignment and Look Angle with Backscatter Response. (Fine Mode April 13 th Non Flooded Image Used)	31
4-8	Histograms for Area B with Saturation Peaks Removed	32
5-1	Boundary Intersection Analysis Between Fine Beam Derived Flood Boundary and SPOT Derived Validation Layer	37
5-2	Differences Noted in Urban Parameters within Area B such as Building Density and Block Pattern Between (a) an Area Showing Large Differences in dB Level During the Flood, and (b) an Area Not Showing any Considerable Change in dB Values	38

LIST OF ILLUSTRATIONS (CONT)

FIGURE	TITLE	PAGE
5-3	Boundary Intersection Analysis Between Standard Beam Derived Flood Boundary and SPOT Derived Validation Layer	39
5-4	Vector Intersection Analysis Results	40
5-5	Accuracy Results from Area Intersection Analysis	41
5-6	Area-based Intersection Matrix of Fine Beam Radar Signal and Validation Dataset	42
5-7	Area-based Intersection Matrix of Standard Beam Radar Signal and Validation Dataset	43
5-8	Misclassification in Various Areas. (a) Area A Showing an Area of Train, (b) Area A Showing Destroyed Buildings, (c) False Negatives Found in Area C, (d) Forest Area Destroyed which Shows as False Positives, (e) Area D Showing Correlation Between Destroyed Buildings and Intact Buildings, and Increase in Backscatter (green) and False Negatives (red), (f) Industrial Area Falsely Classified as Flood Area	45

LIST OF TABLES

TABLE	TITLE	PAGE
2-1	Radarsat-1 Beam Mode Overview	12
2-2	Selected Radarsat-1 Beam Mode Characteristics	13
2-3a	Image Acquisition Characteristics	14
2-3b	Validation Dataset Characteristics	14
4-1	Difference Image Statistics	28
4-2	Average Backscatter Responses and Difference Statistics	30
4-3	Histogram Results and Street Layout from the Six Areas of Analysis	35

SECTION 1 INTRODUCTION

1.1 Importance of Flood Detection

During the last decade, floods have affected more than 1.5 billion people, which equates to 75% of all people affected by a disaster (ESA, 2006). It is predicted that flooding and the resultant impacts on human populations are set to increase because of the continued desire of the public to live in areas that tend to be flood prone, and climate instability as a consequence of climate change. For situation assessment and emergency response, disaster management agencies, policy makers and civil protection authorities (CPAs) also need to know what level of resources will be needed in order to effectively respond to future floods. Flood data can be useful for many post-disaster management activities, including the collection of loss data that will help to assess the magnitude of future risks; this information is particularly useful in establishing the basis for reasonable flood insurance premiums for the public. Ultimately, flood data are essential elements of post-disaster assessment studies that update risk assessments and flood extent predictions.

Efficient flood monitoring and associated damage assessment studies for urban environments are therefore both important and timely. Satellite-based monitoring offers an attractive solution due to its relatively cost-effective nature and widespread coverage for analysis. This is in comparison to stand-alone, spatially restrictive ground sampling, semi-qualitative methods such as resident consultation, examination of administrative documents and claims forms, and costly aerial surveys of flooded areas. Flooding, in particular, can be a very short-lived event, and so it is essential to retrieve a useful satellite-derived product quickly. An important consideration in streamlining the flood assessment process is optimizing the imagery specifications, in terms of parameters such as resolution and swath width.

Urban flooding occurs in a relatively short time span, and so it is essential to retrieve a useful satellite-derived product quickly. To this end, an important consideration in streamlining the flood assessment process is optimizing the imagery specifications. In terms of sensor characteristics, synthetic aperture radar (SAR) imagery offers advantages over optical remote

sensing data. A number of flood detection methodologies have used optical satellite imagery to assess flooding extent and damage (e.g. Bryant and Rainey, 2002; Brakenridge and Anderson, 2005). However, a major limitation to this technique is cloud cover, of particular prevalence in storm-ridden areas. In comparison, using the microwave region of the spectrum bypasses this limitation because of its longer wavelength. As radar is an active system (i.e., it creates its own radar pulse), it negates the need for sunlight, so it can be used at night or during a storm, offering more rapid and reliable damage assessments. However, SAR imagery parameters such as spatial resolution and swath width are also an important consideration that may affect the accuracy achieved. Few prior studies have addressed *urban flood detection using SAR*, and it remains for a comparative analysis of different spatial resolutions to be performed.

1.2 Previous Literature on Radar Use for Flood Detection

1.2.1 Overview

Outside the built environment, radar has proved an extremely useful tool for the purpose of flood detection (e.g. Brivio *et al.*, 2002; Tholey *et al.*, 1997; and Takeuchi *et al.*, 1999). Because it is an active system, it also negates the need for sunlight, so it can be used at night, offering more rapid damage assessment. It has been shown that SAR can potentially be more accurate than certain optical systems, such as Landsat, at delineating flooded areas. Looking at flooding in the Bangladesh monsoon period, Imhoff *et al.* (1987) showed that SAR (SIR-B) retrieved an accuracy of 85% correctly classified, compared with 64% for Landsat MSS, using a simple density slicing threshold method. The differing backscatter response from water and land means that SAR has the capacity to distinguish sharply between these land cover classes (Sanyal and Lu, 2004) making it a potentially useful tool for quick response and rapid detection of flooded areas. It has also been noted that SAR gives higher accuracy flood mapping responses on flat or homogenous floodplain type areas (e.g. Galy and Sanders, 2000). However, areas of human population such as urban environments are usually of more interest to hazard mitigation planners, as these are the areas where losses are likely to be greatest.

Few previous studies have explored SAR implementation for urban flood detection, largely because of complicating complex beam effects (i.e., Kiage *et al.*, 2005; Oberstadler *et al.*, 1997).

It also remains for a systematic evaluation to be completed of the various SAR image sets currently available through multi-mode commercial sensors such as Radarsat, in order to identify the optimal imagery specifications for flood detection. The response of the surface in urban areas is little described and accounted for, and with regard to flood detection, what has been written has often only been preparatory. For instance, Solbø and Solheim (2004) suggest that flood detection can be enhanced in all types of terrain, including urban areas by combining multi-temporal intensity analysis with interferometric coherence data (e.g., Dellepiane *et al.*, 2000; Stabel and Löffler, 2003). Although these researchers investigate a range of sensors and beam modes (ERS and Radarsat; standard and fine beam mode), it was deemed necessary for operational purposes to focus on the simple case scenario, i.e., open agricultural fields. Therefore, these authors did not consider urban and forested regions. Solbø and Solheim (2004) also describe the design and implementation of the SAR processing part of an operational flood mapping service called the *FloodMan* project. This project focuses on near real-time, unsupervised operational flood mapping. It divides up the SAR flooding process into three main areas – (1) open agricultural lands, where SAR flood analysis is fairly straightforward using thresholding techniques, (2) forested areas where double bounce causes an enhanced backscatter response, and (3) urban areas were examined, consisting of a lot of concrete, steel and corners. They conclude that urban material such as concrete makes it difficult to detect flooding, as there will be no dramatic change in scattering mechanisms for flooded areas. Oberstadler *et al.*, (1997), using ERS-1 SAR imagery, present qualitative and quantitative analyses (visual interpretation and an automatic classification method). They used evidence-based interpretation of satellite images (EBIS) which involved visual analysis, an automatic classification method, and filtering techniques to classify flooded areas and create a continuous contour. They found that problems occurred in urban areas because of the increased backscatter of buildings overlaying the backscatter from any flooding, and that often no contour lines could be found. Trees, port and embankment constructions in cities also gave increased backscatter. Despite these issues, they conclude that radar has potential, with visual analysis proving useful for delineating the flood boundary in agricultural land and some urban settlements.

In the specific case of flooding in and around New Orleans, Kiage *et al.*, (2005) used Radarsat-1 100m resolution ScanSAR images from the 2nd and 5th September to look at flooding of the

wetlands of Louisiana after Hurricane Katrina. The authors carried out a preliminary study into the performance of ScanSAR imagery for delineating flooding in New Orleans after the hurricane. The ScanSAR imagery had a 50m pixel resolution. They concluded that in this instance, SAR was not useful because the corner reflections from urban buildings caused increased backscatter response.

Kiage *et al.* (2005) further suggest that since optical SPOT imagery has been useful in the response to Hurricane Katrina, a combined SAR – SPOT approach should be investigated. Another multi-sensor approach is utilized by Fatone, *et al.* (2001), who suggest a data fusion technique may be advantageous for looking at urban areas in detail. They employ a segmentation and de-noising regime, fusing SAR for its textural properties with optical imagery for its high resolution properties. However, in terms of fast operational use for post-disaster monitoring, acquiring both SAR and optical data can take time, and is therefore not focused on here.

While these studies emphasize the importance of radar for flood detection, they also highlight a number of challenges encountered because the urban environment complicates backscatter response. Reviewing the literature, there is a lack of very high-resolution SAR data usage, such as fine beam Radarsat.

1.2.2 Urban Orientation Effects on Radar Response

When structures such as buildings are placed into an environment, they can act as corner reflectors (Dong, *et al.*, 1997; Dousset, 1997). This means that in addition to receiving a direct response from the surface of the first incidence, they can also create a double (or triple) bounce response from ground reflected beams. This phenomenon has been found to complicate urban responses (e.g., Kiage, 2005), and is cited as a significant problem in detecting flood extent in urban areas. In a typical urban environment, Dong, *et al.* (1997), state that there are three main types of radar (surface) scattering. Figure 1-1 shows the importance of sensor flight lines and feature orientation to the backscatter received.

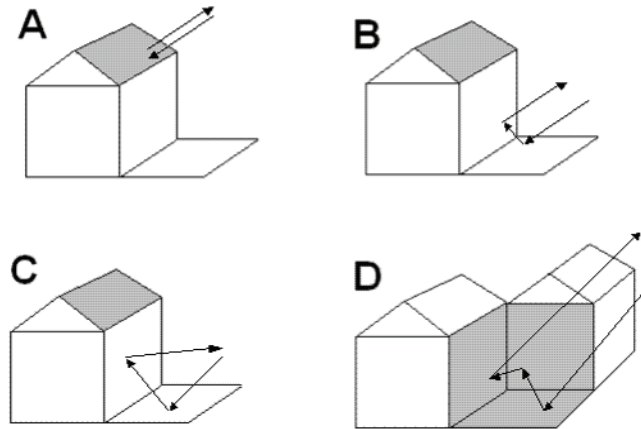


Figure 1-1 Types of Radar Scattering Encountered in Urban Areas. A) Single bounce scattering; B) Double bounce where sensor and feature are aligned, increased backscatter received back to sensor; C) Double bounce where flight line and feature orientation are not aligned and increased backscatter is not received at the sensor; and D) Triple bounce scattering. Adapted from Dong et al. (1997)

From a theoretical standpoint, figure 1-1 illustrates double bounce (dihedral) and triple bounce (trihedral) arrangements. It should be emphasized that single bounce scattering can also occur from the ground at particular incident angles, which miss interactions with buildings. As seen in figure 1-1B and figure 1-1C, the double bounce response is reliant on the relationship between the flight line and the feature orientation (as described in Henderson and Lewis, 1998). Sanyal and Lu (2004) note that the magnitude of the double bounce effect will vary according to radar look angle, wavelength and polarization. In a dihedral corner reflector response, the incoming and outgoing radar response can be reflected back to the sensor, which will give an increased brightness response. However, if the incoming angle is not aligned with the surface orientation, the trajectory will still have a specular-type response, but will ultimately bounce off in a different direction to the radar, resulting in particularly low pixel values. A particularly strong double bounce effect is sometimes seen in urban areas, described by Lee (2001) as the cardinal effect. He explains that lines of strong radar return from the four cardinal directions caused by the grid-like layout of modern cities obscure adjacent targets, leading to loss of information, by in effect blinding the sensor. Even in high-resolution imagery this is a problem because of strong side-lobe generation. Lee (2001) goes on to discuss a technique which allows this total integrated

side-lobe energy (ISL) to be dampened down in the radar pre-processing stage, using SAR range processing techniques.

To summarize, these studies show that double bounce effects can be complex, and may prove to influence the accuracy of results obtained during flood extent detection.

1.2.3 Surface Material Effects on Backscatter Response

As well as building orientation, a main factor influencing backscatter from urban areas is the surface material that the radar signal encounters. For example, Dousset (1997) examined energy balance from a metropolitan area in the Los Angeles basin, using ERS-SAR. It was found that smooth paved surfaces such as asphalt, pavement, airports and bare soil had very low backscatter responses. This was thought to be because of reduced Bragg scatter and low soil moisture that reduces sub-surface scattering. Over industrial areas, isotropic reflectance was found, due to curved surfaces or randomly orientated structures. In downtown and commercial areas, high backscatter from concrete and metallic structures appears to contaminate the signal, so that extraction of ground surface information was not possible. She also found that over some low density residential areas, the increase of backscatter intensity was correlated with the azimuth angle between the radar illumination and the streets. In particular, ‘the regular geometry of reinforced concrete walls, metal roofs and steel beams provides numerous dihedral reflectors, resulting in greatly enhanced backscatter when the illumination azimuth is orthogonal to the buildings’ (Dousset, 1997).

Some studies have assumed that there will not be any difference in backscatter between paved surfaces and flooded surfaces (i.e. Solbø and Solheim 2004). However, this has not been conclusively discussed, especially in relation to the urban environment, e.g., for instance tarmac creates both volumetric and surface scatter, but flood waters produce only a surficial response (Li and Sarabandi, 1999). Add to this the effect of debris and floating matter in flood water, and a more complicated response may arise that could lead to many differences in backscatter between the two situations. Theoretical understanding between flooding signatures in urban areas, and backscatter response from urban materials is therefore limited at present, and requires further investigation.

1.2.4 Previous Methods of Flood Detection

Previous radar flood detection studies have explored a range of different methods for extracting inundation information from satellite scenes. It is possible to extract specular flood response pixels from a single image due to their very dark nature (Malnes *et al.*, 2002). However, more complicated responses are less easy to extract. Stabel and Fischer (2002) note that although it is possible to classify flood water from a single SAR image, it is not possible to extract permanent water from flood water without subsidiary data. Therefore multi-temporal, change-detection involving flooded and non-flooded scenes is also commonly used for flood mapping. A number of studies have used a false color composite approach (e.g., Badji and Dautrebande, 1995; Kannen, 1995) allowing a satisfactory visualization of flood extent seen at the time of acquisition (Brivio *et al.*, 2002). A simple multi-temporal intensity technique may involve taking SAR images from the same area on different dates, and assigning them to the red, green and blue channels in a color image. The visualization allows manual delineation of flood boundaries by tracing around the visible extent.

An alternative way of detecting change due to flooding uses a thresholding method, where a threshold is specified in decibel (dB) above which land is seemingly dry, and below which land is flooded. Threshold values are determined by a number of processes, depending on the study area and overall spectral signature of the imagery. For example, Zhou *et al.* (2000) and Malnes *et al.* (2002) extract a water signature from single radar images using an image histogram, where flooding has two distinct peaks pertaining to the specular dark pixel response of water and the higher backscatter values of the rest of the scene. This approach can be enhanced using filters to maintain edges and texture, and enhance image contrast, but decrease noise effects. Malnes *et al.* (2002) used Bayesian statistics to show that the probability of misclassifying water pixels using this method was 3%. However, it was noted that around 10% of land pixels were misclassified as water. Due to different responses from trees and urban environments and variations with weather conditions, a universal threshold for flood detection is not justified, and as such, must be taken on a case-by-case basis if used (Sanyal and Lu, 2004). Furthermore, it needs extensive filtering of data (Kuehn *et al.* 2002) as the main difficulty with simple image differencing and thresholding techniques is the presence of speckle and noise. It is multiplicative and related to

backscatter, so that an increase in backscatter leads to an increase in noise. As long as filtering and histogram statistics are utilized, it can be a useful technique for flood delineation. When Malnes *et al.* (2002) considered regions of interest, calculating mean and standard deviation statistics, subsequent region growing to neighboring pixels that were within 3σ gave a superior result.

Classification schemes have proven useful for deriving flooded and non-flooded classes of water versus the surrounding land cover. Examples have included neural network solutions (e.g., Wei *et al.*, 2002; Sohn *et al.*, 2005; Pellizzeri *et al.*, 2003), support vector machine (Solbø, 2003) and maximum likelihood classifiers (e.g., Lonbardo and Oliver, 2001), and decision tree approaches (e.g., Parmuchi *et al.*, 2002). Advanced flood detection approaches documented in the literature include active contour methods (Horrit *et al.*, 2001; Ahtonen and Hallikainen, 2005; and Gruen and Li, 1997) and phase coherence studies (Horrit *et al.*, 2001; Dellepiane *et al.*, 2000; and Nico *et al.*, 2000). It is important to note that these methods are not employed within the present evaluation, because of the loss of coherence due to time differences between available images acquired for this study, and limitations of Radarsat imaging geometry for interferometric studies.

While previous studies suggest that radar has considerable potential for flood detection, documented performance within urban environments has been varied, and progress has been limited by methodological challenges such as complicating multi-bounce effects. Before creating elaborate methodologies or conducting advanced data fusion studies, it is necessary to develop a more fundamental understanding of the performance of SAR imagery for urban flood mapping. As part of this exploratory work, it is important to examine all types of response from the flooded urban environment, and not to simply assume the specular dark pixel radar response that prior studies have attributed to flooding. Accordingly, there is a pressing need to extend existing theoretical and methodological bases for extracting flood extent and area in an urban environment using SAR imagery.

1.3 Hurricane Katrina

On the 29th of August 2005, Hurricane Katrina made landfall as a Category 4 storm in Plaquemines Parish, Louisiana (USGS, 2005). Due to the hurricane, storm surges affected large areas of coastlines along Louisiana, Mississippi and Alabama, and also the hydrological system associated with Lake Pontchartrain in close proximity to New Orleans. The storm surge caused by Hurricane Katrina breached a number of the levees on canals linked to Lake Pontchartrain, causing extensive flooding throughout the city, estimated at 80% (USGS, 2005). Because of the extent of the flooding through the urban environment, Katrina is thought to have been the costliest natural disaster in US history with insurance claims and damage estimates still being revised at the time of press. Eroding levees along the Mississippi, the Mississippi River Gulf Outlet (MR-GO) and the Mississippi Sound caused major flooding in St Bernard's Parish and the Lower Ninth Ward. A second surge flowed Westward through the Gulf Intracoastal Waterway further contributing to flooding in this area. More breaches occurred along Lake Pontchartrain, the London Avenue Canal and the 17th Street Canal causing flooding in Eastern and Western New Orleans. By September 1st, the flood water is thought to have equalized to around three feet above sea level (NOVA, 2006). Given the extensive nature of flooding within the city and timely acquisition of multi-resolution SAR imagery, New Orleans is a useful case study for exploring optimal imagery specifications for the monitoring of urban flood events.

1.4 Aims and Objectives

Given the pressing need to improve our theoretical understanding of radar flooding response in urban areas, and to develop operational techniques for flood monitoring in urban environments, the aim of this study is to: *Investigate the performance of multi-resolution SAR data to detect urban flooding*, using the post-Katrina inundation of New Orleans as a case study. Within this broad aim, several objectives are identified:

1. To investigate the general characteristics of radar response from a flooded urban environment
2. To explore multi-temporal change detection-based methodologies for detecting urban flooding

3. To perform a comparative evaluation of SAR standard and fine beam imagery for identifying flooding in New Orleans
4. To undertake validation using multi-source data, in order to establish which SAR imagery specifications and methodology perform best.

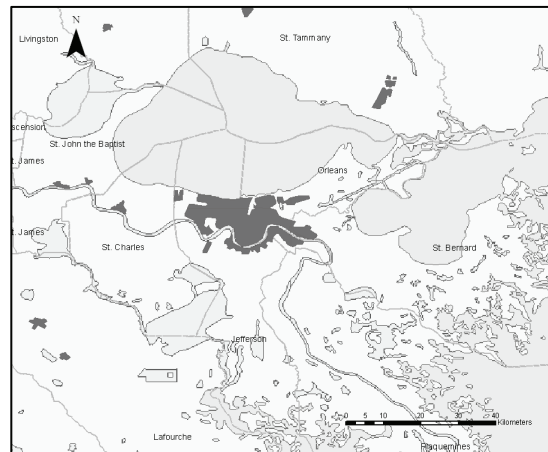
SECTION 2 STUDY AREA

2.1 Area Description

The study area shown in figure 2-1 is the county of Orleans, Louisiana, and specifically the urban areas within this; namely the city of New Orleans, St Bernard's, Plaquemines and Jefferson parishes. The City of New Orleans is centered at 29°57'53" N 90°4'14" W with an estimated population of 469,032 in 2003 (US census Bureau, 2006) and an area of 181 square miles in 2000 (US census Bureau, 2006). It is bordered on the north side by Lake Pontchartrain and on the southern extent by the Mississippi River. The city itself lies predominantly below sea level. Engineered levees enhance the natural silt deposition in the area, leading to land immediately surrounding the Mississippi lying at around 11 feet above sea level (McGlothlin, 2006) and Lake Pontchartrain at around 2 feet above sea level. During the late 19th - early 20th century, a series of canals and pumping stations were created, mainly in the naturally wetland / swamp environments to the North, to essentially drain New Orleans (McGlothlin, 2006). This more stable reclaimed land was then used to expand the city.



(a) Position of New Orleans within the US



(b) Detailed study area showing parishes and main inland water bodies. Populated areas are dark. New Orleans is the main populated area.

Figure 2-1 Study Area

2.2 Multi-mode Radarsat-1 Data

Radarsat -1 was launched on November 4th 1995. It is a C – band SAR (i.e. 5.6cm wavelength), with 7 beam mode capacity and 35 beam positions. It utilizes a sun-synchronous orbit 798km above the earth at an inclination of 98.6 degrees. It has a right-looking radar and can achieve a 24-day repeat period (MDA, 2006).

Different beam modes are characterized by different incidence angles and resolutions as shown in table 2-1. In terms of flood monitoring, the advantages of the system include a frequent revisit period, near real-time processing, cloud free images and swath widths of 50-500km, at incidence angles from 10-59 degrees (MDA, 2006). The maneuverable radar transmitter and receiver means that the elevation angle and beam positions can be modified (Henderson and Lewis, 1998). This flexibility is extremely important, since changes in incidence angle can dramatically change the characteristics of the data captured.

Table 2-1 Radarsat-1 Beam Mode Overview

Beam Mode	Nominal area covered (km)	Nominal resolution (m)
ScanSAR wide	500 x 500	100
ScanSAR narrow	300 x 300	50
Extended low	170 x 170	35
Wide	150 x 150	30
Standard	100 x 100	25
Extended high	75 x 75	25
Fine	50 x 50	8

Radarsat-1 operates in two main instrument modes: single beam and ScanSAR. In Single Beam Mode, the beam is characterized by its nominal incidence angle, nominal swath width, and nominal spatial resolution, and the beam elevation and profile are maintained constant throughout data collection (MDA, 2006). ScanSAR uses a sequential operation, taking two or more single beams to create an artificially wider swath. The radar beam switches to provide two looks per beam. As is often the case, a wider swath is obtained at the expense of spatial resolution (MDA, 2006).

Table 2-2 summarizes the characteristics of the beam modes examined in this study. Fine beam mode offers the best spatial resolution, at the expense of a smaller 50km ground range, to keep the signal within the correct bandwidth. Five Fine beam positions are available on Radarsat, named F1 to F5. These are available to cover the far range of the swath, the incidence angle range from 37 to 47 degrees. Shifting each of these closer or further away from nadir has given Radarsat an extra class of beam positions (e.g. F1N – near or F1F – far). Standard mode has 7 beam modes, and wide beam is similar, although the swath width is extended to 150km instead of 100km (MDA, 2006). In addition to these three modes, there are also extended high (EH) and low (EL) beam mode operating systems. These can collect from 49-60 degrees incidence angle, and 10-23 degrees respectively. Due to their sub-optimum scan angle, a degradation of image is expected compared to the standard mode (MDA, 2006), and as such, they were not used in this study.

Table 2-2 Selected Radarsat-1 Beam Mode Characteristics

Parameter	Standard mode	Fine mode
Beam positions	7 beam positions (S1-S7) (>10% overlap)	5 beam positions (F1-F5) (10% overlap)
Nadir offset	~250km	~500km
Swath Width	100km	Swath Width: 50km
Range Resolution	26m (near) -20m (far)	8-9 m
Azimuth Resolution	28m	9m
Looks	4	1
Incidence angle range	20-49°	35-49°

After Natural Resources Canada (2006)

Four RADARSAT images were acquired from MDA Geospatial Services. A summary of the datasets available for New Orleans is shown in table 2-3a. Both fine beam and standard beam modes were examined. Wide beam mode was not examined due to the lack of suitable archive comparison data. The peak flood event in New Orleans took place on around the 31st August 2005. However, because of the geography of the area, standing flood water was still present weeks after. Images during the flooding were acquired on the 2nd September 2005 for Standard beam mode, and the 9th September 2005 for fine beam mode. Post-flood imagery from the 13th

April 2006 was available for fine beam mode, and April 30th 2006 for standard beam mode. All images acquired were matched to the same orbit and swath as the comparison image for continuity. Images were pre-processed to ground range and pixels were converted to Intensity by MDA.

Table 2-3a Image Acquisition Characteristics

Beam mode	Date acquired	Pixel spacing (m)	Image Centre (Long, Lat, NAD84)	Incidence Angle	Time in relation to flooding
Fine beam mode 5	September 9 th 2005	6.25	29°53'N 090°09'W	46.46	During
Fine beam mode 5	April 13 th 2006	6.25	29°53'N 090°09'W	46.46	After
Standard beam mode 5	September 2 nd 2005	12.5	29°56'N 089°41'W	39.13	During
Standard beam mode 5	April 30 th 2006	12.5	29°57'N 089°40'W	39.13	After

A summary of validation data is shown in table 2-3b. A SPOT-derived flood area was available for the 2nd September. This was available from FEMA and had been derived by researchers at the Dartmouth Flood Observatory (FEMA 2005). The second validation used was a Landsat 5 derived flood area from the 7th September 2005. This was derived by thresholding low pixel values from the visible bands and negating any normal low pixel response (i.e. due to permanent water etc.) by running the same analysis on a non-flooded situation image. It was decided to use these separate sources as flood extent varies a great deal temporally. It was very important to match dates with the radar imagery as much as possible. These validation datasets are shown in Figure 2-2.

Table 2-3b Validation Dataset Characteristics

Validation data	Date	Source
SPOT derived flood area	September 2 nd 2005	Flood area USGS.
Landsat 5 derived flood area	September 7 th 2005	Image USGS Derived flood area ImageCat

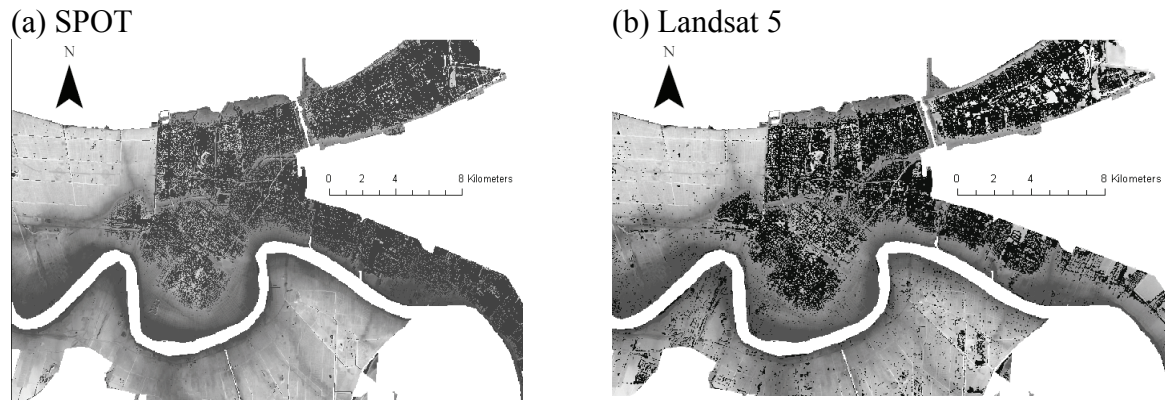


Figure 2-2 Optically Derived Validation Data Sets from (a) SPOT from the 2nd September 2005, and (b) Landsat from the 7th September 2005

SECTION 3 METHODOLOGY

Figure 3-1 summarizes the methodology that was used to investigate the performance of different Radarsat-1 imagery specifications for urban flood detection. The methodology is comprised of five major steps: pre-processing, analysis, validating inputs, flood area validation and flood boundary validation. Within each of these major steps are a series of sub-steps. The discussion that follows elaborates on these more detailed steps.

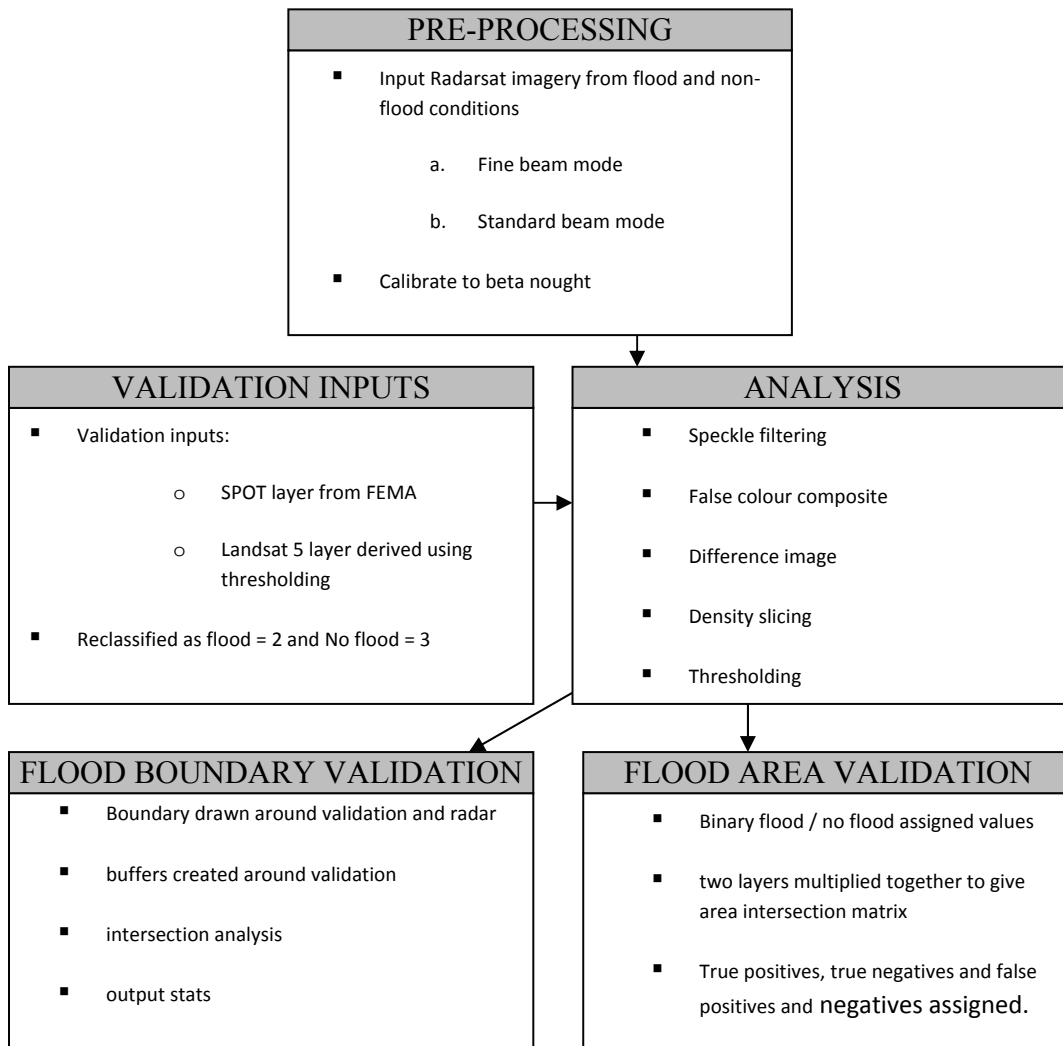


Figure 3-1 Methodology

The following discussion highlights the details of the approach described above, i.e., figure 3-1.

- a.) The images are imported and calibrated to Beta Nought (dB). This is a dimensionless quantity defining the reflectivity per unit area in slant range.
- b.) Geo-registration of the Radarsat images is carried out using the ITT Visual Information Solutions' ENVI radar geoprocessing tool (for more information, see RSI 2000). A 2nd degree polynomial re-sampling technique is used, registered to UTM Zone 15N, and the Molodensky datum transformation is registered to WGS 1984. Once the geo-registration is completed, minor shifts between datasets are assessed by examining some preliminary difference images.
- c.) If minor shifts are discovered, co-registration of the images is needed. This is achieved by using manual tie points in ENVI. All calibrated georeferenced images are then warped to the April 13th 2006 fine beam mode image. In our example, we used 10 tie points, and a polynomial second degree nearest neighbor interpolation. The RMS error was reduced to less than 0.5 pixels in all cases.
- d.) The data layers are then stacked, subset and masked using an urban mask derived from a 1992 National Land Cover map.
- e.) The images are split into specific areas of the city, and summary statistics and histograms are investigated for the different areas. Statistics are derived from the unfiltered imagery.
- f.) To reduce speckle and aid the visual analysis, the amplitude images are filtered. A radar specific filter, the Enhanced Frost filter, is used to dampen down speckle. A 5 x 5 filter size is utilized as a trade-off between reducing speckle and retaining image details. This is suggested as a useful speckle filter for preserving high intensity pixels as well as the edges of features by Ho *et al.* (1998). In particular, the Frost filter is seen to preserve high-intensity pixels, which may be of use in this study.
- g.) As a preliminary change detection technique for identifying flooding using the respective Radarsat beams, false color composites are created for each beam mode. The non-flood image is used in the red and blue channels, with the flooded image as green.
- h.) In order to highlight flooded areas, differencing is undertaken for the fine and standard beams modes, using the flood (September) and non-flood (April) images. A standard

subtract routine is employed. The difference images are then classified by dB difference to better interpret the variation of difference values across the image.

- i.) A threshold is chosen for each beam mode, with a combination of histogram lead knowledge (the lowest dB difference seen for flood versus non-flood) and density slicing to enhance signal, and decrease speckle. This creates a binary flood and no flood image, where flooding has a high positive backscatter difference at the time of the flood, and no flooding has a low backscatter difference or negative difference at the time of the flood. The chosen thresholds are shown below:

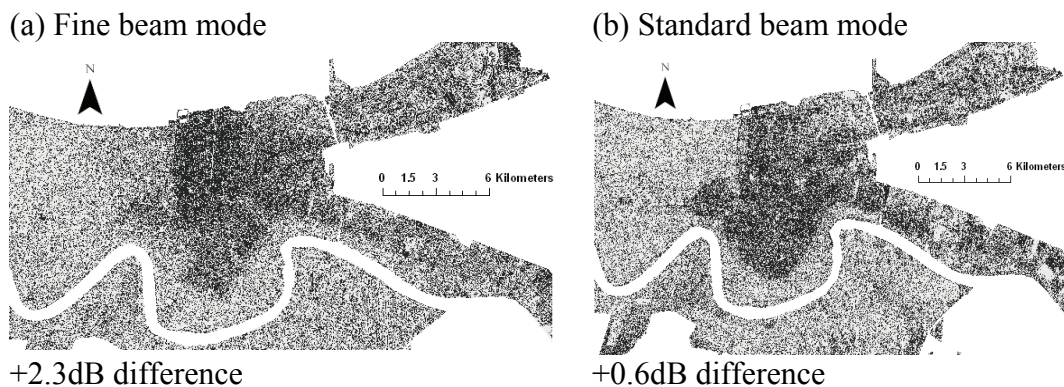


Figure 3-2 Threshold Difference Images from (a) Fine Beam and (b) Standard Beam Modes

- j.) To delineate a flood boundary and consistent flood area from the change detection images, it is necessary to use an aggregation method, as the images are still very speckled, with disparate and coarse textures of response. A median filter is chosen to expel isolated pixel values and aggregate similar regions of pixel values, without biasing the neighborhood result with an outlying pixel, as a low pass filter could. Different window sizes are used to examine the effect on the accuracy of results. Figure 3-3 shows the result of aggregating with different window sizes.

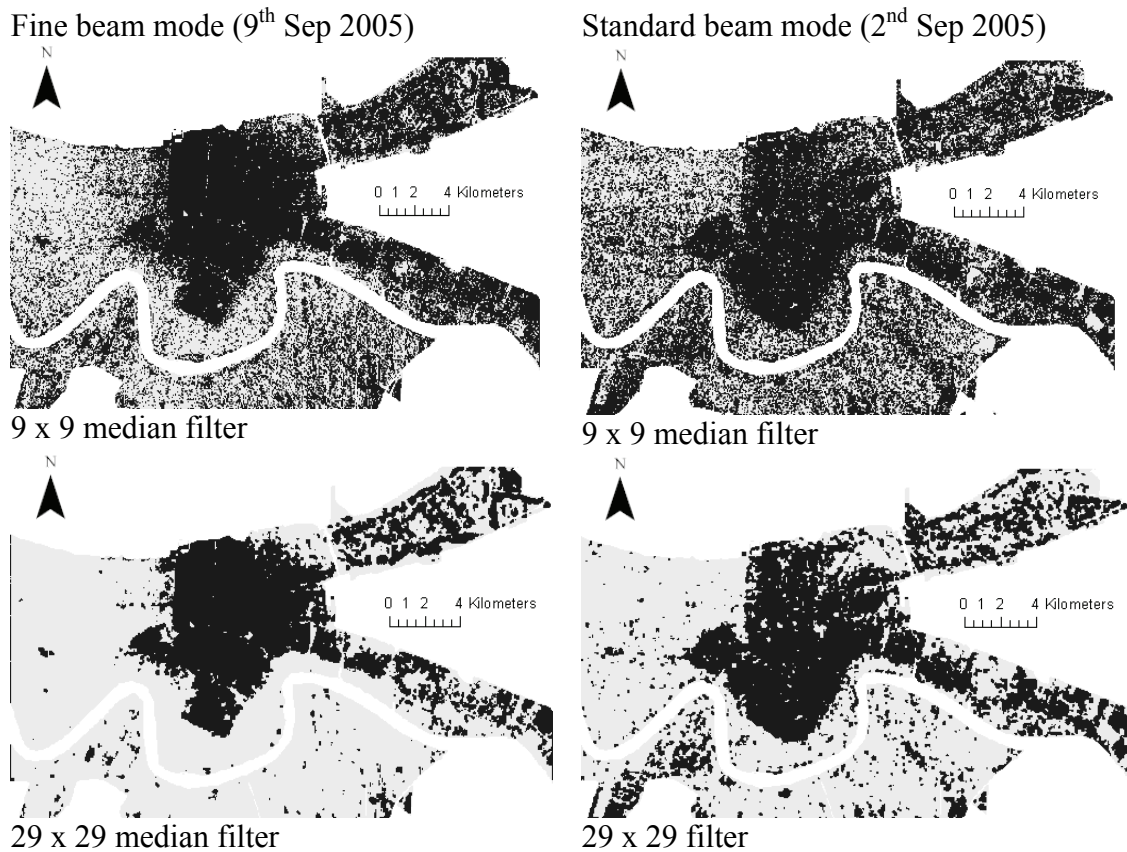


Figure 3-3 Effect of Median Filtering on Threshold Flood Signal

To assess the relative accuracy of the SAR-derived flood extent against independent validation data, two approaches were employed:

- a) A manually-derived flood boundary based approach
- b) An area-based flood detection approach

For the boundary-based validation, a flood boundary was manually delineated on the standard beam mode and fine beam mode aggregated difference images. Originally, the unfiltered images were used, but this left a lot of subjectivity in the delineation. The fine beam mode boundary was compared with the Landsat 5 derived boundary as they were the most similar in date. The standard beam boundary was compared with a boundary derived from a SPOT flood area created by FEMA. To compare the radar-delineated flood boundaries with the validation boundaries, a multi-ring buffer was created on the validation boundary. Each buffer segment was treated separately and overlaid with the radar flood delineation boundary so that only boundary

segments within that distance were derived. The length of the floodlines within each boundary was then calculated. Lastly, the percentage of each flood boundary within a certain buffer zone was calculated giving an estimate on the closeness of fit between the two layers.

For flood area delineation, the binary flood and no-flood radar maps created in step (j) were intersected with the binary flood and no-flood validation layers shown in figure 3-1. The validation and radar layers were multiplied together to create a four class contingency matrix image, showing areas of flood agreement and disagreement, false positives and negatives. Overall accuracy, user and producer and statistics were derived for each classification and kappa coefficients were calculated to examine the probability of the result occurring by chance. The following section discusses the results of this analysis.

SECTION 4

RESULTS

4.1 Amplitude Images

Figure 4-1 shows fine beam mode and standard beam mode Radarsat images of New Orleans. These have been filtered and masked to the urban extent of the city. A visual analysis of the imagery from the time of the event compared with the imagery post event shows that as well as slight changes possibly due to natural variability, both beam modes show two main areas of increased backscatter, which require further investigation. These are marked A to D in figure 4-1.

Both of these areas consist of many point target responses due to the nature of the urban area. Analog to digital conversion (ADC) of the radar signal was undertaken by MDA before receipt of the imagery. Absolute radiometric correction is important when results from multiple acquisitions are compared (Nicoll *et al.*, 2002). One major contributor for high contrast targets is saturation power loss. In the images processed, area B in particular shows high saturation levels. It is thought that in this particular area, the analog signal was stronger than the limits of the ADC, forcing the upper end of the continuous analog signal into 1 DN bin at the furthest extent of the histogram. This area, therefore, contains poor signal to distortion ratio. The same cut-off was not seen at the lower end of the histogram.

Radarsat uses Automatic Gain Control (AGC) onboard the sensor prior to the input to the analog to digital converter. The AGC samples a subset of the data; in the case of Radarsat, these values are set based on signals received from part of the swath in the half closest to the satellite. This determines a signal gain to be applied immediately before digitization at the ADC for a number of pulses. If the sub-sample is not a good representation of the backscatter for the pulse, then significant saturation can occur, and the whole line will be processed darker than its neighbors will. Therefore, a series of light and dark bands occurs frequently when the satellite images coastlines and the AGC is used (Nicoll *et al.*, 2002). If areas are dark on the near range and brighter on the far range, areas in the far range may be saturated. The near range here does contain some dark wetland and lake areas which is why the AGC has not performed well. To

perform a power loss correction for Radarsat AGC requires reprocessing from signal data. Signal data was not available in this instance.

It is acknowledged that the saturation artefacts in the image are not ideal, however the imagery will still be useful to examine as it is seen to vary temporally. It is important to remember that the incidence angle, sensor heading, and swath characteristics for the flood and non-flood imagery are the same, and so the AGC should compensate similarly for both images. Other differences in backscatter should be due to temporal effects, which will still be valid to investigate.

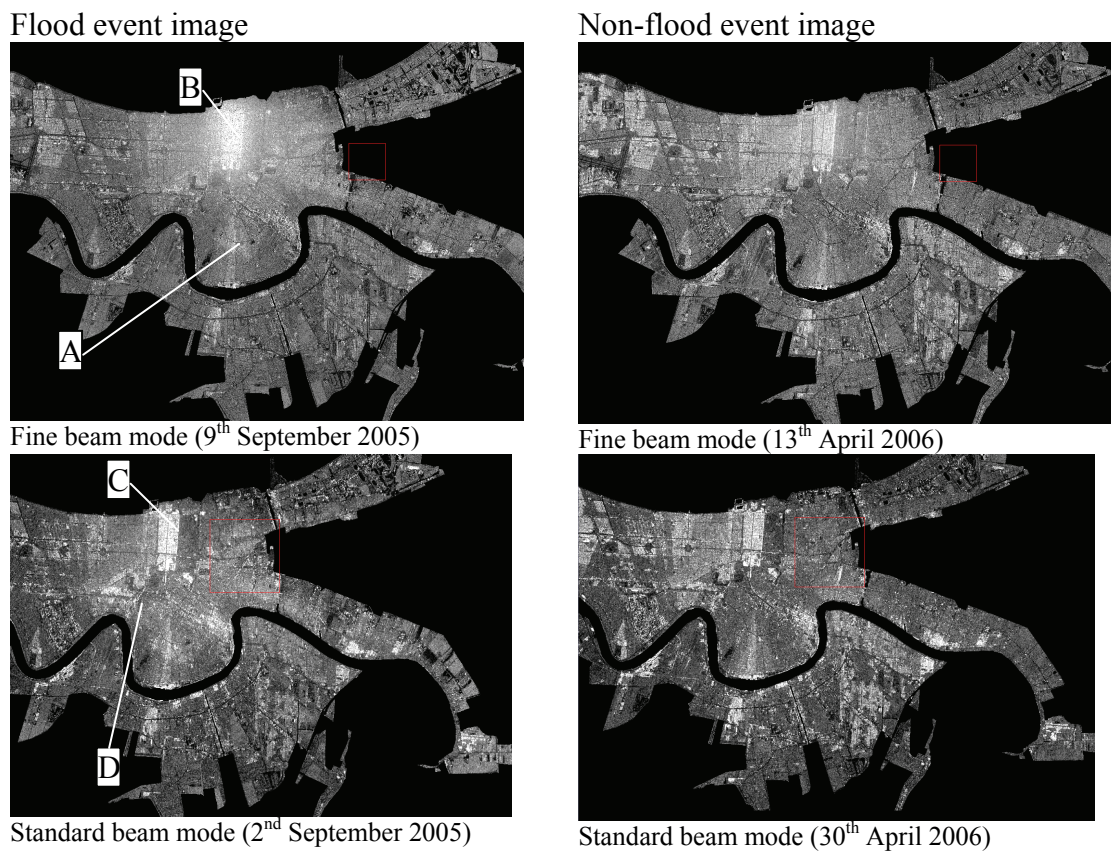


Figure 4-1 Raw Radarsat Imagery

4.2 False Color Composite

A False Color Composite (FCC) was utilized to visually explore in more detail the multi-temporal difference in backscatter (figure 4-2). Considering the flooded image was assigned to the green channel, and the non-flooded image was assigned to the red and blue channels, areas of

green in the False Color Composite (FCC) would relate to increased backscatter seen at the time of the flood. Areas of pink would relate to areas where little consistent change was seen between dates. This visualization presents a number of general patterns of response that are present in both fine and standard mode results. It firstly enhances area A, identified in section 4-1, where increased backscatter is seen at the time of the flood. The anomalously high backscatter in area B is seen in both images, in both beam modes, as this creates a white signal (high in all channels). In addition to this, areas which were not so obvious in the single images alone have also shown a change in response, as green areas are seen to the east of the city. These new areas of change have been marked C and D in figures 4-2 and 4-3. These green areas, as well as exhibiting higher backscatter in the flooded image, also contain small areas of intense pink coloring, which relate to areas where backscatter has decreased at the time of the flood. Areas of no major consistent change are classed as E and are characterized by a pink signal.



Figure 4-2 Fine Beam Mode False Color Composite Where Red = 13th April Pre-Flood, Green = 9th September – Flood, and Blue = 13th April Pre-Flood

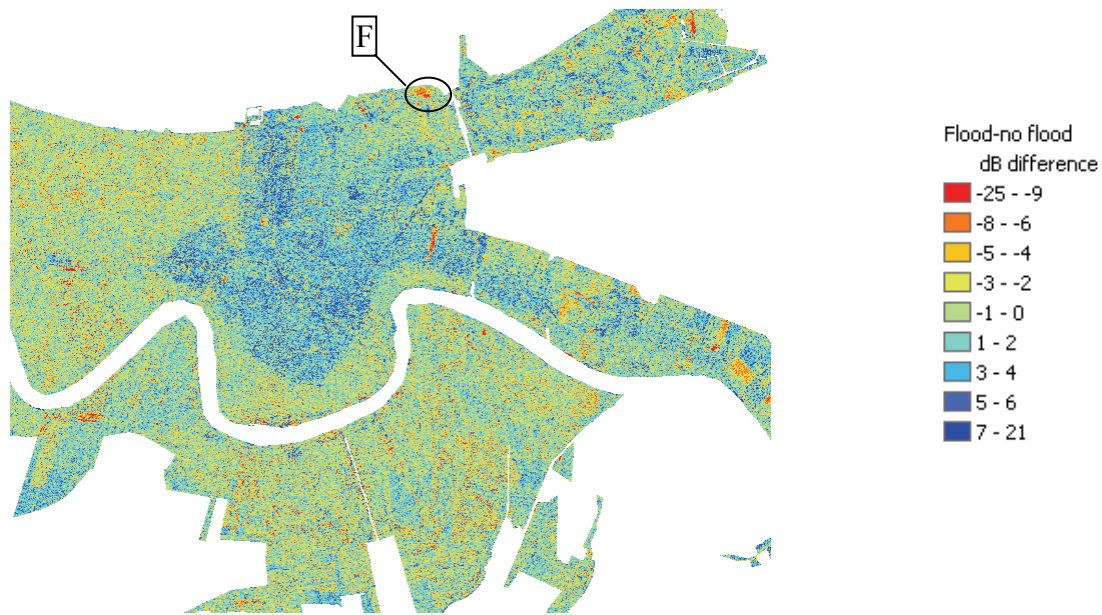


Figure 4-3 Standard Beam Mode False Color Composite Where Red = 30th April Pre-Flood, Green = 2nd September Flood, and Blue = 30th April Pre-Flood

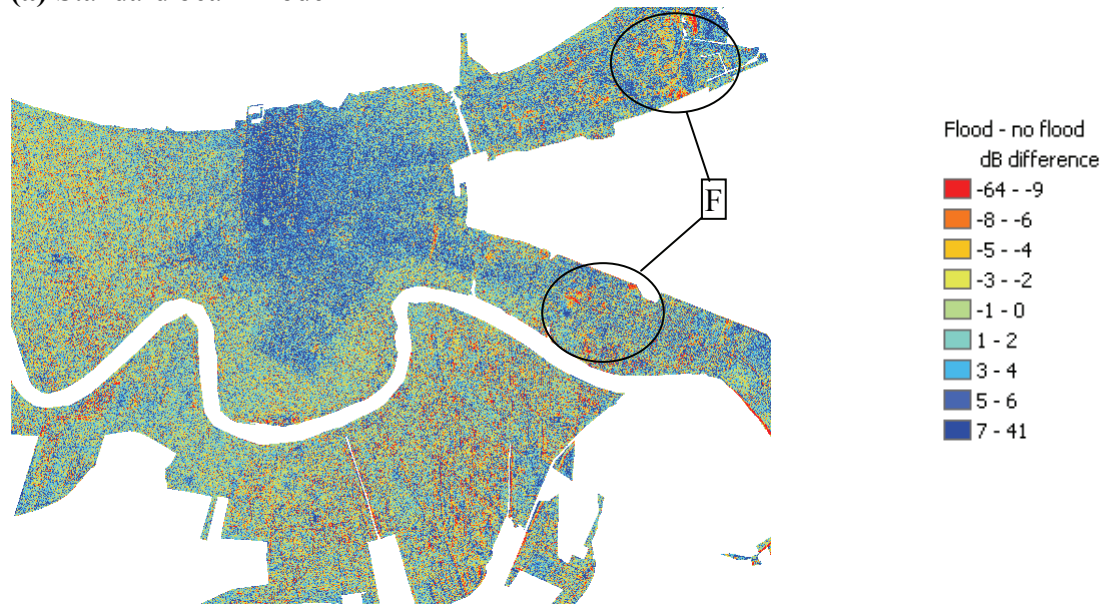
Although this change in backscatter is seen at the time of the flood for both fine and standard beam modes, the extent is shown to differ. The green area of A in the standard beam mode is seen to have a wider extent than fine beam mode, for instance. It is suggested that this difference in extent may be linked to the difference in acquisition dates of the images, however this needs to be investigated further. In summary, the color composites are seen to identify a definite and consistent change which should be investigated further to demonstrate that *higher backscatter seen may be related to the flooding of New Orleans due to Hurricane Katrina*.

4.3 Difference Image

Leading on from the false color composite analysis, a more thorough investigation of dB values was undertaken. A difference image was employed to examine the magnitude and direction of dB change. This is shown in figure 4-4, with a comparable scale used to display values for fine and standard modes.



(a) Standard beam mode



(b) Fine beam mode

Figure 4-4 Decibel Difference Images for a) Standard and b) Fine Beam Modes. Circled are Localized Areas of Large Negative Difference (area F)

The difference map further highlights variations in backscatter across New Orleans between the flooded and non-flooded scenes. Both maps show features A-D from the false color composite, as areas of blue, which corresponds to high positive difference values. Area B, in particular, appears to have a concentration of positive difference values. Areas C and D also include some negative differences. Area E is characterized by small magnitude difference values which show

no consistent pattern. Finally there are localized occurrences of large negative differences in all areas, possibly pertaining to specular responses which were not present before.

Comparing the standard and fine difference maps, both are seen to show the same general pattern, however the fine beam mode image has more blue which means a greater concentration of positive dB difference values than the standard mode. The maximum positive and negative values are also higher on the fine beam mode map. This is reflected in the normalized frequency distribution shown in figure 4-5, and by the increase in mean and standard deviation shown in table 4-1. This effect can be seen across the whole of figure 4-5, although it is most appreciable in areas A-D. Again, area A appears to cover a larger geographic area in the standard beam mode compared with the fine beam mode, probably because of the difference in acquisition dates.

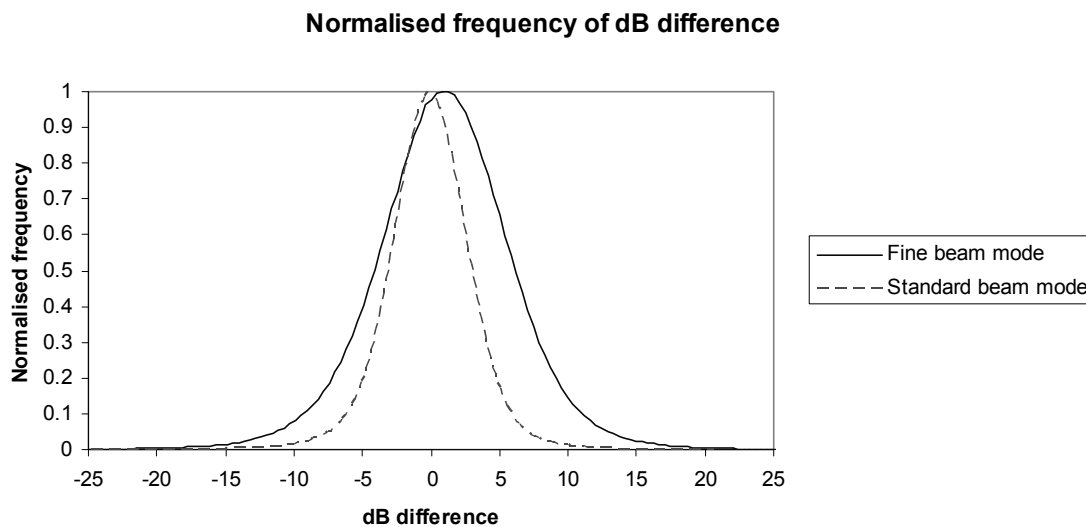


Figure 4-5 Normalized Frequency of Db Difference for Fine and Standard Beam Modes, Clipped to 99%

Table 4-1 Difference Image Statistics

Beam mode	Min	Max	Mean	SD
Fine	-65	41	1.15	5.10
Standard	-25	21	-0.04	3.12

4.4 Statistical Analysis

Regions of interest were extracted from areas A-F. The areas were designated depending on a number of factors. Firstly they were based on the different backscatter responses identified in figure 4-3. They also corresponded roughly to different areas of the city; the densely built up centre of New Orleans, and the surrounding parishes. This procedure allowed statistics to be calculated for selected samples within those areas, assigning values to the patterns that were identified (see figure 4-6). Each area contained distinctive responses, which are summarized by the area names assigned below.

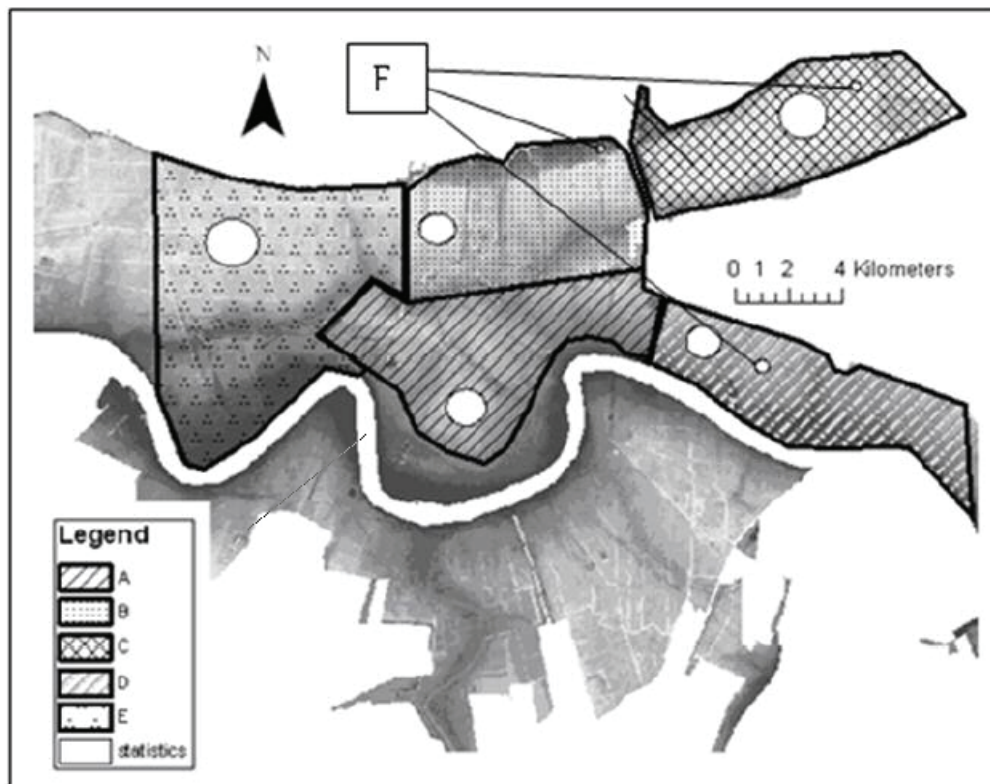


Figure 4-6 Study Area Split into 6 Zones of Investigation, and Sample Areas for Statistical Analysis (Circles)

Table 4.2 – Average Backscatter Responses and Difference Statistics

Area	Description	Flood (average dB)	No-Flood (average dB)	Difference (average dB)
A (Fine)	Flooded area	-7.3	-10.5	3.2
A (Standard)	Flooded area	-5.3	-3.4	1.9
B (Fine)	Saturated area	1.7	-3.5	5.2
B (Standard)	Saturated area	1.8	0.2	1.6
C (Fine)	Mixed response	-11.4	-13.7	2.3
C (Standard)	Mixed response	-7.3	-7.9	0.6
D (Fine)	Small response	-8.2	-11.1	2.9
D (Standard)	Small response	-5.0	-5.7	0.7
E (Fine)	Non-flooded area	-17	-14	-3.4
E (Standard)	Non-flooded area	-9	-7.3	-2.6
F (Fine)	Open areas of land	-9	-8.1	-0.9
F (Standard)	Open areas of land	-3.6	-5	-1.5

4.4.1 Area A

Area A is a flooded area. Considering table 4-3A, this area is characterized by a definite increase in backscatter at the time of the flood. This area is seen to be flooded using both Landsat and SPOT validation data. The mean backscatter between the flood and no flood event imagery differs by 3.2dB for fine beam mode. Backscatter at the time of the flood was recorded at an average of -7.3 dB. In the non-flood situation, the mean backscatter is recorded at -10.5 dB. In standard beam mode, the margin of increase is less pronounced. Mean backscatter between the flood and no flood event imagery differs by 1.9dB with a mean backscatter of -5.3dB during a non flood situation and -3.4dB during a flood situation. In both fine and standard modes, the distribution is similar to the no flood image, despite being shifted by these amounts. Examining the optical imagery, this flood signature relates to an area composed of high-density residential structures in a strict grid pattern. Houses are relatively large, and there is relatively little open or green space.

4.4.2 Area B

Area B is characterized by a saturated area. Table 4-3B demonstrates a large frequency of extremely high dB values exist for both flood and non-flood conditions. The histograms respectively peak at a frequency of >10,000 pixels for a value of 8.3dB for fine beam mode, and

>2,500 pixels with a value of 9.8dB for standard beam mode, which is where the ADC did not adequately sample the high radar signal received at the center. Similar to area A, this region of New Orleans is composed of high-density residential structures, with relatively little green or open space in the vicinity. Unlike area A, the streets are all aligned in a very specific direction, an orientation effect that may be responsible for the large frequency of high dB values obtained. Figure 4-7 further illustrates the relationship between the saturation and the street row configuration. In particular, the first row of houses of each block in this orientation gives a very strong response. They also appear to be perpendicular to the incoming radar beam direction. The sensor platform heading for the fine beam descending mode image was 193° , equating to a 283° look direction. The average angle of streets in the very high backscatter area is around $81-84^\circ$, making the look direction almost parallel to the street angle. This suggests that the saturation is induced by an increased double bounce effect from the particular orientation of these streets and buildings.

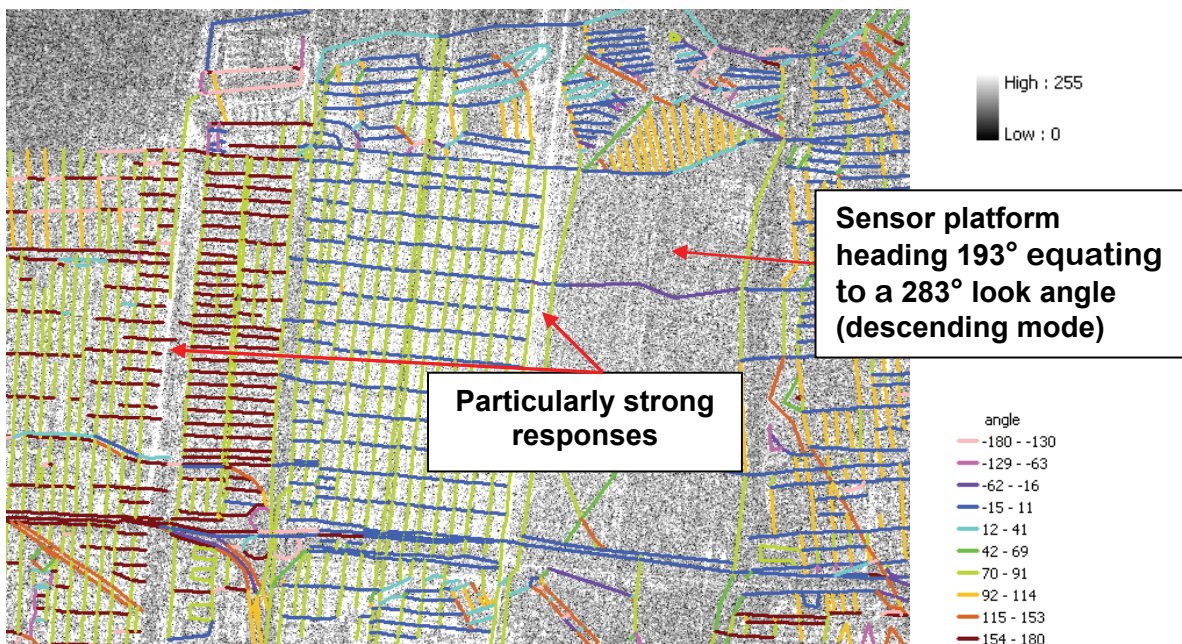


Figure 4-7 Area B Overlain with Tiger Lines™ Comparing Street Alignment and Look Angle with Backscatter Response. (Fine Mode April 13th Non Flooded Image Used).

To attempt a simple multi-temporal investigation, the saturated values were simply excluded from analysis in this area. Figure 4-8 illustrates the area B histograms after eliminating values relating to the saturation effect. In fine beam mode, the mean values increase from -3.5 dB at non-flood conditions to 1.7dB during the flood, a difference of 5.2dB. For standard mode, the mean values are lower at 0.2dB and 1.8dB respectively, with a smaller difference of 1.6dB. This suggests that in spite of the saturation effect, area B exhibits a similar pattern of response to area A, with an increase in backscatter at the time of the flood.

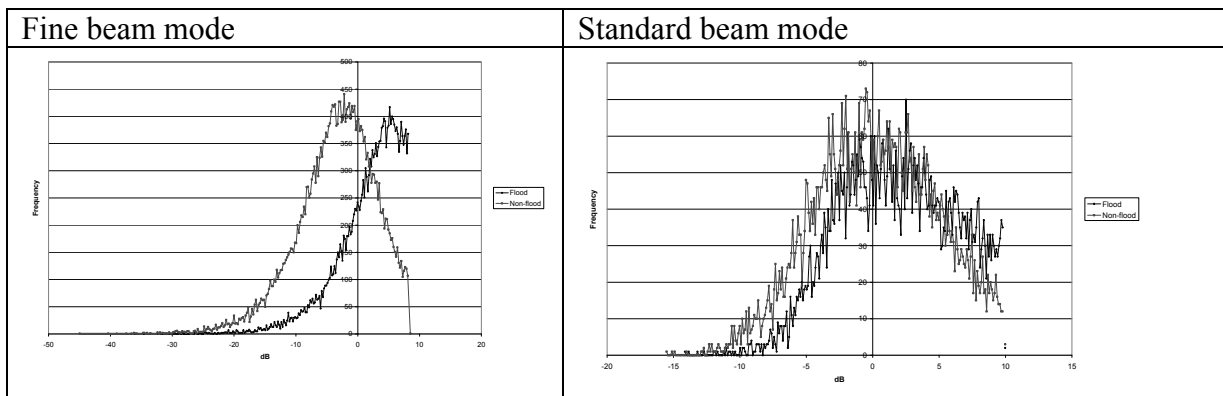


Figure 4-8 Histograms for Area B with Saturation Peaks Removed

4.4.3 Area C

Although flooded, table 4-3C shows less change in mean backscatter than the first two areas in both beam modes, and is characterized by a mixed response. In fine beam mode, a 2.3dB mean difference is still seen, from -13.7dB during the non-flood situation to -11.4dB at the time of the flood. The standard beam mode decibel difference showed negligible change. 0.6dB change was seen, where dB values were -7.9dB during non flood conditions and 7.3dB at the time of the flood. This area also has a low average dB range compared to most other areas. It is suggested that these low values are related to the land cover in this area. Considering table 4-3C, there are a large amount of canal and lake features in this area, as well as relatively large areas of open space such as parks and wetlands. Residential structures are still on a grid system. However the predominant street angle is around 40-45 degrees different to the alignment of streets in central New Orleans. Some blocks also have recognizably more expansive garden surrounds to their homes. The absence of a distinctive flood signature in this area requires further investigation of the relationship between radar response and urban configuration.

4.4.4 Area D

Flooded neighborhoods in table 4-3D shows slight increases in dB values at the time of the flood for both beam modes. For fine beam mode, 2.9dB of change was observed, from a mean decibel level of -11.1dB at non-flood conditions to -8.2dB at flood conditions. In standard beam mode, 0.7dB change was seen from -5.7dB under non-flood conditions to -5.0dB at the time of the flood. The standard deviation in this area was not seen to change considerably for either beam mode. As in area C, the flood signature in this region is less distinct. Again, it may be related to landcover type; this area is characterized by a mixture of different residential structures, industrial areas and open park areas. From table 4-3D, a localized increase in backscatter areas is mainly associated with residential areas. A decrease in backscatter coincides with open park areas, and also certain residential areas where the distinctive grid structure of the buildings and road configuration is degraded due to the complete destruction of the areas.

4.4.5 Area E

This area is the first sample to show a decrease in backscatter at the time of the flood, and is also the first to come from a non-flooded area as specified by the optical validation data. Fine beam mode shows -3.4dB difference (mean of -17dB at the time of the flood, compared a mean of -14dB for non-flood). In standard beam mode there is -2.6dB difference with a mean of -9.9dB at the time of the flood and -7.3dB from the non-flood image. From table 4-3F, these neighborhoods are high-density residential. Importantly, they were not flooded during Hurricane Katrina, further suggesting that the flood signature is characterized an increase in backscatter.

4.4.6 Area F

This is the second area investigated where the mean backscatter decreases at the time of the flood. There is a -0.9dB mean difference in fine beam mode, with -9dB at the time of the flood and -8.1dB under non-flood conditions. There is also a -1.5dB difference in standard beam mode, with the non-flood image exhibiting a slightly higher dB value than the flood image (-5dB as opposed to -3.6dB). These areas were chosen because of their large decrease in backscatter values at the time of the flood, but they are located in areas affected by the flood as defined by the optical validation dataset. They correspond with areas of flat open land such as car parks, or

grass areas. This suggests that the flooding created an enhanced specular response, leading to decreased return signal back to the radar.

4.4.7 Summary

In summary, this analysis suggests that areas identified as flooded by the optical validation data have, in general, recorded higher backscatter values at the time of the flood in radar imagery. A decrease in backscatter was seen from the sample taken from the non-flooded area. The distinctive positive difference in backscatter mainly corresponds with high-density residential areas, particularly where street patterns and buildings are aligned in a grid pattern, and where streets were perpendicular to the look angle of the radar. This change in values was accentuated more in fine beam mode than in standard mode. Parks, open spaces and completely destroyed areas within the flood zone tended to show a less distinctive change in backscatter values, suggesting a specular flood response.

Table 4-3 Histogram Results and Street Layout from the Six Areas of Analysis

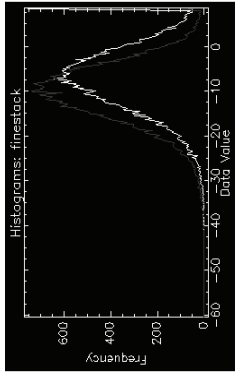
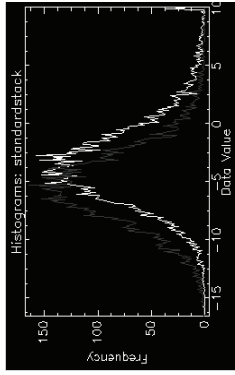


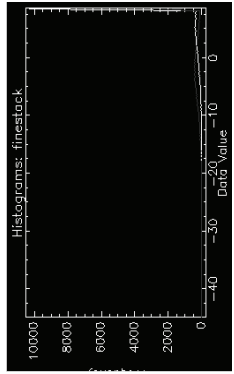
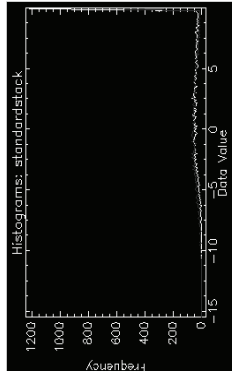


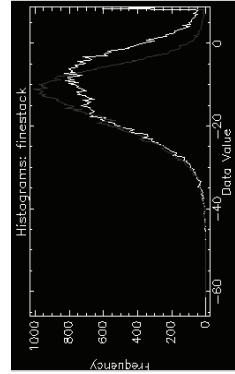
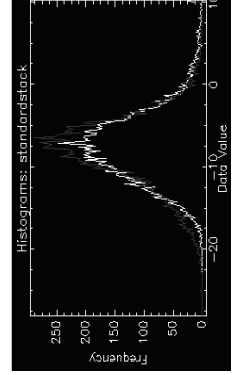
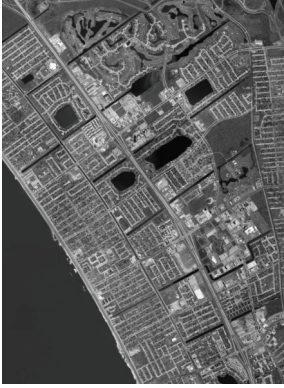

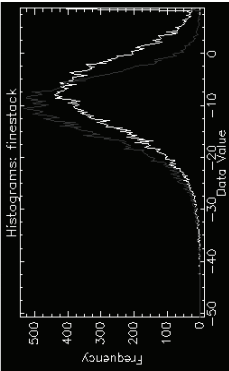
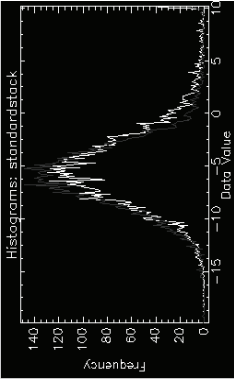


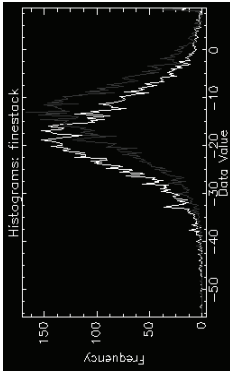
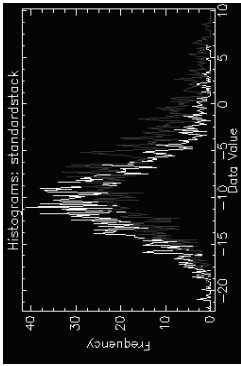


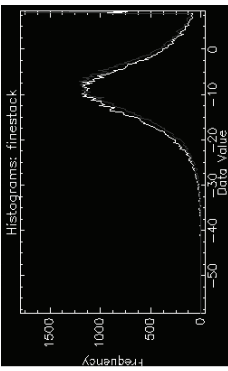
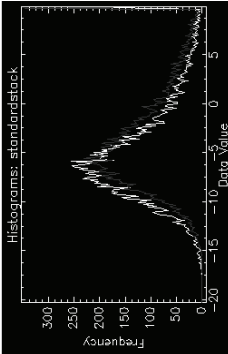


	Fine beam histogram	Standard beam histogram	Street layout	Housing type
A				
B				
C				

Table 4-3 (cont) Histogram Results and Street Layout from the Six Areas of Analysis

	Fine beam histogram	Standard beam histogram	Street layout	Housing type
D				
E				
F				

SECTION 5 VALIDATION

Two validation methods were chosen to investigate the accuracy and spatial variability of the detected change signal throughout the urban area of New Orleans and its suitability for mapping urban flooding. After thresholding and filtering, the first intersection analysis focuses on validating a flood boundary derived from manual delineation. This examines the maximum extent of the flooding. The second area intersection analysis focuses on the consistency of signal within the flood areas.

5.1 Boundary Intersection Analysis

Figures 5-1 and 5-3 show the results of the intersection analysis for fine and standard beam modes. In both cases, green shows good agreement between the validation and radar-derived flood boundary (within 150m). Yellow to orange is medium agreement (within 550m), and red is poor agreement (500m+)



Figure 5-1 Boundary Intersection Analysis Between Fine Beam Derived Flood Boundary and SPOT Derived Validation Layer

Fine beam mode showed generally good results, with 58% of radar boundary length falling within 150m of the validation boundary, and 82% of boundary length falling within 550m of the validation boundary. This is shown in figure 5-1. This proved to be a more accurate result than standard beam mode. Within this result, accuracies were spatially variable.

The numbers marked in figure 5-1 show points of poor correlation with the validation. Points 1 and 2 fall within the area of saturation (area A). It is clear that in this area high backscatter values spread beyond the boundary of the flood because of the effect that the saturation has on the surrounding pixel values. Point 3 is an area where some flooding was not distinguished. It is characterized by both different block formation (although similar road angle) and different housing type than those to the west that did show a large change in dB levels (figure 5-2). Useful parameters to investigate further could include building density, building orientation, street orientation and building height.

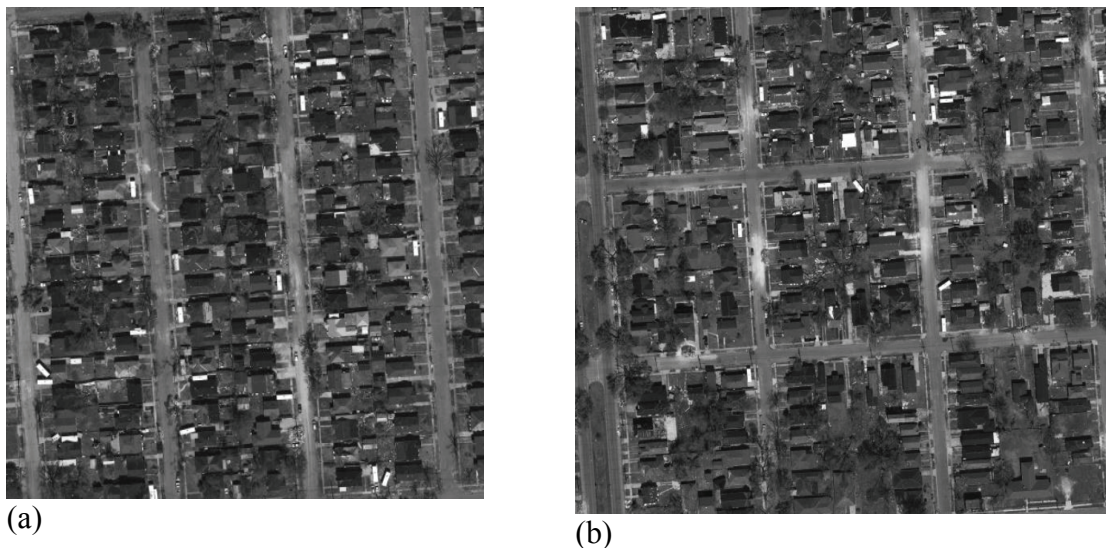


Figure 5-2 Differences Noted in Urban Parameters within Area B such as Building Density and Block Pattern between (a) an Area Showing Large Differences in dB Level During the Flood, and (b) an Area Not Showing any Considerable Change in dB Values. Both Areas were Flooded as Confirmed by Validation Data.

The area marked 4 did not show high backscatter values as it is actually a small area of wetland not masked out of the area. Point 5 is an area where houses were completely destroyed. No backscatter increase was seen at this area although it was flooded leading to an inaccurate

boundary. Finally point 6 gives an inconsistent response. There is not an obvious change in land cover or building configuration in this area. Therefore the inaccuracy may stem from either the difference in dates between the validation and the radar data or other building parameters which need to be investigated more thoroughly.

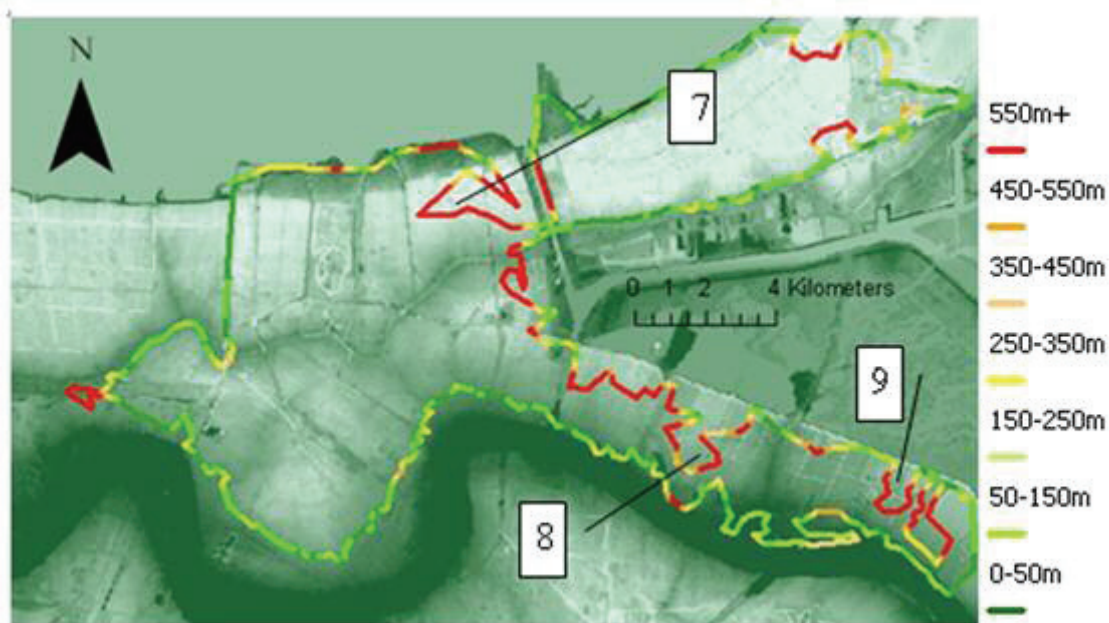


Figure 5-3 Boundary Intersection Analysis between Standard Beam Derived Flood Boundary and SPOT Derived Validation Layer

As shown in figures 5-3 and 5-4, Standard beam mode showed fair results. 46% of radar boundary length falls within 150m of the validation boundary layer, and 78% falls within 550m. This is seen to be less accurate than fine beam mode. Again, the result is spatially variable. Three main areas of boundary inaccuracy were found. Point 7 underestimated the flood boundary to a greater extent than fine beam mode. The urban configuration in this area has been explained in figure 5-2 and is a possible explanation for the low backscatter observed. No big errors are seen due to saturation effects here. This may be due to the difference in range described in figure 4-5. Points 8 and 9 stem from areas of woodland which were not marked as flooded in the validation (because the validation was derived from optical sources, it was probably not possible to distinguish flooding below the canopy, whereas the radar signal was able to show a difference in backscatter).

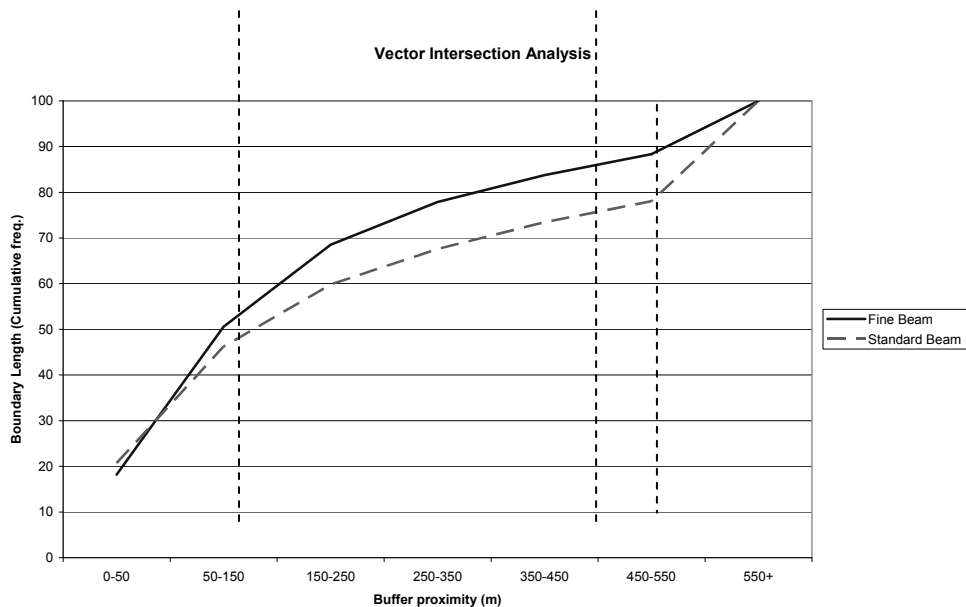


Figure 5-4 Vector Intersection Analysis Results

5.2 Area Intersection Analysis

Generally, fair results were seen from the area intersection analysis. Comparing the area flooded with validation datasets for various filter sizes, total accuracies were generally better as filter sizes increased, as shown in figure 5-5. User, producer and kappa coefficients increased in much the same pattern. The best filter examined for both beam modes was the 29 x 29 filter. This was seen to be adequate to remove speckle, and to create coherent flood and no-flood areas.

Continuing with the results from the best analysis using the 29 x 29 filter, the overall accuracy of the flood classification for fine beam mode was calculated as 77%. For standard beam mode this dropped slightly to 73%. Producer accuracy shows what percentage of each validation class is correctly classified. Very good results were seen for both non-flood classes with a fine beam producer accuracy of. Few false positives and negatives were seen outside of the flood area, helping to validate the fact that the change detection was a valid method to use, and that changes seen are correlated to non-random change in backscatter values. Flood class producer accuracy was recorded between 50-60% for both beam modes. Some false positives and negatives were seen within the flood area, showing that the change in backscatter is not consistent throughout the whole zone. Fine beam mode performed better than standard beam mode. User accuracy

shows what percentage of each classification class was classified correctly. Again, fine beam mode performed better than standard beam mode. Non-flood classification was very good, with both beam modes over 80% after 15 x 15 filtering. The flood class was less accurate with the best result of 56% using the fine beam 29x29 filter. There were generally more false positives than false negatives in both beam modes. This is due to small areas of woodland showing higher backscatter at the time of the flood, and possibly some spread of high backscatter signal.

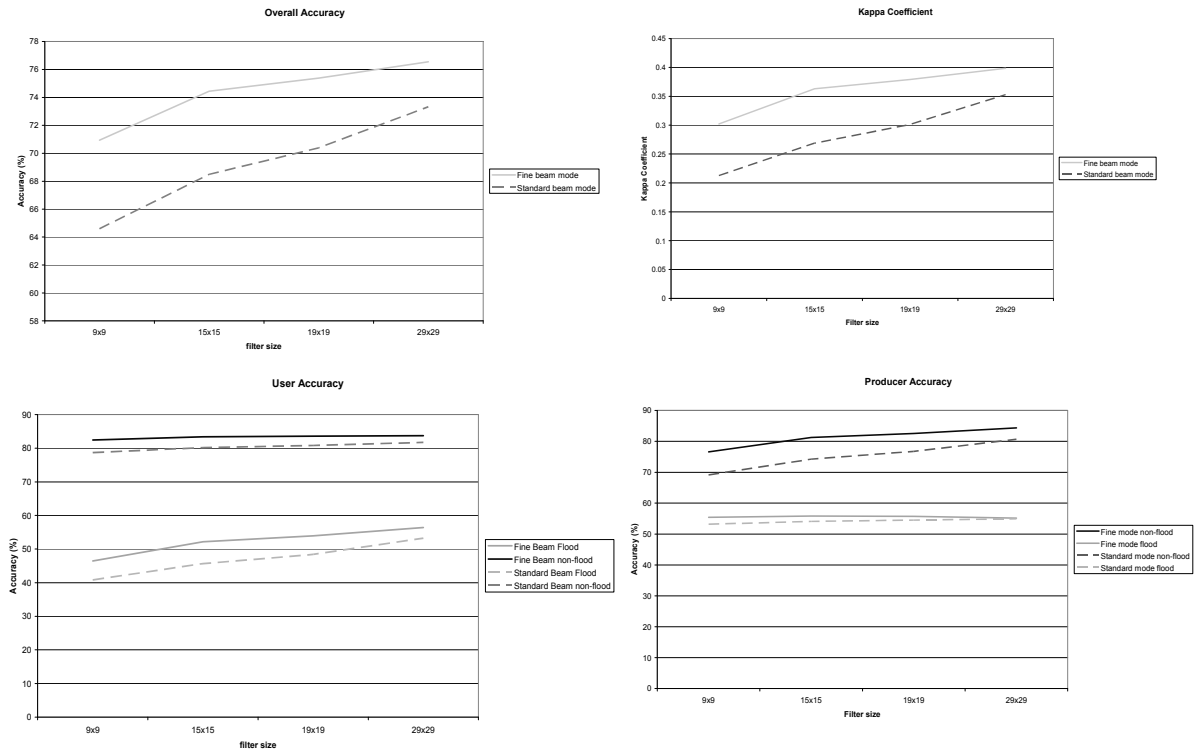


Figure 5-5 Accuracy Results from Area Intersection Analysis

Kappa coefficient is a statistical measure to calculate the probability of the results appearing by chance. In this instance, the kappa coefficient value was shown to be 0.40 for fine beam mode, and 0.35 for standard beam mode. Following the determinations of Landis and Koch (1977), this shows that there is a fair agreement between the radar-derived change in backscatter signal, and the flood validation layer, and that it is unlikely to have occurred by chance.

Figures 5-6 and 5-7 show the graphical results of the area intersection analysis, with green as flood agreement, black as non-flood agreement, red as false negatives, and yellow as false positives. Although the accuracies above are an average for the whole classification area, the results are seen to be spatially variable. Starting to suggest reasons for this variability will help determine under what conditions flood may be able to be detected using the change in backscatter.

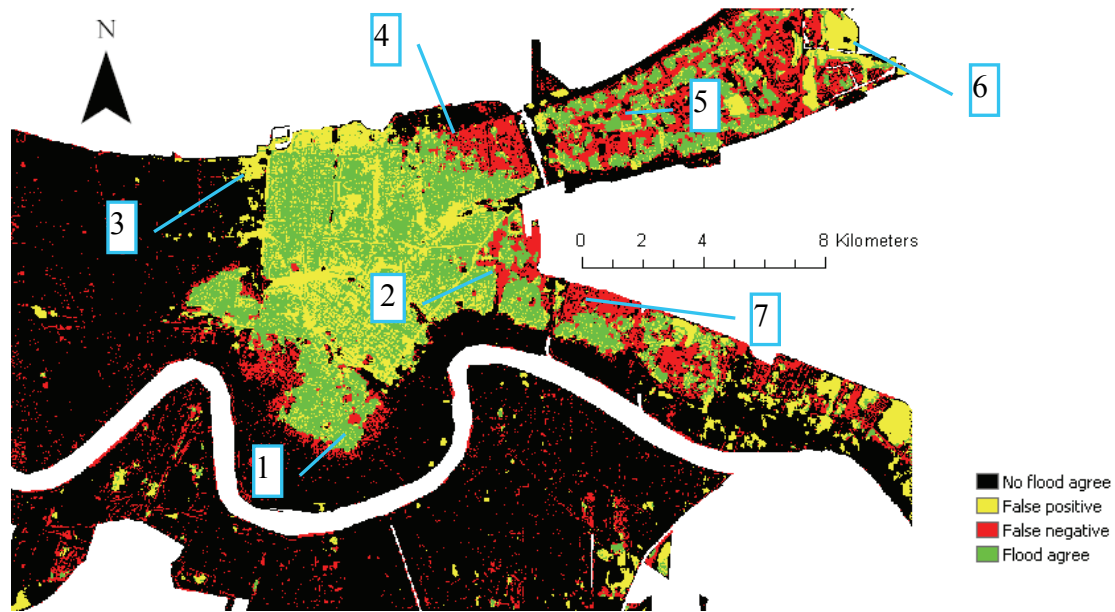


Figure 5-6 Area-based Intersection Matrix of Fine Beam Radar Signal and Validation Dataset

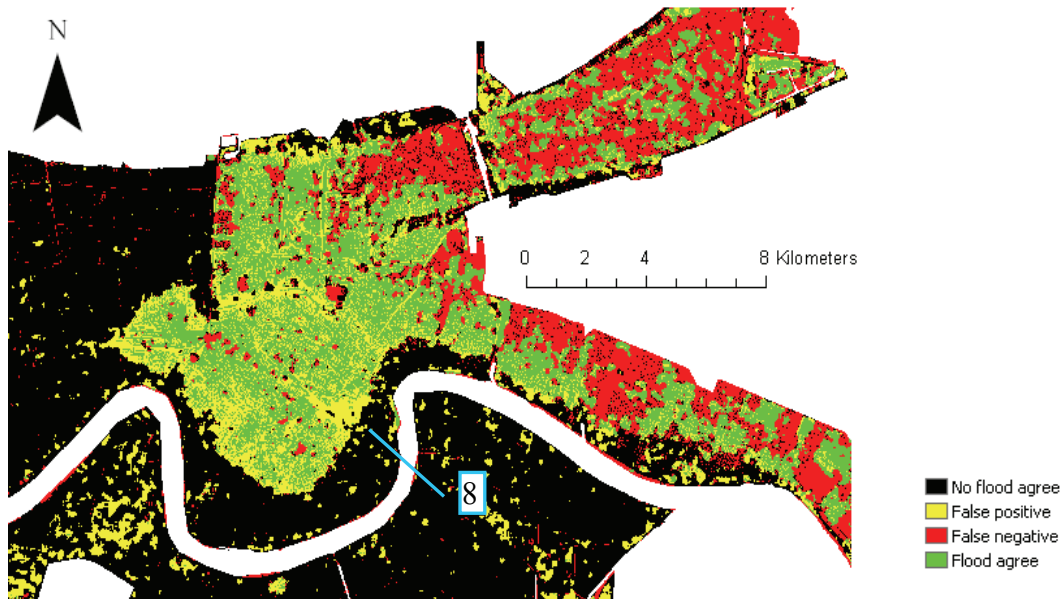


Figure 5-7 Area-based Intersection Matrix of Standard Beam Radar Signal and Validation Dataset

5.2.1 Fine Beam Mode

Considering figure 5-6, the flooded area, area A generally showed good agreement. There were some false negative areas, however. This is thought to be due to the difference in dates (two days) between acquisition and validation data, and the recession of the flood within that time. Further false negatives were seen at point 2. Figures 5-8a and b expand this area, and show two major factors contributing to this area of misclassification, i.e., the railway which was not seen to give an increased backscatter at the time of the flood, and an area of completely destroyed buildings. High-residential areas around these features give an increased backscatter response and are correctly classified as flood. Both of these findings give empirical evidence that residential buildings are an important factor in the increase in backscatter seen.

The saturation area (B) showed generally good agreement apart from a small area of false positive response (marked as 3 in figure 5-6) and an area of false negative marked 4. These effects were introduced in sections 4.4.2 and 5.1 and are caused by saturation and a change in building configuration, respectively.

Areas C contains areas of high backscatter associated with flooded areas, but also shows a lot of areas where this increase was not seen so strongly, resulting in false negatives. Considering

figure 5-8c it is apparent that most of the difference in backscatter is coming from the center of blocks of streets. Roads and houses on the periphery of these blocks are less likely to have a strong difference in response. But the pattern of results is complex, and needs further investigative work to understand the relationship between different urban parameters and the change in backscatter. The false positive (yellow) in areas C and D comes from areas of woodland which not masked out by the urban mask. They were seen to be badly damaged by the storm surge (see figure 5-8d). These areas were certainly flooded as is shown by the SPOT validation from the 2nd September. It is possible that the radar is better at picking up flooded forest than the Landsat data, so this may not necessarily be a misclassification. Other reasons may be the change in structure of the destroyed forest, perhaps due to decay and clearing between the 9th September (during) and the 13th April (after) radar imagery. As the purpose of this paper was to examine radar change within urban areas, this area was not investigated further.

Area D again shows a complex mixed response. The area marked 7 was introduced in figure 5-8b and gives a false negative due to completely destroyed buildings in this area. Figure 5-8e shows the relatively clear division between an area where buildings are moved from their foundations or destroyed, and the intact buildings giving an increased backscatter signal.

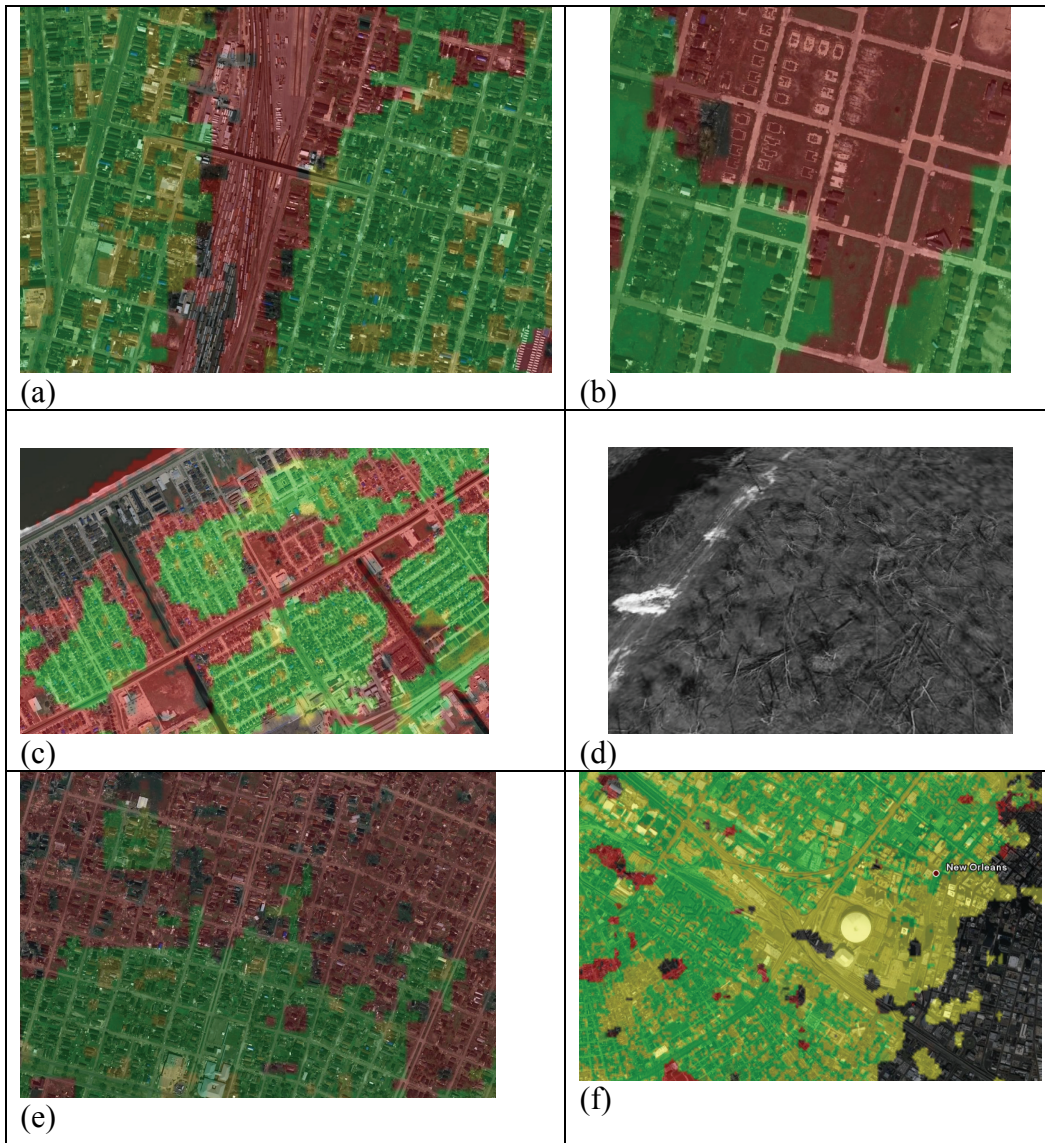


Figure 5-8 Misclassification in Various Areas. (a) Area A Showing an Area of Train, (b) Area A Showing Destroyed Buildings, (c) False Negatives Found in Area C, (d) Forest Area Destroyed which Shows as False Positives, (e) Area D Showing Correlation between Destroyed Buildings and Intact Buildings, and Increase in Backscatter (green) and False Negatives (red), (f) Industrial Area Falsely Classified as a Flood Area

Most of area E shows good non-flood agreement. Area F contained areas showing a large drop in decibel values at the time of the flood. These are mainly from open park and land areas. These were not encapsulated in the change detection methodology, to concentrate on urban increase in backscatter effects, and so show up as false negatives.

5.2.2 Standard Beam Mode

Examining figure 5-7, standard beam mode generally showed the same patterns of response as fine beam mode. The false negative at area A thought to be due to flood recession is not seen here, as the validation and the radar were acquired on the same day. However, instead, a small area of false positive (detected flood where there was not flood) was encountered (marked 8 on figure 5-7). This is an industrial area (figure 5-8f). This area could, therefore, be related to the spread of increased backscatter values resulting in a misclassification by the radar.

Less saturation effect was seen around area B than the fine beam mode. This is probably correlated to the difference in range identified in figure 4-5. Mixed results are seen at area C and D, however there is more extensive false negative results seen from the Standard beam mode than fine beam mode. Again this is probably correlated to the difference in range identified in figure 4-5.

Compared with fine beam mode, false positives are not seen in these areas. This shows that the forested areas were flooded at this time. Some false positives were seen at area F however, which again correlate to forested areas which were not totally masked out. All these areas were affected by the hurricane and resemble figure 5-8b.

In summary, validating the results showed an overall fair agreement with optically derived validation. Fine beam mode results gave greater accuracy than standard beam mode results for both delineating a flood boundary, and comparing flood area. Accuracies were seen to be class related. Non-flood was classified very well, whereas the accurate assignment of a flood class from high backscatter values was seen to depend on spatial variability. Areas generally consisting of high-density residential structures gave better results than areas of relatively generously spaced urban layout interspersed with parks and open space. Generally, a high backscatter change was not seen in areas where buildings had been completely destroyed. Other factors that were empirically seen to affect the signal were street and block alignment, and building type. These factors need further investigation.

SECTION 6

KEY FINDINGS AND FUTURE WORK

Image processing techniques and GIS analysis were utilized to explore the general characteristics of the flooded urban environment using radar. Using multi-temporal change detection methods, it was found that urban areas affected by flooding showed increased backscatter at the time of the flood. As a result of this, a flood boundary could be delineated and a threshold analysis undertaken to examine the spatial extent of the flood.

When manually delineating a flood boundary from the filtered imagery, fair agreement was found with optically-derived boundaries. 58% of fine-beam radar derived boundaries fell within 150m of the optically derived data, and 82% fell within 550m.

The optimum results were gained from fine beam mode, demonstrating that 58% of the radar derived boundaries fell within 150m of the optically derived data, and 82% fell within 550m. A second analysis used an area-based contingency matrix method to compare radar classified flood with the validation layers. The most accurate result was obtained using fine beam mode imagery with large window size filtering. Results show user accuracies of 56% for flooded and 84% for non-flooded regions, and producer accuracies of 55% and 81% for flood and non-flood classes respectively.

Considering the area-based analysis, validation showed that this result had a fair statistical significance. The most accurate result was obtained using fine beam mode imagery with large window size filtering. Results show user accuracies of 56% for flooded and 84% for non-flooded regions, and producer accuracies of 55% and 81% for flood and non-flood classes respectively. It is a fair assumption that this relationship did not occur by chance, as a calculated kappa coefficient was recorded at 0.40. Very good agreement was found in areas of non-flood, showing that the change detection methodology was valid. Within areas affected by flood, spatial variability was experienced.

Considering empirical evidence comparing classification results and visual analysis, differences in accuracy were not straightforward. Many factors are thought to be involved. Firstly, some

small areas of forest and wetland were not completely removed from analysis by the urban mask, leading to some false positives from loss of coherence. Park areas, car parks, railways and other transport structures did not usually have high backscatter values attached to them. Many of these areas are fairly open and flat. It was more likely that flooded areas in these classes have a specular response to radar, leading to a decrease in dB values at the time of the flood. Within intact residential areas, variability in the correlation between high backscatter and flood was seen. Empirically, this seemed to be related to urban parameters such as building size, density of buildings, and orientation of buildings. Particularly pertinent evidence for the importance of residential structures in the signal response came from examples where complete destruction of buildings led to areas of false negative response. Industrial areas were more likely to show a false positive response.

As well as classification differences due to land cover and urban structure, a few non-scene related issues were encountered. Firstly the ADC processing undertaken by Radarsat before receipt of imagery, and in particular the AGC process lead to saturation of very high backscatter values in a particular area in central New Orleans where the street orientation was almost perpendicular to the oncoming radar beam. This led to some small misclassification areas.

Secondly, the validation datasets come with their own assumptions. In particular, differences in resolution, derivation method and date can lead to discrepancies in classification which may not always be false.

It is difficult to compare the accuracy of the method with other similar studies; as mentioned in the introduction radar is not generally used inside urban areas to detect flood because of confounding double bounce effects. As far as the author is aware, no studies have examined the accuracy of this method before. It should be remembered that this is only one study. Capturing radar imagery from other large scale urban floods will be highly recommended to repeat these observations for other areas. However, it can be said that urban flood monitoring by radar has not been demonstrated to be as accurate as expert interpretation of high-resolution optical satellite or aerial imagery, or ground based measurements. Its main advantage is that it can be explored if cloud cover means that optical imagery is not available. In this case it may be the best method

for quick evaluation of flooding in a large urban area, and it is for this purpose that the research is important. Flood mapping by radar outside of urban areas, where water gives a specular dark response, is well established. This preliminary work strongly suggests that it is also worth investigating the radar response inside urban areas, and should not be dismissed out of hand.

It is clear that the radar beam interacts with urban areas in a complex way, making the response complicated and seemingly random at times, and is less instinctive to interpret than optical imagery. The beam manifests as a series of pathways from the radar (which do not come in at a nadir angle). Once through the atmosphere, they are affected by the sizes, angles, composition and roughness of objects on the surface they hit. They can be scattered in many directions. Some of these beams bounce back in a favourable way (i.e. back towards the sensor on the satellite) and it is these beams which we can interpret. One way of minimizing this complex scatter, as used in this study, is to concentrate on differences between two responses in a single area from different times, using the same acquisition parameters. Therefore major differences in the composition of the scatter are often due to the actual physical differences on the surface that the radar hits. However the nature of the beam means that random scatter, and phase interactions can still complicate the picture. Along with this automatic gain control at the satellite mean that comparison should still be done with caution.

Assuming that acquisition parameters are similar, it is important to get temporally close images, so that extraneous variation is minimized (for instance changes to vegetation growth, or building work).

It is clear that much future work needs to be undertaken. There are a few key areas to be explored. First is the image acquisition specifications. It would be interesting to explore raw SAR data without AGC processing, so that the beam response can be better matched between different beam modes. This can also help avoid saturation signals in images where a large amount of backscatter is being reflected, allowing more detailed study. Secondly, more work needs to be undertaken in order to investigate exactly how urban parameters change backscatter values, as even in the non-flood case these are not fully understood. Modelling urban areas and radar signals to investigate changes in response at different angles, with different beam

parameters will allow a deeper understanding of the fundamental responses in these complex areas.

Only when this is known can we really understand how the addition of flood water may change those backscatter values. In this case it is suggested that different water depths are modeled, and backscatter response monitored to investigate relationships between water depth, height of buildings, and radar beam interactions. The layout and size of roads, street furniture (i.e. lampposts) and spaces within the city (i.e. car parks, parklands) are all further variables which can be investigated.

Finally it is hoped that the continuing capture and archiving of flood events over urban areas by radar will enable further research to validate models produced. A number of test cases would allow a more comprehensive understanding of radar beams in a variety of urban settings, and the similarities and differences in each case.

In conclusion, this preliminary research shows potential for further research into an area previously discounted.

SECTION 7

REFERENCES

Ahtonen and Hallikainen, (2005), Flood detection with spaceborne SAR images by using the Active Contour Model *Geophysical Research Abstracts*, Vol. 7, 02920.

Badji, M. and Dautrebande, S., (1995), Characterization of flood inundated areas and delineation of poor drainage soil using ERS-1 SAR imagery. *Hydrological Processes*, 11, 1441–1450.

Bryant, R. G. and Rainey, M. P., (2002), Investigation of flood inundation on playas within the Zone of Chotts, using a time-series of AVHRR *Remote Sensing of Environment*, 82, 360-375.

Brivio P. A., Colombo R., Maggi, M. and Tomasoni, R., (2002), Integration of remote sensing data and GIS for accurate mapping of flooded areas. *International Journal of Remote Sensing*, 23, pp. 429-441

Brakenridge, R.G. and Anderson, E., (2005), MODIS-based flood detection, mapping, and measurement: the potential for operational hydrological applications. In: *Transboundary Floods, Proc. of NATO Advanced Research Workshop*, Baile Felix – Oradea, Romania, May 4-8, 2005.

Dellepiane, S., Bo, G., Monni, S. and Buck, C., (2000), SAR images and interferometric coherence for flood monitoring. *Proceedings of the 2000 IEEE Geoscience and Remote Sensing Symposium (IGARSS'00)*, Honolulu, Hawaii, USA, 24–28 July 2000 (Piscataway, NJ: IEEE), vol. 4, pp. 2608–2610.

Dong, Y., Forster, B.C. and Ticehurst, C., (1997), Radar Backscatter Analysis for Urban Environments, *International Journal of Remote Sensing*, 1997, 18 1351 – 1364.

Dousset, B., (1997), Interpretation of ERS-SAR images over urban surfaces. *Proceedings of the Third ERS Symposium on Space at the service of our Environment*, Florence, Italy, 14-21 March, 1997. ESA pp.53.

ESA, (2006), Katrina (Florida) Hurricane, August 2005 Available online at: http://earth.esa.int/ew/cyclones/Katrina_Hurricane-aug05/ (accessed 9th March 2006)

Fatone, L., Maponi, P. and Zirilli, F., (2001), Fusion of SAR/optical images to detect urban areas, *Remote Sensing and Data Fusion Over Urban Areas: IEEE/ISPRS Joint Workshop Proceedings 2001* pp. 217-221.

FEMA, (2005), FEMA Mapping and Analysis Center Available online at: <http://www.gismaps.fema.gov/2005pages/rsdrkatrina.shtm> (Accessed 10th March 2006).

Galy, H. M. and Sanders, R. A., (2000), Using SAR Imagery for Flood Modeling Available online at: http://www.intermap.com/images/papers/rgs_paper.pdf RGS-IBG Annual Conference, University of Sussex, January 4th – 7th 2000. (Accessed 5th August 2006).

Gruen, A. and Li, H., (1997), Linear feature extraction with 3-D LSB-Snakes, *Automatic Extraction of Man-Made Objects from Aerial and Space Images (II)*, Birkhaeuser Verlag, Basel.

Henderson, F. M. and Lewis, A. J. (Eds.), (1998), *Principles and Applications of Imaging Radar* 3rd edition. John Wiley & Sons, 866 pages.

Ho, A.T.S.; Seumahu, E.S.; Siu Chung Tam; Teck Wei Chin and Hock Seng Lim, (1998), Improving SAR image classification in tropical region through fusion with SPOT data, *Geoscience and Remote Sensing Symposium Proceedings*, 3 pp.1596 - 1598.

Horrit, M. S. and Mason, D. C., (2001), Flood boundary delineation from synthetic aperture radar imagery using a statistical active contour model, *International Journal of Remote Sensing*, 22, 2489–2507.

Imhoff, M.L., Vermillion, C., Story, M.H., Chouhury, A.M., Gafoor, A. and Polcyn, F., (1987), Monsoon flood boundary delineation and damage assessment using space borne imaging radar and Landsat data, *Photogrammetric Engineering and Remote Sensing*, 53, 405–413.

Kiage, L.M., Walker, N.D., Balasubramanian, S., Babin, A. and Barras, J., (2005), Applications of Radarsat-1 synthetic aperture radar imagery to assess hurricane-related flooding of coastal Louisiana, *International Journal of Remote Sensing* 26, 5359–5380.

Kannen, A., (1995), Use of SAR data for flood mapping and monitoring in Thuringen, Germany, *Proceedings of the 2nd ERS applications workshop, 6–8 December 1995* (London: ESA) pp. 237–241.

Kuehn, S., Benz, U. and Hurley, J., (2002), Efficient flood monitoring based on RADARSAT-1 images data and information fusion with object-oriented technology, *IEEE International Geoscience and Remote Sensing Symposium Proceedings*, 5, pp. 2862-8264.

Landis, J.R. and Koch, G.G., (1977), The Measurement of Observer Agreement for Categorical Data, *Biometrics*, 33, 159-174.

Lee, W. K., (2001), Reduction of cardinal effects in SAR imagery of densely populated urban areas by suppressing strong multiple returns *IEEE International Geoscience and Remote Sensing Symposium Proceedings*, 2001, IGARSS '01. 5, pp. 2328-2330.

Li, E.S. and Sarabandi, K., (1999), Low grazing incidence millimetre-wave scattering models and measurements for various road surfaces, *IEEE Transactions on Antennas and Propagation*, 47, 851-86.

Lonbardo, P. and Oliver, C., (2001), Maximum likelihood approach to the detection of changes between multi-temporal SAR images, *IEEE Proceedings on Radar, Sonar and Navigation*, 148, 200.210.

Malnes, E., Guneriussen, T. and Høgda, K. A., (2002), Mapping of flood-area by Radarsat in Vansjø Norway, *ISRSE-2002 (International Symposium on Remote Sensing of Environment)*, Buenos Aires, Argentina 8-12 April.

McGlothlin, J.T., (2006), The Geography of New Orleans. Available online at: http://www.southbear.com/New_Orleans/Geography.html (accessed 15th August 2006)

MDA, (2006), Radarsat 1. Available online at: <http://gs.mdacorporation.com/products/sensor/radarsat/radarsat1.asp> (accessed on 15th July 2006).

Natural Resources Canada, (2006), Radarsat-1 SAR. More technical details available online at <http://ccrs.nrcan.gc.ca/radar/spaceborne/radarsat1/specs/rsattable.php> (accessed 1st July 2006).

Nico, G., Pappalepore, M., Pasquariello, G., Refice, A. and Samarelli, S., (2000), Comparison of SAR amplitude vs. coherence flood detection methods—a GIS application, *International Journal of Remote Sensing*, **21**, 1619–1631

Nicoll, J, Gens, R. and Denny, P., (2002), Pre-processing compensation for saturation power loss in SAR data, *Geoscience and Remote Sensing Symposium, 2002, IGARSS '02, 2002 IEEE International 5*, 2744- 2746.

NOVA, (2006), How New Orleans Flooded. Available online at: <http://www.pbs.org/wgbh/nova/orleans/how.html> (accessed 1st August 2006).

Oberstadler, R., Honsch, H. and Huth, D., (1997), Assessment of the mapping capabilities of ERS-1 SAR data for flood mapping: a case study in Germany, *Hydrological Processes*, **11**, 1415–1425.

Parmuchi, M.G., Karszenbaum, H. and Kandus, P., (2002), Mapping wetlands using multi-temporal RADARSAT-1 data and a decision-based classifier, *Canadian Journal of Remote Sensing*, **28**, 175-186.

Pellizzeri, T.M., Gamba, P., Lombardo, P., Dell'Acqua, F. and Tottora, A., (2003), Flood monitoring in urban areas: Statistical vs. neurofuzzy approach, *Proceedings 2nd GRSS/ISPRS Joint Workshop on Remote Sensing and Data Fusion over Urban Areas*, pp. 211-215.

RSI, (2000), ENVI User's manual. Available online at www.gisits.com/otros/userguid.pdf accessed 4th October 2006

Sanyal, J, and Lu, X.X., (2004), Application of Remote Sensing in Flood Management with Special Reference to Monsoon Asia: A Review. *Natural Hazards* **33**, 283-301.

Sohn, H.G., Song, Y.S. and Kim, G.H., (2005), Detecting water area during flood event from SAR image computational science and its applications, *ICCSA 2005, pt 2 lecture notes in computer science*, **3480**, 771-780.

Solbø, S., (2003), Published Literature on water detection from SAR data. Available online at: <http://projects.itek.norut.no/floodman/Publications/Papers/artikkelsoek.pdf> (accessed 13th July 2006).

Solbø, S. and Solheim, I., (2004), Towards Operational Flood Mapping with Satellite SAR, *Proceedings of the 2004 Envisat & ERS Symposium (ESA SP-572, 6-10 September 2004, Salzburg, Austria*, Edited by H. Lacoste and L. Ouwehand, Published on CD-Rom., #264.1.

Stabel, E. and Löffler, E., (2003), Optimized Mapping of Flood Extent and Floodplain Structures by Radar EO-Methods, In: *Proceedings of FRINGE 2003 Workshop*, Frascati, Italy, 1 – 5 December 2003.

Stabel, E. and Fischer, P., (2002), Detection of Structural Changes in River Dynamics by Radar-Based Earth Observation Methods, In: *Proceedings of the 1st Biennial Meeting of the iEMSS – Integrated assessment and decision support* Lugano, Switzerland, 24-27, June 2002.

Takeuchi, S., Konishi, T., Suga, Y. and Kishi, S., (1999), Comparative study for flood detection using JERS-1 SAR and LandsatTM data, In *Geoscience and Remote Sensing Symposium, 1999, IGARSS '99 Proceedings. IEEE 1999 International*, 6-7th June, 1999, pp. 873-875.

Tholey, N., Clandillon, S. and De Fraipont, P., (1997), The contribution of spaceborne SAR and optical data in monitoring flood events: examples in northern and southern France. *Hydrological processes*, 11, 1409-1413.

US Census Bureau, (2006), State & County QuickFacts – New Orleans. Available online at: <http://quickfacts.census.gov/qfd/states/22/2255000.html> (accessed 2nd August 2006).

USGS, (2005), Hurricane Katrina Impact Studies. Available online at <http://coastal.er.usgs.gov/hurricanes/katrina/> (accessed 3 June 2006).

Wei, Y., Xu, W., Fan, Y. and Tasi, H.T., (2002), Artificial neural network based predictive method for flood disaster, *Computers and Industrial Engineering*, 42, 383-390.

Zhou, C., Luo, J., Yang, C., Li, B. and Wang, S., (2000), Flood Monitoring Using Multi-Temporal AVHRR and RADARSAT Imagery, *Photogrammetric Engineering & Remote Sensing*, 66, 633-638.

MCEER Technical Reports

MCEER publishes technical reports on a variety of subjects written by authors funded through MCEER. These reports are available from both MCEER Publications and the National Technical Information Service (NTIS). Requests for reports should be directed to MCEER Publications, MCEER, University at Buffalo, State University of New York, Red Jacket Quadrangle, Buffalo, New York 14261. Reports can also be requested through NTIS, 5285 Port Royal Road, Springfield, Virginia 22161. NTIS accession numbers are shown in parenthesis, if available.

- NCEER-87-0001 "First-Year Program in Research, Education and Technology Transfer," 3/5/87, (PB88-134275, A04, MF-A01).
- NCEER-87-0002 "Experimental Evaluation of Instantaneous Optimal Algorithms for Structural Control," by R.C. Lin, T.T. Soong and A.M. Reinhorn, 4/20/87, (PB88-134341, A04, MF-A01).
- NCEER-87-0003 "Experimentation Using the Earthquake Simulation Facilities at University at Buffalo," by A.M. Reinhorn and R.L. Ketter, to be published.
- NCEER-87-0004 "The System Characteristics and Performance of a Shaking Table," by J.S. Hwang, K.C. Chang and G.C. Lee, 6/1/87, (PB88-134259, A03, MF-A01). This report is available only through NTIS (see address given above).
- NCEER-87-0005 "A Finite Element Formulation for Nonlinear Viscoplastic Material Using a Q Model," by O. Gyebe and G. Dasgupta, 11/2/87, (PB88-213764, A08, MF-A01).
- NCEER-87-0006 "Symbolic Manipulation Program (SMP) - Algebraic Codes for Two and Three Dimensional Finite Element Formulations," by X. Lee and G. Dasgupta, 11/9/87, (PB88-218522, A05, MF-A01).
- NCEER-87-0007 "Instantaneous Optimal Control Laws for Tall Buildings Under Seismic Excitations," by J.N. Yang, A. Akbarpour and P. Ghaemmaghami, 6/10/87, (PB88-134333, A06, MF-A01). This report is only available through NTIS (see address given above).
- NCEER-87-0008 "IDARC: Inelastic Damage Analysis of Reinforced Concrete Frame - Shear-Wall Structures," by Y.J. Park, A.M. Reinhorn and S.K. Kunnath, 7/20/87, (PB88-134325, A09, MF-A01). This report is only available through NTIS (see address given above).
- NCEER-87-0009 "Liquefaction Potential for New York State: A Preliminary Report on Sites in Manhattan and Buffalo," by M. Budhu, V. Vijayakumar, R.F. Giese and L. Baumgras, 8/31/87, (PB88-163704, A03, MF-A01). This report is available only through NTIS (see address given above).
- NCEER-87-0010 "Vertical and Torsional Vibration of Foundations in Inhomogeneous Media," by A.S. Veletsos and K.W. Dotson, 6/1/87, (PB88-134291, A03, MF-A01). This report is only available through NTIS (see address given above).
- NCEER-87-0011 "Seismic Probabilistic Risk Assessment and Seismic Margins Studies for Nuclear Power Plants," by Howard H.M. Hwang, 6/15/87, (PB88-134267, A03, MF-A01). This report is only available through NTIS (see address given above).
- NCEER-87-0012 "Parametric Studies of Frequency Response of Secondary Systems Under Ground-Acceleration Excitations," by Y. Yong and Y.K. Lin, 6/10/87, (PB88-134309, A03, MF-A01). This report is only available through NTIS (see address given above).
- NCEER-87-0013 "Frequency Response of Secondary Systems Under Seismic Excitation," by J.A. HoLung, J. Cai and Y.K. Lin, 7/31/87, (PB88-134317, A05, MF-A01). This report is only available through NTIS (see address given above).
- NCEER-87-0014 "Modelling Earthquake Ground Motions in Seismically Active Regions Using Parametric Time Series Methods," by G.W. Ellis and A.S. Cakmak, 8/25/87, (PB88-134283, A08, MF-A01). This report is only available through NTIS (see address given above).
- NCEER-87-0015 "Detection and Assessment of Seismic Structural Damage," by E. DiPasquale and A.S. Cakmak, 8/25/87, (PB88-163712, A05, MF-A01). This report is only available through NTIS (see address given above).

- NCEER-87-0016 "Pipeline Experiment at Parkfield, California," by J. Isenberg and E. Richardson, 9/15/87, (PB88-163720, A03, MF-A01). This report is available only through NTIS (see address given above).
- NCEER-87-0017 "Digital Simulation of Seismic Ground Motion," by M. Shinozuka, G. Deodatis and T. Harada, 8/31/87, (PB88-155197, A04, MF-A01). This report is available only through NTIS (see address given above).
- NCEER-87-0018 "Practical Considerations for Structural Control: System Uncertainty, System Time Delay and Truncation of Small Control Forces," J.N. Yang and A. Akbarpour, 8/10/87, (PB88-163738, A08, MF-A01). This report is only available through NTIS (see address given above).
- NCEER-87-0019 "Modal Analysis of Nonclassically Damped Structural Systems Using Canonical Transformation," by J.N. Yang, S. Sarkani and F.X. Long, 9/27/87, (PB88-187851, A04, MF-A01).
- NCEER-87-0020 "A Nonstationary Solution in Random Vibration Theory," by J.R. Red-Horse and P.D. Spanos, 11/3/87, (PB88-163746, A03, MF-A01).
- NCEER-87-0021 "Horizontal Impedances for Radially Inhomogeneous Viscoelastic Soil Layers," by A.S. Veletsos and K.W. Dotson, 10/15/87, (PB88-150859, A04, MF-A01).
- NCEER-87-0022 "Seismic Damage Assessment of Reinforced Concrete Members," by Y.S. Chung, C. Meyer and M. Shinozuka, 10/9/87, (PB88-150867, A05, MF-A01). This report is available only through NTIS (see address given above).
- NCEER-87-0023 "Active Structural Control in Civil Engineering," by T.T. Soong, 11/11/87, (PB88-187778, A03, MF-A01).
- NCEER-87-0024 "Vertical and Torsional Impedances for Radially Inhomogeneous Viscoelastic Soil Layers," by K.W. Dotson and A.S. Veletsos, 12/87, (PB88-187786, A03, MF-A01).
- NCEER-87-0025 "Proceedings from the Symposium on Seismic Hazards, Ground Motions, Soil-Liquefaction and Engineering Practice in Eastern North America," October 20-22, 1987, edited by K.H. Jacob, 12/87, (PB88-188115, A23, MF-A01). This report is available only through NTIS (see address given above).
- NCEER-87-0026 "Report on the Whittier-Narrows, California, Earthquake of October 1, 1987," by J. Pantelic and A. Reinhorn, 11/87, (PB88-187752, A03, MF-A01). This report is available only through NTIS (see address given above).
- NCEER-87-0027 "Design of a Modular Program for Transient Nonlinear Analysis of Large 3-D Building Structures," by S. Srivastav and J.F. Abel, 12/30/87, (PB88-187950, A05, MF-A01). This report is only available through NTIS (see address given above).
- NCEER-87-0028 "Second-Year Program in Research, Education and Technology Transfer," 3/8/88, (PB88-219480, A04, MF-A01).
- NCEER-88-0001 "Workshop on Seismic Computer Analysis and Design of Buildings With Interactive Graphics," by W. McGuire, J.F. Abel and C.H. Conley, 1/18/88, (PB88-187760, A03, MF-A01). This report is only available through NTIS (see address given above).
- NCEER-88-0002 "Optimal Control of Nonlinear Flexible Structures," by J.N. Yang, F.X. Long and D. Wong, 1/22/88, (PB88-213772, A06, MF-A01).
- NCEER-88-0003 "Substructuring Techniques in the Time Domain for Primary-Secondary Structural Systems," by G.D. Manolis and G. Juhn, 2/10/88, (PB88-213780, A04, MF-A01).
- NCEER-88-0004 "Iterative Seismic Analysis of Primary-Secondary Systems," by A. Singhal, L.D. Lutes and P.D. Spanos, 2/23/88, (PB88-213798, A04, MF-A01).
- NCEER-88-0005 "Stochastic Finite Element Expansion for Random Media," by P.D. Spanos and R. Ghanem, 3/14/88, (PB88-213806, A03, MF-A01).

- NCEER-88-0006 "Combining Structural Optimization and Structural Control," by F.Y. Cheng and C.P. Pantelides, 1/10/88, (PB88-213814, A05, MF-A01).
- NCEER-88-0007 "Seismic Performance Assessment of Code-Designed Structures," by H.H-M. Hwang, J-W. Jaw and H-J. Shau, 3/20/88, (PB88-219423, A04, MF-A01). This report is only available through NTIS (see address given above).
- NCEER-88-0008 "Reliability Analysis of Code-Designed Structures Under Natural Hazards," by H.H-M. Hwang, H. Ushiba and M. Shinozuka, 2/29/88, (PB88-229471, A07, MF-A01). This report is only available through NTIS (see address given above).
- NCEER-88-0009 "Seismic Fragility Analysis of Shear Wall Structures," by J-W Jaw and H.H-M. Hwang, 4/30/88, (PB89-102867, A04, MF-A01).
- NCEER-88-0010 "Base Isolation of a Multi-Story Building Under a Harmonic Ground Motion - A Comparison of Performances of Various Systems," by F-G Fan, G. Ahmadi and I.G. Tadjbakhsh, 5/18/88, (PB89-122238, A06, MF-A01). This report is only available through NTIS (see address given above).
- NCEER-88-0011 "Seismic Floor Response Spectra for a Combined System by Green's Functions," by F.M. Lavelle, L.A. Bergman and P.D. Spanos, 5/1/88, (PB89-102875, A03, MF-A01).
- NCEER-88-0012 "A New Solution Technique for Randomly Excited Hysteretic Structures," by G.Q. Cai and Y.K. Lin, 5/16/88, (PB89-102883, A03, MF-A01).
- NCEER-88-0013 "A Study of Radiation Damping and Soil-Structure Interaction Effects in the Centrifuge," by K. Weissman, supervised by J.H. Prevost, 5/24/88, (PB89-144703, A06, MF-A01).
- NCEER-88-0014 "Parameter Identification and Implementation of a Kinematic Plasticity Model for Frictional Soils," by J.H. Prevost and D.V. Griffiths, to be published.
- NCEER-88-0015 "Two- and Three- Dimensional Dynamic Finite Element Analyses of the Long Valley Dam," by D.V. Griffiths and J.H. Prevost, 6/17/88, (PB89-144711, A04, MF-A01).
- NCEER-88-0016 "Damage Assessment of Reinforced Concrete Structures in Eastern United States," by A.M. Reinhorn, M.J. Seidel, S.K. Kunnath and Y.J. Park, 6/15/88, (PB89-122220, A04, MF-A01). This report is only available through NTIS (see address given above).
- NCEER-88-0017 "Dynamic Compliance of Vertically Loaded Strip Foundations in Multilayered Viscoelastic Soils," by S. Ahmad and A.S.M. Israil, 6/17/88, (PB89-102891, A04, MF-A01).
- NCEER-88-0018 "An Experimental Study of Seismic Structural Response With Added Viscoelastic Dampers," by R.C. Lin, Z. Liang, T.T. Soong and R.H. Zhang, 6/30/88, (PB89-122212, A05, MF-A01). This report is available only through NTIS (see address given above).
- NCEER-88-0019 "Experimental Investigation of Primary - Secondary System Interaction," by G.D. Manolis, G. Juhn and A.M. Reinhorn, 5/27/88, (PB89-122204, A04, MF-A01).
- NCEER-88-0020 "A Response Spectrum Approach For Analysis of Nonclassically Damped Structures," by J.N. Yang, S. Sarkani and F.X. Long, 4/22/88, (PB89-102909, A04, MF-A01).
- NCEER-88-0021 "Seismic Interaction of Structures and Soils: Stochastic Approach," by A.S. Veletsos and A.M. Prasad, 7/21/88, (PB89-122196, A04, MF-A01). This report is only available through NTIS (see address given above).
- NCEER-88-0022 "Identification of the Serviceability Limit State and Detection of Seismic Structural Damage," by E. DiPasquale and A.S. Cakmak, 6/15/88, (PB89-122188, A05, MF-A01). This report is available only through NTIS (see address given above).
- NCEER-88-0023 "Multi-Hazard Risk Analysis: Case of a Simple Offshore Structure," by B.K. Bhartia and E.H. Vanmarcke, 7/21/88, (PB89-145213, A05, MF-A01).

- NCEER-88-0024 "Automated Seismic Design of Reinforced Concrete Buildings," by Y.S. Chung, C. Meyer and M. Shinozuka, 7/5/88, (PB89-122170, A06, MF-A01). This report is available only through NTIS (see address given above).
- NCEER-88-0025 "Experimental Study of Active Control of MDOF Structures Under Seismic Excitations," by L.L. Chung, R.C. Lin, T.T. Soong and A.M. Reinhorn, 7/10/88, (PB89-122600, A04, MF-A01).
- NCEER-88-0026 "Earthquake Simulation Tests of a Low-Rise Metal Structure," by J.S. Hwang, K.C. Chang, G.C. Lee and R.L. Ketter, 8/1/88, (PB89-102917, A04, MF-A01).
- NCEER-88-0027 "Systems Study of Urban Response and Reconstruction Due to Catastrophic Earthquakes," by F. Kozin and H.K. Zhou, 9/22/88, (PB90-162348, A04, MF-A01).
- NCEER-88-0028 "Seismic Fragility Analysis of Plane Frame Structures," by H.H-M. Hwang and Y.K. Low, 7/31/88, (PB89-131445, A06, MF-A01).
- NCEER-88-0029 "Response Analysis of Stochastic Structures," by A. Kardara, C. Bucher and M. Shinozuka, 9/22/88, (PB89-174429, A04, MF-A01).
- NCEER-88-0030 "Nonnormal Accelerations Due to Yielding in a Primary Structure," by D.C.K. Chen and L.D. Lutes, 9/19/88, (PB89-131437, A04, MF-A01).
- NCEER-88-0031 "Design Approaches for Soil-Structure Interaction," by A.S. Veletsos, A.M. Prasad and Y. Tang, 12/30/88, (PB89-174437, A03, MF-A01). This report is available only through NTIS (see address given above).
- NCEER-88-0032 "A Re-evaluation of Design Spectra for Seismic Damage Control," by C.J. Turkstra and A.G. Tallin, 11/7/88, (PB89-145221, A05, MF-A01).
- NCEER-88-0033 "The Behavior and Design of Noncontact Lap Splices Subjected to Repeated Inelastic Tensile Loading," by V.E. Sagan, P. Gergely and R.N. White, 12/8/88, (PB89-163737, A08, MF-A01).
- NCEER-88-0034 "Seismic Response of Pile Foundations," by S.M. Mamoon, P.K. Banerjee and S. Ahmad, 11/1/88, (PB89-145239, A04, MF-A01).
- NCEER-88-0035 "Modeling of R/C Building Structures With Flexible Floor Diaphragms (IDARC2)," by A.M. Reinhorn, S.K. Kunnath and N. Panahshahi, 9/7/88, (PB89-207153, A07, MF-A01).
- NCEER-88-0036 "Solution of the Dam-Reservoir Interaction Problem Using a Combination of FEM, BEM with Particular Integrals, Modal Analysis, and Substructuring," by C-S. Tsai, G.C. Lee and R.L. Ketter, 12/31/88, (PB89-207146, A04, MF-A01).
- NCEER-88-0037 "Optimal Placement of Actuators for Structural Control," by F.Y. Cheng and C.P. Pantelides, 8/15/88, (PB89-162846, A05, MF-A01).
- NCEER-88-0038 "Teflon Bearings in Aseismic Base Isolation: Experimental Studies and Mathematical Modeling," by A. Mokha, M.C. Constantinou and A.M. Reinhorn, 12/5/88, (PB89-218457, A10, MF-A01). This report is available only through NTIS (see address given above).
- NCEER-88-0039 "Seismic Behavior of Flat Slab High-Rise Buildings in the New York City Area," by P. Weidlinger and M. Ettouney, 10/15/88, (PB90-145681, A04, MF-A01).
- NCEER-88-0040 "Evaluation of the Earthquake Resistance of Existing Buildings in New York City," by P. Weidlinger and M. Ettouney, 10/15/88, to be published.
- NCEER-88-0041 "Small-Scale Modeling Techniques for Reinforced Concrete Structures Subjected to Seismic Loads," by W. Kim, A. El-Attar and R.N. White, 11/22/88, (PB89-189625, A05, MF-A01).
- NCEER-88-0042 "Modeling Strong Ground Motion from Multiple Event Earthquakes," by G.W. Ellis and A.S. Cakmak, 10/15/88, (PB89-174445, A03, MF-A01).

- NCEER-88-0043 "Nonstationary Models of Seismic Ground Acceleration," by M. Grigoriu, S.E. Ruiz and E. Rosenblueth, 7/15/88, (PB89-189617, A04, MF-A01).
- NCEER-88-0044 "SARCF User's Guide: Seismic Analysis of Reinforced Concrete Frames," by Y.S. Chung, C. Meyer and M. Shinozuka, 11/9/88, (PB89-174452, A08, MF-A01).
- NCEER-88-0045 "First Expert Panel Meeting on Disaster Research and Planning," edited by J. Pantelic and J. Stoyke, 9/15/88, (PB89-174460, A05, MF-A01).
- NCEER-88-0046 "Preliminary Studies of the Effect of Degrading Infill Walls on the Nonlinear Seismic Response of Steel Frames," by C.Z. Chrysostomou, P. Gergely and J.F. Abel, 12/19/88, (PB89-208383, A05, MF-A01).
- NCEER-88-0047 "Reinforced Concrete Frame Component Testing Facility - Design, Construction, Instrumentation and Operation," by S.P. Pessiki, C. Conley, T. Bond, P. Gergely and R.N. White, 12/16/88, (PB89-174478, A04, MF-A01).
- NCEER-89-0001 "Effects of Protective Cushion and Soil Compliancy on the Response of Equipment Within a Seismically Excited Building," by J.A. HoLung, 2/16/89, (PB89-207179, A04, MF-A01).
- NCEER-89-0002 "Statistical Evaluation of Response Modification Factors for Reinforced Concrete Structures," by H.H-M. Hwang and J-W. Jaw, 2/17/89, (PB89-207187, A05, MF-A01).
- NCEER-89-0003 "Hysteretic Columns Under Random Excitation," by G-Q. Cai and Y.K. Lin, 1/9/89, (PB89-196513, A03, MF-A01).
- NCEER-89-0004 "Experimental Study of 'Elephant Foot Bulge' Instability of Thin-Walled Metal Tanks," by Z-H. Jia and R.L. Ketter, 2/22/89, (PB89-207195, A03, MF-A01).
- NCEER-89-0005 "Experiment on Performance of Buried Pipelines Across San Andreas Fault," by J. Isenberg, E. Richardson and T.D. O'Rourke, 3/10/89, (PB89-218440, A04, MF-A01). This report is available only through NTIS (see address given above).
- NCEER-89-0006 "A Knowledge-Based Approach to Structural Design of Earthquake-Resistant Buildings," by M. Subramani, P. Gergely, C.H. Conley, J.F. Abel and A.H. Zaghaw, 1/15/89, (PB89-218465, A06, MF-A01).
- NCEER-89-0007 "Liquefaction Hazards and Their Effects on Buried Pipelines," by T.D. O'Rourke and P.A. Lane, 2/1/89, (PB89-218481, A09, MF-A01).
- NCEER-89-0008 "Fundamentals of System Identification in Structural Dynamics," by H. Imai, C-B. Yun, O. Maruyama and M. Shinozuka, 1/26/89, (PB89-207211, A04, MF-A01).
- NCEER-89-0009 "Effects of the 1985 Michoacan Earthquake on Water Systems and Other Buried Lifelines in Mexico," by A.G. Ayala and M.J. O'Rourke, 3/8/89, (PB89-207229, A06, MF-A01).
- NCEER-89-R010 "NCEER Bibliography of Earthquake Education Materials," by K.E.K. Ross, Second Revision, 9/1/89, (PB90-125352, A05, MF-A01). This report is replaced by NCEER-92-0018.
- NCEER-89-0011 "Inelastic Three-Dimensional Response Analysis of Reinforced Concrete Building Structures (IDARC-3D), Part I - Modeling," by S.K. Kunnath and A.M. Reinhorn, 4/17/89, (PB90-114612, A07, MF-A01). This report is available only through NTIS (see address given above).
- NCEER-89-0012 "Recommended Modifications to ATC-14," by C.D. Poland and J.O. Malley, 4/12/89, (PB90-108648, A15, MF-A01).
- NCEER-89-0013 "Repair and Strengthening of Beam-to-Column Connections Subjected to Earthquake Loading," by M. Corazao and A.J. Durrani, 2/28/89, (PB90-109885, A06, MF-A01).
- NCEER-89-0014 "Program EXKAL2 for Identification of Structural Dynamic Systems," by O. Maruyama, C-B. Yun, M. Hoshiya and M. Shinozuka, 5/19/89, (PB90-109877, A09, MF-A01).

- NCEER-89-0015 "Response of Frames With Bolted Semi-Rigid Connections, Part I - Experimental Study and Analytical Predictions," by P.J. DiCorso, A.M. Reinhorn, J.R. Dickerson, J.B. Radzinski and W.L. Harper, 6/1/89, to be published.
- NCEER-89-0016 "ARMA Monte Carlo Simulation in Probabilistic Structural Analysis," by P.D. Spanos and M.P. Mignolet, 7/10/89, (PB90-109893, A03, MF-A01).
- NCEER-89-P017 "Preliminary Proceedings from the Conference on Disaster Preparedness - The Place of Earthquake Education in Our Schools," Edited by K.E.K. Ross, 6/23/89, (PB90-108606, A03, MF-A01).
- NCEER-89-0017 "Proceedings from the Conference on Disaster Preparedness - The Place of Earthquake Education in Our Schools," Edited by K.E.K. Ross, 12/31/89, (PB90-207895, A012, MF-A02). This report is available only through NTIS (see address given above).
- NCEER-89-0018 "Multidimensional Models of Hysteretic Material Behavior for Vibration Analysis of Shape Memory Energy Absorbing Devices, by E.J. Graesser and F.A. Cozzarelli, 6/7/89, (PB90-164146, A04, MF-A01).
- NCEER-89-0019 "Nonlinear Dynamic Analysis of Three-Dimensional Base Isolated Structures (3D-BASIS)," by S. Nagarajaiah, A.M. Reinhorn and M.C. Constantinou, 8/3/89, (PB90-161936, A06, MF-A01). This report has been replaced by NCEER-93-0011.
- NCEER-89-0020 "Structural Control Considering Time-Rate of Control Forces and Control Rate Constraints," by F.Y. Cheng and C.P. Pantelides, 8/3/89, (PB90-120445, A04, MF-A01).
- NCEER-89-0021 "Subsurface Conditions of Memphis and Shelby County," by K.W. Ng, T-S. Chang and H-H.M. Hwang, 7/26/89, (PB90-120437, A03, MF-A01).
- NCEER-89-0022 "Seismic Wave Propagation Effects on Straight Jointed Buried Pipelines," by K. Elhmadi and M.J. O'Rourke, 8/24/89, (PB90-162322, A10, MF-A02).
- NCEER-89-0023 "Workshop on Serviceability Analysis of Water Delivery Systems," edited by M. Grigoriu, 3/6/89, (PB90-127424, A03, MF-A01).
- NCEER-89-0024 "Shaking Table Study of a 1/5 Scale Steel Frame Composed of Tapered Members," by K.C. Chang, J.S. Hwang and G.C. Lee, 9/18/89, (PB90-160169, A04, MF-A01).
- NCEER-89-0025 "DYNA1D: A Computer Program for Nonlinear Seismic Site Response Analysis - Technical Documentation," by Jean H. Prevost, 9/14/89, (PB90-161944, A07, MF-A01). This report is available only through NTIS (see address given above).
- NCEER-89-0026 "1:4 Scale Model Studies of Active Tendon Systems and Active Mass Dampers for Aseismic Protection," by A.M. Reinhorn, T.T. Soong, R.C. Lin, Y.P. Yang, Y. Fukao, H. Abe and M. Nakai, 9/15/89, (PB90-173246, A10, MF-A02). This report is available only through NTIS (see address given above).
- NCEER-89-0027 "Scattering of Waves by Inclusions in a Nonhomogeneous Elastic Half Space Solved by Boundary Element Methods," by P.K. Hadley, A. Askar and A.S. Cakmak, 6/15/89, (PB90-145699, A07, MF-A01).
- NCEER-89-0028 "Statistical Evaluation of Deflection Amplification Factors for Reinforced Concrete Structures," by H.H.M. Hwang, J-W. Jaw and A.L. Ch'ng, 8/31/89, (PB90-164633, A05, MF-A01).
- NCEER-89-0029 "Bedrock Accelerations in Memphis Area Due to Large New Madrid Earthquakes," by H.H.M. Hwang, C.H.S. Chen and G. Yu, 11/7/89, (PB90-162330, A04, MF-A01).
- NCEER-89-0030 "Seismic Behavior and Response Sensitivity of Secondary Structural Systems," by Y.Q. Chen and T.T. Soong, 10/23/89, (PB90-164658, A08, MF-A01).
- NCEER-89-0031 "Random Vibration and Reliability Analysis of Primary-Secondary Structural Systems," by Y. Ibrahim, M. Grigoriu and T.T. Soong, 11/10/89, (PB90-161951, A04, MF-A01).

- NCEER-89-0032 "Proceedings from the Second U.S. - Japan Workshop on Liquefaction, Large Ground Deformation and Their Effects on Lifelines, September 26-29, 1989," Edited by T.D. O'Rourke and M. Hamada, 12/1/89, (PB90-209388, A22, MF-A03).
- NCEER-89-0033 "Deterministic Model for Seismic Damage Evaluation of Reinforced Concrete Structures," by J.M. Bracci, A.M. Reinhorn, J.B. Mander and S.K. Kunnath, 9/27/89, (PB91-108803, A06, MF-A01).
- NCEER-89-0034 "On the Relation Between Local and Global Damage Indices," by E. DiPasquale and A.S. Cakmak, 8/15/89, (PB90-173865, A05, MF-A01).
- NCEER-89-0035 "Cyclic Undrained Behavior of Nonplastic and Low Plasticity Silts," by A.J. Walker and H.E. Stewart, 7/26/89, (PB90-183518, A10, MF-A01).
- NCEER-89-0036 "Liquefaction Potential of Surficial Deposits in the City of Buffalo, New York," by M. Budhu, R. Giese and L. Baumgrass, 1/17/89, (PB90-208455, A04, MF-A01).
- NCEER-89-0037 "A Deterministic Assessment of Effects of Ground Motion Incoherence," by A.S. Veletsos and Y. Tang, 7/15/89, (PB90-164294, A03, MF-A01).
- NCEER-89-0038 "Workshop on Ground Motion Parameters for Seismic Hazard Mapping," July 17-18, 1989, edited by R.V. Whitman, 12/1/89, (PB90-173923, A04, MF-A01).
- NCEER-89-0039 "Seismic Effects on Elevated Transit Lines of the New York City Transit Authority," by C.J. Costantino, C.A. Miller and E. Heymsfield, 12/26/89, (PB90-207887, A06, MF-A01).
- NCEER-89-0040 "Centrifugal Modeling of Dynamic Soil-Structure Interaction," by K. Weissman, Supervised by J.H. Prevost, 5/10/89, (PB90-207879, A07, MF-A01).
- NCEER-89-0041 "Linearized Identification of Buildings With Cores for Seismic Vulnerability Assessment," by I-K. Ho and A.E. Aktan, 11/1/89, (PB90-251943, A07, MF-A01).
- NCEER-90-0001 "Geotechnical and Lifeline Aspects of the October 17, 1989 Loma Prieta Earthquake in San Francisco," by T.D. O'Rourke, H.E. Stewart, F.T. Blackburn and T.S. Dickerman, 1/90, (PB90-208596, A05, MF-A01).
- NCEER-90-0002 "Nonnormal Secondary Response Due to Yielding in a Primary Structure," by D.C.K. Chen and L.D. Lutes, 2/28/90, (PB90-251976, A07, MF-A01).
- NCEER-90-0003 "Earthquake Education Materials for Grades K-12," by K.E.K. Ross, 4/16/90, (PB91-251984, A05, MF-A05). This report has been replaced by NCEER-92-0018.
- NCEER-90-0004 "Catalog of Strong Motion Stations in Eastern North America," by R.W. Busby, 4/3/90, (PB90-251984, A05, MF-A01).
- NCEER-90-0005 "NCEER Strong-Motion Data Base: A User Manual for the GeoBase Release (Version 1.0 for the Sun3)," by P. Friberg and K. Jacob, 3/31/90 (PB90-258062, A04, MF-A01).
- NCEER-90-0006 "Seismic Hazard Along a Crude Oil Pipeline in the Event of an 1811-1812 Type New Madrid Earthquake," by H.H.M. Hwang and C-H.S. Chen, 4/16/90, (PB90-258054, A04, MF-A01).
- NCEER-90-0007 "Site-Specific Response Spectra for Memphis Sheahan Pumping Station," by H.H.M. Hwang and C.S. Lee, 5/15/90, (PB91-108811, A05, MF-A01).
- NCEER-90-0008 "Pilot Study on Seismic Vulnerability of Crude Oil Transmission Systems," by T. Ariman, R. Dobry, M. Grigoriu, F. Kozin, M. O'Rourke, T. O'Rourke and M. Shinozuka, 5/25/90, (PB91-108837, A06, MF-A01).
- NCEER-90-0009 "A Program to Generate Site Dependent Time Histories: EQGEN," by G.W. Ellis, M. Srinivasan and A.S. Cakmak, 1/30/90, (PB91-108829, A04, MF-A01).
- NCEER-90-0010 "Active Isolation for Seismic Protection of Operating Rooms," by M.E. Talbott, Supervised by M. Shinozuka, 6/8/9, (PB91-110205, A05, MF-A01).

- NCEER-90-0011 "Program LINEARID for Identification of Linear Structural Dynamic Systems," by C-B. Yun and M. Shinozuka, 6/25/90, (PB91-110312, A08, MF-A01).
- NCEER-90-0012 "Two-Dimensional Two-Phase Elasto-Plastic Seismic Response of Earth Dams," by A.N. Yiagos, Supervised by J.H. Prevost, 6/20/90, (PB91-110197, A13, MF-A02).
- NCEER-90-0013 "Secondary Systems in Base-Isolated Structures: Experimental Investigation, Stochastic Response and Stochastic Sensitivity," by G.D. Manolis, G. Juhn, M.C. Constantinou and A.M. Reinhorn, 7/1/90, (PB91-110320, A08, MF-A01).
- NCEER-90-0014 "Seismic Behavior of Lightly-Reinforced Concrete Column and Beam-Column Joint Details," by S.P. Pessiki, C.H. Conley, P. Gergely and R.N. White, 8/22/90, (PB91-108795, A11, MF-A02).
- NCEER-90-0015 "Two Hybrid Control Systems for Building Structures Under Strong Earthquakes," by J.N. Yang and A. Daniellians, 6/29/90, (PB91-125393, A04, MF-A01).
- NCEER-90-0016 "Instantaneous Optimal Control with Acceleration and Velocity Feedback," by J.N. Yang and Z. Li, 6/29/90, (PB91-125401, A03, MF-A01).
- NCEER-90-0017 "Reconnaissance Report on the Northern Iran Earthquake of June 21, 1990," by M. Mehrain, 10/4/90, (PB91-125377, A03, MF-A01).
- NCEER-90-0018 "Evaluation of Liquefaction Potential in Memphis and Shelby County," by T.S. Chang, P.S. Tang, C.S. Lee and H. Hwang, 8/10/90, (PB91-125427, A09, MF-A01).
- NCEER-90-0019 "Experimental and Analytical Study of a Combined Sliding Disc Bearing and Helical Steel Spring Isolation System," by M.C. Constantinou, A.S. Mokha and A.M. Reinhorn, 10/4/90, (PB91-125385, A06, MF-A01). This report is available only through NTIS (see address given above).
- NCEER-90-0020 "Experimental Study and Analytical Prediction of Earthquake Response of a Sliding Isolation System with a Spherical Surface," by A.S. Mokha, M.C. Constantinou and A.M. Reinhorn, 10/11/90, (PB91-125419, A05, MF-A01).
- NCEER-90-0021 "Dynamic Interaction Factors for Floating Pile Groups," by G. Gazetas, K. Fan, A. Kaynia and E. Kausel, 9/10/90, (PB91-170381, A05, MF-A01).
- NCEER-90-0022 "Evaluation of Seismic Damage Indices for Reinforced Concrete Structures," by S. Rodriguez-Gomez and A.S. Cakmak, 9/30/90, PB91-171322, A06, MF-A01).
- NCEER-90-0023 "Study of Site Response at a Selected Memphis Site," by H. Desai, S. Ahmad, E.S. Gazetas and M.R. Oh, 10/11/90, (PB91-196857, A03, MF-A01).
- NCEER-90-0024 "A User's Guide to Strongmo: Version 1.0 of NCEER's Strong-Motion Data Access Tool for PCs and Terminals," by P.A. Friberg and C.A.T. Susch, 11/15/90, (PB91-171272, A03, MF-A01).
- NCEER-90-0025 "A Three-Dimensional Analytical Study of Spatial Variability of Seismic Ground Motions," by L-L. Hong and A.H.-S. Ang, 10/30/90, (PB91-170399, A09, MF-A01).
- NCEER-90-0026 "MUMOID User's Guide - A Program for the Identification of Modal Parameters," by S. Rodriguez-Gomez and E. DiPasquale, 9/30/90, (PB91-171298, A04, MF-A01).
- NCEER-90-0027 "SARCF-II User's Guide - Seismic Analysis of Reinforced Concrete Frames," by S. Rodriguez-Gomez, Y.S. Chung and C. Meyer, 9/30/90, (PB91-171280, A05, MF-A01).
- NCEER-90-0028 "Viscous Dampers: Testing, Modeling and Application in Vibration and Seismic Isolation," by N. Makris and M.C. Constantinou, 12/20/90 (PB91-190561, A06, MF-A01).
- NCEER-90-0029 "Soil Effects on Earthquake Ground Motions in the Memphis Area," by H. Hwang, C.S. Lee, K.W. Ng and T.S. Chang, 8/2/90, (PB91-190751, A05, MF-A01).

- NCEER-91-0001 "Proceedings from the Third Japan-U.S. Workshop on Earthquake Resistant Design of Lifeline Facilities and Countermeasures for Soil Liquefaction, December 17-19, 1990," edited by T.D. O'Rourke and M. Hamada, 2/1/91, (PB91-179259, A99, MF-A04).
- NCEER-91-0002 "Physical Space Solutions of Non-Proportionally Damped Systems," by M. Tong, Z. Liang and G.C. Lee, 1/15/91, (PB91-179242, A04, MF-A01).
- NCEER-91-0003 "Seismic Response of Single Piles and Pile Groups," by K. Fan and G. Gazetas, 1/10/91, (PB92-174994, A04, MF-A01).
- NCEER-91-0004 "Damping of Structures: Part 1 - Theory of Complex Damping," by Z. Liang and G. Lee, 10/10/91, (PB92-197235, A12, MF-A03).
- NCEER-91-0005 "3D-BASIS - Nonlinear Dynamic Analysis of Three Dimensional Base Isolated Structures: Part II," by S. Nagarajaiah, A.M. Reinhorn and M.C. Constantinou, 2/28/91, (PB91-190553, A07, MF-A01). This report has been replaced by NCEER-93-0011.
- NCEER-91-0006 "A Multidimensional Hysteretic Model for Plasticity Deforming Metals in Energy Absorbing Devices," by E.J. Graesser and F.A. Cozzarelli, 4/9/91, (PB92-108364, A04, MF-A01).
- NCEER-91-0007 "A Framework for Customizable Knowledge-Based Expert Systems with an Application to a KBES for Evaluating the Seismic Resistance of Existing Buildings," by E.G. Ibarra-Anaya and S.J. Fennes, 4/9/91, (PB91-210930, A08, MF-A01).
- NCEER-91-0008 "Nonlinear Analysis of Steel Frames with Semi-Rigid Connections Using the Capacity Spectrum Method," by G.G. Deierlein, S-H. Hsieh, Y-J. Shen and J.F. Abel, 7/2/91, (PB92-113828, A05, MF-A01).
- NCEER-91-0009 "Earthquake Education Materials for Grades K-12," by K.E.K. Ross, 4/30/91, (PB91-212142, A06, MF-A01). This report has been replaced by NCEER-92-0018.
- NCEER-91-0010 "Phase Wave Velocities and Displacement Phase Differences in a Harmonically Oscillating Pile," by N. Makris and G. Gazetas, 7/8/91, (PB92-108356, A04, MF-A01).
- NCEER-91-0011 "Dynamic Characteristics of a Full-Size Five-Story Steel Structure and a 2/5 Scale Model," by K.C. Chang, G.C. Yao, G.C. Lee, D.S. Hao and Y.C. Yeh," 7/2/91, (PB93-116648, A06, MF-A02).
- NCEER-91-0012 "Seismic Response of a 2/5 Scale Steel Structure with Added Viscoelastic Dampers," by K.C. Chang, T.T. Soong, S-T. Oh and M.L. Lai, 5/17/91, (PB92-110816, A05, MF-A01).
- NCEER-91-0013 "Earthquake Response of Retaining Walls; Full-Scale Testing and Computational Modeling," by S. Alampalli and A-W.M. Elgamal, 6/20/91, to be published.
- NCEER-91-0014 "3D-BASIS-M: Nonlinear Dynamic Analysis of Multiple Building Base Isolated Structures," by P.C. Tsopelas, S. Nagarajaiah, M.C. Constantinou and A.M. Reinhorn, 5/28/91, (PB92-113885, A09, MF-A02).
- NCEER-91-0015 "Evaluation of SEAOC Design Requirements for Sliding Isolated Structures," by D. Theodossiou and M.C. Constantinou, 6/10/91, (PB92-114602, A11, MF-A03).
- NCEER-91-0016 "Closed-Loop Modal Testing of a 27-Story Reinforced Concrete Flat Plate-Core Building," by H.R. Somaprasad, T. Toksoy, H. Yoshiyuki and A.E. Aktan, 7/15/91, (PB92-129980, A07, MF-A02).
- NCEER-91-0017 "Shake Table Test of a 1/6 Scale Two-Story Lightly Reinforced Concrete Building," by A.G. El-Attar, R.N. White and P. Gergely, 2/28/91, (PB92-222447, A06, MF-A02).
- NCEER-91-0018 "Shake Table Test of a 1/8 Scale Three-Story Lightly Reinforced Concrete Building," by A.G. El-Attar, R.N. White and P. Gergely, 2/28/91, (PB93-116630, A08, MF-A02).
- NCEER-91-0019 "Transfer Functions for Rigid Rectangular Foundations," by A.S. Veletsos, A.M. Prasad and W.H. Wu, 7/31/91, to be published.

- NCEER-91-0020 "Hybrid Control of Seismic-Excited Nonlinear and Inelastic Structural Systems," by J.N. Yang, Z. Li and A. Daniellians, 8/1/91, (PB92-143171, A06, MF-A02).
- NCEER-91-0021 "The NCEER-91 Earthquake Catalog: Improved Intensity-Based Magnitudes and Recurrence Relations for U.S. Earthquakes East of New Madrid," by L. Seeber and J.G. Armbruster, 8/28/91, (PB92-176742, A06, MF-A02).
- NCEER-91-0022 "Proceedings from the Implementation of Earthquake Planning and Education in Schools: The Need for Change - The Roles of the Changemakers," by K.E.K. Ross and F. Winslow, 7/23/91, (PB92-129998, A12, MF-A03).
- NCEER-91-0023 "A Study of Reliability-Based Criteria for Seismic Design of Reinforced Concrete Frame Buildings," by H.H.M. Hwang and H-M. Hsu, 8/10/91, (PB92-140235, A09, MF-A02).
- NCEER-91-0024 "Experimental Verification of a Number of Structural System Identification Algorithms," by R.G. Ghanem, H. Gavin and M. Shinozuka, 9/18/91, (PB92-176577, A18, MF-A04).
- NCEER-91-0025 "Probabilistic Evaluation of Liquefaction Potential," by H.H.M. Hwang and C.S. Lee," 11/25/91, (PB92-143429, A05, MF-A01).
- NCEER-91-0026 "Instantaneous Optimal Control for Linear, Nonlinear and Hysteretic Structures - Stable Controllers," by J.N. Yang and Z. Li, 11/15/91, (PB92-163807, A04, MF-A01).
- NCEER-91-0027 "Experimental and Theoretical Study of a Sliding Isolation System for Bridges," by M.C. Constantinou, A. Kartoum, A.M. Reinhorn and P. Bradford, 11/15/91, (PB92-176973, A10, MF-A03).
- NCEER-92-0001 "Case Studies of Liquefaction and Lifeline Performance During Past Earthquakes, Volume 1: Japanese Case Studies," Edited by M. Hamada and T. O'Rourke, 2/17/92, (PB92-197243, A18, MF-A04).
- NCEER-92-0002 "Case Studies of Liquefaction and Lifeline Performance During Past Earthquakes, Volume 2: United States Case Studies," Edited by T. O'Rourke and M. Hamada, 2/17/92, (PB92-197250, A20, MF-A04).
- NCEER-92-0003 "Issues in Earthquake Education," Edited by K. Ross, 2/3/92, (PB92-222389, A07, MF-A02).
- NCEER-92-0004 "Proceedings from the First U.S. - Japan Workshop on Earthquake Protective Systems for Bridges," Edited by I.G. Buckle, 2/4/92, (PB94-142239, A99, MF-A06).
- NCEER-92-0005 "Seismic Ground Motion from a Haskell-Type Source in a Multiple-Layered Half-Space," A.P. Theoharis, G. Deodatis and M. Shinozuka, 1/2/92, to be published.
- NCEER-92-0006 "Proceedings from the Site Effects Workshop," Edited by R. Whitman, 2/29/92, (PB92-197201, A04, MF-A01).
- NCEER-92-0007 "Engineering Evaluation of Permanent Ground Deformations Due to Seismically-Induced Liquefaction," by M.H. Baziar, R. Dobry and A-W.M. Elgamal, 3/24/92, (PB92-222421, A13, MF-A03).
- NCEER-92-0008 "A Procedure for the Seismic Evaluation of Buildings in the Central and Eastern United States," by C.D. Poland and J.O. Malley, 4/2/92, (PB92-222439, A20, MF-A04).
- NCEER-92-0009 "Experimental and Analytical Study of a Hybrid Isolation System Using Friction Controllable Sliding Bearings," by M.Q. Feng, S. Fujii and M. Shinozuka, 5/15/92, (PB93-150282, A06, MF-A02).
- NCEER-92-0010 "Seismic Resistance of Slab-Column Connections in Existing Non-Ductile Flat-Plate Buildings," by A.J. Durrani and Y. Du, 5/18/92, (PB93-116812, A06, MF-A02).
- NCEER-92-0011 "The Hysteretic and Dynamic Behavior of Brick Masonry Walls Upgraded by Ferrocement Coatings Under Cyclic Loading and Strong Simulated Ground Motion," by H. Lee and S.P. Prawl, 5/11/92, to be published.
- NCEER-92-0012 "Study of Wire Rope Systems for Seismic Protection of Equipment in Buildings," by G.F. Demetriades, M.C. Constantinou and A.M. Reinhorn, 5/20/92, (PB93-116655, A08, MF-A02).

- NCEER-92-0013 "Shape Memory Structural Dampers: Material Properties, Design and Seismic Testing," by P.R. Witting and F.A. Cozzarelli, 5/26/92, (PB93-116663, A05, MF-A01).
- NCEER-92-0014 "Longitudinal Permanent Ground Deformation Effects on Buried Continuous Pipelines," by M.J. O'Rourke, and C. Nordberg, 6/15/92, (PB93-116671, A08, MF-A02).
- NCEER-92-0015 "A Simulation Method for Stationary Gaussian Random Functions Based on the Sampling Theorem," by M. Grigoriu and S. Balopoulou, 6/11/92, (PB93-127496, A05, MF-A01).
- NCEER-92-0016 "Gravity-Load-Designed Reinforced Concrete Buildings: Seismic Evaluation of Existing Construction and Detailing Strategies for Improved Seismic Resistance," by G.W. Hoffmann, S.K. Kunnath, A.M. Reinhorn and J.B. Mander, 7/15/92, (PB94-142007, A08, MF-A02).
- NCEER-92-0017 "Observations on Water System and Pipeline Performance in the Limón Area of Costa Rica Due to the April 22, 1991 Earthquake," by M. O'Rourke and D. Ballantyne, 6/30/92, (PB93-126811, A06, MF-A02).
- NCEER-92-0018 "Fourth Edition of Earthquake Education Materials for Grades K-12," Edited by K.E.K. Ross, 8/10/92, (PB93-114023, A07, MF-A02).
- NCEER-92-0019 "Proceedings from the Fourth Japan-U.S. Workshop on Earthquake Resistant Design of Lifeline Facilities and Countermeasures for Soil Liquefaction," Edited by M. Hamada and T.D. O'Rourke, 8/12/92, (PB93-163939, A99, MF-E11).
- NCEER-92-0020 "Active Bracing System: A Full Scale Implementation of Active Control," by A.M. Reinhorn, T.T. Soong, R.C. Lin, M.A. Riley, Y.P. Wang, S. Aizawa and M. Higashino, 8/14/92, (PB93-127512, A06, MF-A02).
- NCEER-92-0021 "Empirical Analysis of Horizontal Ground Displacement Generated by Liquefaction-Induced Lateral Spreads," by S.F. Bartlett and T.L. Youd, 8/17/92, (PB93-188241, A06, MF-A02).
- NCEER-92-0022 "IDARC Version 3.0: Inelastic Damage Analysis of Reinforced Concrete Structures," by S.K. Kunnath, A.M. Reinhorn and R.F. Lobo, 8/31/92, (PB93-227502, A07, MF-A02).
- NCEER-92-0023 "A Semi-Empirical Analysis of Strong-Motion Peaks in Terms of Seismic Source, Propagation Path and Local Site Conditions, by M. Kamiyama, M.J. O'Rourke and R. Flores-Berrones, 9/9/92, (PB93-150266, A08, MF-A02).
- NCEER-92-0024 "Seismic Behavior of Reinforced Concrete Frame Structures with Nonductile Details, Part I: Summary of Experimental Findings of Full Scale Beam-Column Joint Tests," by A. Beres, R.N. White and P. Gergely, 9/30/92, (PB93-227783, A05, MF-A01).
- NCEER-92-0025 "Experimental Results of Repaired and Retrofitted Beam-Column Joint Tests in Lightly Reinforced Concrete Frame Buildings," by A. Beres, S. El-Borgi, R.N. White and P. Gergely, 10/29/92, (PB93-227791, A05, MF-A01).
- NCEER-92-0026 "A Generalization of Optimal Control Theory: Linear and Nonlinear Structures," by J.N. Yang, Z. Li and S. Vongchavalitkul, 11/2/92, (PB93-188621, A05, MF-A01).
- NCEER-92-0027 "Seismic Resistance of Reinforced Concrete Frame Structures Designed Only for Gravity Loads: Part I - Design and Properties of a One-Third Scale Model Structure," by J.M. Bracci, A.M. Reinhorn and J.B. Mander, 12/1/92, (PB94-104502, A08, MF-A02).
- NCEER-92-0028 "Seismic Resistance of Reinforced Concrete Frame Structures Designed Only for Gravity Loads: Part II - Experimental Performance of Subassemblages," by L.E. Aycaardi, J.B. Mander and A.M. Reinhorn, 12/1/92, (PB94-104510, A08, MF-A02).
- NCEER-92-0029 "Seismic Resistance of Reinforced Concrete Frame Structures Designed Only for Gravity Loads: Part III - Experimental Performance and Analytical Study of a Structural Model," by J.M. Bracci, A.M. Reinhorn and J.B. Mander, 12/1/92, (PB93-227528, A09, MF-A01).

- NCEER-92-0030 "Evaluation of Seismic Retrofit of Reinforced Concrete Frame Structures: Part I - Experimental Performance of Retrofitted Subassemblages," by D. Choudhuri, J.B. Mander and A.M. Reinhorn, 12/8/92, (PB93-198307, A07, MF-A02).
- NCEER-92-0031 "Evaluation of Seismic Retrofit of Reinforced Concrete Frame Structures: Part II - Experimental Performance and Analytical Study of a Retrofitted Structural Model," by J.M. Bracci, A.M. Reinhorn and J.B. Mander, 12/8/92, (PB93-198315, A09, MF-A03).
- NCEER-92-0032 "Experimental and Analytical Investigation of Seismic Response of Structures with Supplemental Fluid Viscous Dampers," by M.C. Constantinou and M.D. Symans, 12/21/92, (PB93-191435, A10, MF-A03). This report is available only through NTIS (see address given above).
- NCEER-92-0033 "Reconnaissance Report on the Cairo, Egypt Earthquake of October 12, 1992," by M. Khater, 12/23/92, (PB93-188621, A03, MF-A01).
- NCEER-92-0034 "Low-Level Dynamic Characteristics of Four Tall Flat-Plate Buildings in New York City," by H. Gavin, S. Yuan, J. Grossman, E. Pekelis and K. Jacob, 12/28/92, (PB93-188217, A07, MF-A02).
- NCEER-93-0001 "An Experimental Study on the Seismic Performance of Brick-Infilled Steel Frames With and Without Retrofit," by J.B. Mander, B. Nair, K. Wojtkowski and J. Ma, 1/29/93, (PB93-227510, A07, MF-A02).
- NCEER-93-0002 "Social Accounting for Disaster Preparedness and Recovery Planning," by S. Cole, E. Pantoja and V. Razak, 2/22/93, (PB94-142114, A12, MF-A03).
- NCEER-93-0003 "Assessment of 1991 NEHRP Provisions for Nonstructural Components and Recommended Revisions," by T.T. Soong, G. Chen, Z. Wu, R-H. Zhang and M. Grigoriu, 3/1/93, (PB93-188639, A06, MF-A02).
- NCEER-93-0004 "Evaluation of Static and Response Spectrum Analysis Procedures of SEAOC/UBC for Seismic Isolated Structures," by C.W. Winters and M.C. Constantinou, 3/23/93, (PB93-198299, A10, MF-A03).
- NCEER-93-0005 "Earthquakes in the Northeast - Are We Ignoring the Hazard? A Workshop on Earthquake Science and Safety for Educators," edited by K.E.K. Ross, 4/2/93, (PB94-103066, A09, MF-A02).
- NCEER-93-0006 "Inelastic Response of Reinforced Concrete Structures with Viscoelastic Braces," by R.F. Lobo, J.M. Bracci, K.L. Shen, A.M. Reinhorn and T.T. Soong, 4/5/93, (PB93-227486, A05, MF-A02).
- NCEER-93-0007 "Seismic Testing of Installation Methods for Computers and Data Processing Equipment," by K. Kosar, T.T. Soong, K.L. Shen, J.A. HoLung and Y.K. Lin, 4/12/93, (PB93-198299, A07, MF-A02).
- NCEER-93-0008 "Retrofit of Reinforced Concrete Frames Using Added Dampers," by A. Reinhorn, M. Constantinou and C. Li, to be published.
- NCEER-93-0009 "Seismic Behavior and Design Guidelines for Steel Frame Structures with Added Viscoelastic Dampers," by K.C. Chang, M.L. Lai, T.T. Soong, D.S. Hao and Y.C. Yeh, 5/1/93, (PB94-141959, A07, MF-A02).
- NCEER-93-0010 "Seismic Performance of Shear-Critical Reinforced Concrete Bridge Piers," by J.B. Mander, S.M. Waheed, M.T.A. Chaudhary and S.S. Chen, 5/12/93, (PB93-227494, A08, MF-A02).
- NCEER-93-0011 "3D-BASIS-TABS: Computer Program for Nonlinear Dynamic Analysis of Three Dimensional Base Isolated Structures," by S. Nagarajaiah, C. Li, A.M. Reinhorn and M.C. Constantinou, 8/2/93, (PB94-141819, A09, MF-A02).
- NCEER-93-0012 "Effects of Hydrocarbon Spills from an Oil Pipeline Break on Ground Water," by O.J. Helweg and H.H.M. Hwang, 8/3/93, (PB94-141942, A06, MF-A02).
- NCEER-93-0013 "Simplified Procedures for Seismic Design of Nonstructural Components and Assessment of Current Code Provisions," by M.P. Singh, L.E. Suarez, E.E. Matheu and G.O. Maldonado, 8/4/93, (PB94-141827, A09, MF-A02).
- NCEER-93-0014 "An Energy Approach to Seismic Analysis and Design of Secondary Systems," by G. Chen and T.T. Soong, 8/6/93, (PB94-142767, A11, MF-A03).

- NCEER-93-0015 "Proceedings from School Sites: Becoming Prepared for Earthquakes - Commemorating the Third Anniversary of the Loma Prieta Earthquake," Edited by F.E. Winslow and K.E.K. Ross, 8/16/93, (PB94-154275, A16, MF-A02).
- NCEER-93-0016 "Reconnaissance Report of Damage to Historic Monuments in Cairo, Egypt Following the October 12, 1992 Dahshur Earthquake," by D. Sykora, D. Look, G. Croci, E. Karaesmen and E. Karaesmen, 8/19/93, (PB94-142221, A08, MF-A02).
- NCEER-93-0017 "The Island of Guam Earthquake of August 8, 1993," by S.W. Swan and S.K. Harris, 9/30/93, (PB94-141843, A04, MF-A01).
- NCEER-93-0018 "Engineering Aspects of the October 12, 1992 Egyptian Earthquake," by A.W. Elgamal, M. Amer, K. Adalier and A. Abul-Fadl, 10/7/93, (PB94-141983, A05, MF-A01).
- NCEER-93-0019 "Development of an Earthquake Motion Simulator and its Application in Dynamic Centrifuge Testing," by I. Krstelj, Supervised by J.H. Prevost, 10/23/93, (PB94-181773, A-10, MF-A03).
- NCEER-93-0020 "NCEER-Taisei Corporation Research Program on Sliding Seismic Isolation Systems for Bridges: Experimental and Analytical Study of a Friction Pendulum System (FPS)," by M.C. Constantinou, P. Tsopelas, Y-S. Kim and S. Okamoto, 11/1/93, (PB94-142775, A08, MF-A02).
- NCEER-93-0021 "Finite Element Modeling of Elastomeric Seismic Isolation Bearings," by L.J. Billings, Supervised by R. Shepherd, 11/8/93, to be published.
- NCEER-93-0022 "Seismic Vulnerability of Equipment in Critical Facilities: Life-Safety and Operational Consequences," by K. Porter, G.S. Johnson, M.M. Zadeh, C. Scawthorn and S. Eder, 11/24/93, (PB94-181765, A16, MF-A03).
- NCEER-93-0023 "Hokkaido Nansei-oki, Japan Earthquake of July 12, 1993, by P.I. Yanev and C.R. Scawthorn, 12/23/93, (PB94-181500, A07, MF-A01).
- NCEER-94-0001 "An Evaluation of Seismic Serviceability of Water Supply Networks with Application to the San Francisco Auxiliary Water Supply System," by I. Markov, Supervised by M. Grigoriu and T. O'Rourke, 1/21/94, (PB94-204013, A07, MF-A02).
- NCEER-94-0002 "NCEER-Taisei Corporation Research Program on Sliding Seismic Isolation Systems for Bridges: Experimental and Analytical Study of Systems Consisting of Sliding Bearings, Rubber Restoring Force Devices and Fluid Dampers," Volumes I and II, by P. Tsopelas, S. Okamoto, M.C. Constantinou, D. Ozaki and S. Fujii, 2/4/94, (PB94-181740, A09, MF-A02 and PB94-181757, A12, MF-A03).
- NCEER-94-0003 "A Markov Model for Local and Global Damage Indices in Seismic Analysis," by S. Rahman and M. Grigoriu, 2/18/94, (PB94-206000, A12, MF-A03).
- NCEER-94-0004 "Proceedings from the NCEER Workshop on Seismic Response of Masonry Infills," edited by D.P. Abrams, 3/1/94, (PB94-180783, A07, MF-A02).
- NCEER-94-0005 "The Northridge, California Earthquake of January 17, 1994: General Reconnaissance Report," edited by J.D. Goltz, 3/11/94, (PB94-193943, A10, MF-A03).
- NCEER-94-0006 "Seismic Energy Based Fatigue Damage Analysis of Bridge Columns: Part I - Evaluation of Seismic Capacity," by G.A. Chang and J.B. Mander, 3/14/94, (PB94-219185, A11, MF-A03).
- NCEER-94-0007 "Seismic Isolation of Multi-Story Frame Structures Using Spherical Sliding Isolation Systems," by T.M. Al-Hussaini, V.A. Zayas and M.C. Constantinou, 3/17/94, (PB94-193745, A09, MF-A02).
- NCEER-94-0008 "The Northridge, California Earthquake of January 17, 1994: Performance of Highway Bridges," edited by I.G. Buckle, 3/24/94, (PB94-193851, A06, MF-A02).
- NCEER-94-0009 "Proceedings of the Third U.S.-Japan Workshop on Earthquake Protective Systems for Bridges," edited by I.G. Buckle and I. Friedland, 3/31/94, (PB94-195815, A99, MF-A06).

- NCEER-94-0010 "3D-BASIS-ME: Computer Program for Nonlinear Dynamic Analysis of Seismically Isolated Single and Multiple Structures and Liquid Storage Tanks," by P.C. Tsopelas, M.C. Constantinou and A.M. Reinhorn, 4/12/94, (PB94-204922, A09, MF-A02).
- NCEER-94-0011 "The Northridge, California Earthquake of January 17, 1994: Performance of Gas Transmission Pipelines," by T.D. O'Rourke and M.C. Palmer, 5/16/94, (PB94-204989, A05, MF-A01).
- NCEER-94-0012 "Feasibility Study of Replacement Procedures and Earthquake Performance Related to Gas Transmission Pipelines," by T.D. O'Rourke and M.C. Palmer, 5/25/94, (PB94-206638, A09, MF-A02).
- NCEER-94-0013 "Seismic Energy Based Fatigue Damage Analysis of Bridge Columns: Part II - Evaluation of Seismic Demand," by G.A. Chang and J.B. Mander, 6/1/94, (PB95-18106, A08, MF-A02).
- NCEER-94-0014 "NCEER-Taisei Corporation Research Program on Sliding Seismic Isolation Systems for Bridges: Experimental and Analytical Study of a System Consisting of Sliding Bearings and Fluid Restoring Force/Damping Devices," by P. Tsopelas and M.C. Constantinou, 6/13/94, (PB94-219144, A10, MF-A03).
- NCEER-94-0015 "Generation of Hazard-Consistent Fragility Curves for Seismic Loss Estimation Studies," by H. Hwang and J-R. Huo, 6/14/94, (PB95-181996, A09, MF-A02).
- NCEER-94-0016 "Seismic Study of Building Frames with Added Energy-Absorbing Devices," by W.S. Pong, C.S. Tsai and G.C. Lee, 6/20/94, (PB94-219136, A10, A03).
- NCEER-94-0017 "Sliding Mode Control for Seismic-Excited Linear and Nonlinear Civil Engineering Structures," by J. Yang, J. Wu, A. Agrawal and Z. Li, 6/21/94, (PB95-138483, A06, MF-A02).
- NCEER-94-0018 "3D-BASIS-TABS Version 2.0: Computer Program for Nonlinear Dynamic Analysis of Three Dimensional Base Isolated Structures," by A.M. Reinhorn, S. Nagarajaiah, M.C. Constantinou, P. Tsopelas and R. Li, 6/22/94, (PB95-182176, A08, MF-A02).
- NCEER-94-0019 "Proceedings of the International Workshop on Civil Infrastructure Systems: Application of Intelligent Systems and Advanced Materials on Bridge Systems," Edited by G.C. Lee and K.C. Chang, 7/18/94, (PB95-252474, A20, MF-A04).
- NCEER-94-0020 "Study of Seismic Isolation Systems for Computer Floors," by V. Lambrou and M.C. Constantinou, 7/19/94, (PB95-138533, A10, MF-A03).
- NCEER-94-0021 "Proceedings of the U.S.-Italian Workshop on Guidelines for Seismic Evaluation and Rehabilitation of Unreinforced Masonry Buildings," Edited by D.P. Abrams and G.M. Calvi, 7/20/94, (PB95-138749, A13, MF-A03).
- NCEER-94-0022 "NCEER-Taisei Corporation Research Program on Sliding Seismic Isolation Systems for Bridges: Experimental and Analytical Study of a System Consisting of Lubricated PTFE Sliding Bearings and Mild Steel Dampers," by P. Tsopelas and M.C. Constantinou, 7/22/94, (PB95-182184, A08, MF-A02).
- NCEER-94-0023 "Development of Reliability-Based Design Criteria for Buildings Under Seismic Load," by Y.K. Wen, H. Hwang and M. Shinozuka, 8/1/94, (PB95-211934, A08, MF-A02).
- NCEER-94-0024 "Experimental Verification of Acceleration Feedback Control Strategies for an Active Tendon System," by S.J. Dyke, B.F. Spencer, Jr., P. Quast, M.K. Sain, D.C. Kaspari, Jr. and T.T. Soong, 8/29/94, (PB95-212320, A05, MF-A01).
- NCEER-94-0025 "Seismic Retrofitting Manual for Highway Bridges," Edited by I.G. Buckle and I.F. Friedland, published by the Federal Highway Administration (PB95-212676, A15, MF-A03).
- NCEER-94-0026 "Proceedings from the Fifth U.S.-Japan Workshop on Earthquake Resistant Design of Lifeline Facilities and Countermeasures Against Soil Liquefaction," Edited by T.D. O'Rourke and M. Hamada, 11/7/94, (PB95-220802, A99, MF-E08).

- NCEER-95-0001 “Experimental and Analytical Investigation of Seismic Retrofit of Structures with Supplemental Damping: Part 1 - Fluid Viscous Damping Devices,” by A.M. Reinhorn, C. Li and M.C. Constantinou, 1/3/95, (PB95-266599, A09, MF-A02).
- NCEER-95-0002 “Experimental and Analytical Study of Low-Cycle Fatigue Behavior of Semi-Rigid Top-And-Seat Angle Connections,” by G. Pekcan, J.B. Mander and S.S. Chen, 1/5/95, (PB95-220042, A07, MF-A02).
- NCEER-95-0003 “NCEER-ATC Joint Study on Fragility of Buildings,” by T. Anagnos, C. Rojahn and A.S. Kiremidjian, 1/20/95, (PB95-220026, A06, MF-A02).
- NCEER-95-0004 “Nonlinear Control Algorithms for Peak Response Reduction,” by Z. Wu, T.T. Soong, V. Gattulli and R.C. Lin, 2/16/95, (PB95-220349, A05, MF-A01).
- NCEER-95-0005 “Pipeline Replacement Feasibility Study: A Methodology for Minimizing Seismic and Corrosion Risks to Underground Natural Gas Pipelines,” by R.T. Eguchi, H.A. Seligson and D.G. Honegger, 3/2/95, (PB95-252326, A06, MF-A02).
- NCEER-95-0006 “Evaluation of Seismic Performance of an 11-Story Frame Building During the 1994 Northridge Earthquake,” by F. Naeim, R. DiSulio, K. Benuska, A. Reinhorn and C. Li, to be published.
- NCEER-95-0007 “Prioritization of Bridges for Seismic Retrofitting,” by N. Basöz and A.S. Kiremidjian, 4/24/95, (PB95-252300, A08, MF-A02).
- NCEER-95-0008 “Method for Developing Motion Damage Relationships for Reinforced Concrete Frames,” by A. Singhal and A.S. Kiremidjian, 5/11/95, (PB95-266607, A06, MF-A02).
- NCEER-95-0009 “Experimental and Analytical Investigation of Seismic Retrofit of Structures with Supplemental Damping: Part II - Friction Devices,” by C. Li and A.M. Reinhorn, 7/6/95, (PB96-128087, A11, MF-A03).
- NCEER-95-0010 “Experimental Performance and Analytical Study of a Non-Ductile Reinforced Concrete Frame Structure Retrofitted with Elastomeric Spring Dampers,” by G. Pekcan, J.B. Mander and S.S. Chen, 7/14/95, (PB96-137161, A08, MF-A02).
- NCEER-95-0011 “Development and Experimental Study of Semi-Active Fluid Damping Devices for Seismic Protection of Structures,” by M.D. Symans and M.C. Constantinou, 8/3/95, (PB96-136940, A23, MF-A04).
- NCEER-95-0012 “Real-Time Structural Parameter Modification (RSPM): Development of Innervated Structures,” by Z. Liang, M. Tong and G.C. Lee, 4/11/95, (PB96-137153, A06, MF-A01).
- NCEER-95-0013 “Experimental and Analytical Investigation of Seismic Retrofit of Structures with Supplemental Damping: Part III - Viscous Damping Walls,” by A.M. Reinhorn and C. Li, 10/1/95, (PB96-176409, A11, MF-A03).
- NCEER-95-0014 “Seismic Fragility Analysis of Equipment and Structures in a Memphis Electric Substation,” by J-R. Huo and H.H.M. Hwang, 8/10/95, (PB96-128087, A09, MF-A02).
- NCEER-95-0015 “The Hanshin-Awaji Earthquake of January 17, 1995: Performance of Lifelines,” Edited by M. Shinozuka, 11/3/95, (PB96-176383, A15, MF-A03).
- NCEER-95-0016 “Highway Culvert Performance During Earthquakes,” by T.L. Youd and C.J. Beckman, available as NCEER-96-0015.
- NCEER-95-0017 “The Hanshin-Awaji Earthquake of January 17, 1995: Performance of Highway Bridges,” Edited by I.G. Buckle, 12/1/95, to be published.
- NCEER-95-0018 “Modeling of Masonry Infill Panels for Structural Analysis,” by A.M. Reinhorn, A. Madan, R.E. Valles, Y. Reichmann and J.B. Mander, 12/8/95, (PB97-110886, MF-A01, A06).
- NCEER-95-0019 “Optimal Polynomial Control for Linear and Nonlinear Structures,” by A.K. Agrawal and J.N. Yang, 12/11/95, (PB96-168737, A07, MF-A02).

- NCEER-95-0020 "Retrofit of Non-Ductile Reinforced Concrete Frames Using Friction Dampers," by R.S. Rao, P. Gergely and R.N. White, 12/22/95, (PB97-133508, A10, MF-A02).
- NCEER-95-0021 "Parametric Results for Seismic Response of Pile-Supported Bridge Bents," by G. Mylonakis, A. Nikolaou and G. Gazetas, 12/22/95, (PB97-100242, A12, MF-A03).
- NCEER-95-0022 "Kinematic Bending Moments in Seismically Stressed Piles," by A. Nikolaou, G. Mylonakis and G. Gazetas, 12/23/95, (PB97-113914, MF-A03, A13).
- NCEER-96-0001 "Dynamic Response of Unreinforced Masonry Buildings with Flexible Diaphragms," by A.C. Costley and D.P. Abrams, 10/10/96, (PB97-133573, MF-A03, A15).
- NCEER-96-0002 "State of the Art Review: Foundations and Retaining Structures," by I. Po Lam, to be published.
- NCEER-96-0003 "Ductility of Rectangular Reinforced Concrete Bridge Columns with Moderate Confinement," by N. Wehbe, M. Saiidi, D. Sanders and B. Douglas, 11/7/96, (PB97-133557, A06, MF-A02).
- NCEER-96-0004 "Proceedings of the Long-Span Bridge Seismic Research Workshop," edited by I.G. Buckle and I.M. Friedland, to be published.
- NCEER-96-0005 "Establish Representative Pier Types for Comprehensive Study: Eastern United States," by J. Kulicki and Z. Prucz, 5/28/96, (PB98-119217, A07, MF-A02).
- NCEER-96-0006 "Establish Representative Pier Types for Comprehensive Study: Western United States," by R. Imbsen, R.A. Schamber and T.A. Osterkamp, 5/28/96, (PB98-118607, A07, MF-A02).
- NCEER-96-0007 "Nonlinear Control Techniques for Dynamical Systems with Uncertain Parameters," by R.G. Ghanem and M.I. Bujakov, 5/27/96, (PB97-100259, A17, MF-A03).
- NCEER-96-0008 "Seismic Evaluation of a 30-Year Old Non-Ductile Highway Bridge Pier and Its Retrofit," by J.B. Mander, B. Mahmoodzadegan, S. Bhadra and S.S. Chen, 5/31/96, (PB97-110902, MF-A03, A10).
- NCEER-96-0009 "Seismic Performance of a Model Reinforced Concrete Bridge Pier Before and After Retrofit," by J.B. Mander, J.H. Kim and C.A. Ligozio, 5/31/96, (PB97-110910, MF-A02, A10).
- NCEER-96-0010 "IDARC2D Version 4.0: A Computer Program for the Inelastic Damage Analysis of Buildings," by R.E. Valles, A.M. Reinhorn, S.K. Kunnath, C. Li and A. Madan, 6/3/96, (PB97-100234, A17, MF-A03).
- NCEER-96-0011 "Estimation of the Economic Impact of Multiple Lifeline Disruption: Memphis Light, Gas and Water Division Case Study," by S.E. Chang, H.A. Seligson and R.T. Eguchi, 8/16/96, (PB97-133490, A11, MF-A03).
- NCEER-96-0012 "Proceedings from the Sixth Japan-U.S. Workshop on Earthquake Resistant Design of Lifeline Facilities and Countermeasures Against Soil Liquefaction, Edited by M. Hamada and T. O'Rourke, 9/11/96, (PB97-133581, A99, MF-A06).
- NCEER-96-0013 "Chemical Hazards, Mitigation and Preparedness in Areas of High Seismic Risk: A Methodology for Estimating the Risk of Post-Earthquake Hazardous Materials Release," by H.A. Seligson, R.T. Eguchi, K.J. Tierney and K. Richmond, 11/7/96, (PB97-133565, MF-A02, A08).
- NCEER-96-0014 "Response of Steel Bridge Bearings to Reversed Cyclic Loading," by J.B. Mander, D-K. Kim, S.S. Chen and G.J. Premus, 11/13/96, (PB97-140735, A12, MF-A03).
- NCEER-96-0015 "Highway Culvert Performance During Past Earthquakes," by T.L. Youd and C.J. Beckman, 11/25/96, (PB97-133532, A06, MF-A01).
- NCEER-97-0001 "Evaluation, Prevention and Mitigation of Pounding Effects in Building Structures," by R.E. Valles and A.M. Reinhorn, 2/20/97, (PB97-159552, A14, MF-A03).
- NCEER-97-0002 "Seismic Design Criteria for Bridges and Other Highway Structures," by C. Rojahn, R. Mayes, D.G. Anderson, J. Clark, J.H. Hom, R.V. Nutt and M.J. O'Rourke, 4/30/97, (PB97-194658, A06, MF-A03).

- NCEER-97-0003 "Proceedings of the U.S.-Italian Workshop on Seismic Evaluation and Retrofit," Edited by D.P. Abrams and G.M. Calvi, 3/19/97, (PB97-194666, A13, MF-A03).
- NCEER-97-0004 "Investigation of Seismic Response of Buildings with Linear and Nonlinear Fluid Viscous Dampers," by A.A. Seleemah and M.C. Constantinou, 5/21/97, (PB98-109002, A15, MF-A03).
- NCEER-97-0005 "Proceedings of the Workshop on Earthquake Engineering Frontiers in Transportation Facilities," edited by G.C. Lee and I.M. Friedland, 8/29/97, (PB98-128911, A25, MR-A04).
- NCEER-97-0006 "Cumulative Seismic Damage of Reinforced Concrete Bridge Piers," by S.K. Kunnath, A. El-Bahy, A. Taylor and W. Stone, 9/2/97, (PB98-108814, A11, MF-A03).
- NCEER-97-0007 "Structural Details to Accommodate Seismic Movements of Highway Bridges and Retaining Walls," by R.A. Imbsen, R.A. Schamber, E. Thorkildsen, A. Kartoum, B.T. Martin, T.N. Rosser and J.M. Kulicki, 9/3/97, (PB98-108996, A09, MF-A02).
- NCEER-97-0008 "A Method for Earthquake Motion-Damage Relationships with Application to Reinforced Concrete Frames," by A. Singhal and A.S. Kiremidjian, 9/10/97, (PB98-108988, A13, MF-A03).
- NCEER-97-0009 "Seismic Analysis and Design of Bridge Abutments Considering Sliding and Rotation," by K. Fishman and R. Richards, Jr., 9/15/97, (PB98-108897, A06, MF-A02).
- NCEER-97-0010 "Proceedings of the FHWA/NCEER Workshop on the National Representation of Seismic Ground Motion for New and Existing Highway Facilities," edited by I.M. Friedland, M.S. Power and R.L. Mayes, 9/22/97, (PB98-128903, A21, MF-A04).
- NCEER-97-0011 "Seismic Analysis for Design or Retrofit of Gravity Bridge Abutments," by K.L. Fishman, R. Richards, Jr. and R.C. Divito, 10/2/97, (PB98-128937, A08, MF-A02).
- NCEER-97-0012 "Evaluation of Simplified Methods of Analysis for Yielding Structures," by P. Tsopelas, M.C. Constantinou, C.A. Kircher and A.S. Whittaker, 10/31/97, (PB98-128929, A10, MF-A03).
- NCEER-97-0013 "Seismic Design of Bridge Columns Based on Control and Repairability of Damage," by C-T. Cheng and J.B. Mander, 12/8/97, (PB98-144249, A11, MF-A03).
- NCEER-97-0014 "Seismic Resistance of Bridge Piers Based on Damage Avoidance Design," by J.B. Mander and C-T. Cheng, 12/10/97, (PB98-144223, A09, MF-A02).
- NCEER-97-0015 "Seismic Response of Nominally Symmetric Systems with Strength Uncertainty," by S. Balopoulou and M. Grigoriu, 12/23/97, (PB98-153422, A11, MF-A03).
- NCEER-97-0016 "Evaluation of Seismic Retrofit Methods for Reinforced Concrete Bridge Columns," by T.J. Wipf, F.W. Klaiber and F.M. Russo, 12/28/97, (PB98-144215, A12, MF-A03).
- NCEER-97-0017 "Seismic Fragility of Existing Conventional Reinforced Concrete Highway Bridges," by C.L. Mullen and A.S. Cakmak, 12/30/97, (PB98-153406, A08, MF-A02).
- NCEER-97-0018 "Loss Assessment of Memphis Buildings," edited by D.P. Abrams and M. Shinozuka, 12/31/97, (PB98-144231, A13, MF-A03).
- NCEER-97-0019 "Seismic Evaluation of Frames with Infill Walls Using Quasi-static Experiments," by K.M. Mosalam, R.N. White and P. Gergely, 12/31/97, (PB98-153455, A07, MF-A02).
- NCEER-97-0020 "Seismic Evaluation of Frames with Infill Walls Using Pseudo-dynamic Experiments," by K.M. Mosalam, R.N. White and P. Gergely, 12/31/97, (PB98-153430, A07, MF-A02).
- NCEER-97-0021 "Computational Strategies for Frames with Infill Walls: Discrete and Smeared Crack Analyses and Seismic Fragility," by K.M. Mosalam, R.N. White and P. Gergely, 12/31/97, (PB98-153414, A10, MF-A02).

- NCEER-97-0022 "Proceedings of the NCEER Workshop on Evaluation of Liquefaction Resistance of Soils," edited by T.L. Youd and I.M. Idriss, 12/31/97, (PB98-155617, A15, MF-A03).
- MCEER-98-0001 "Extraction of Nonlinear Hysteretic Properties of Seismically Isolated Bridges from Quick-Release Field Tests," by Q. Chen, B.M. Douglas, E.M. Maragakis and I.G. Buckle, 5/26/98, (PB99-118838, A06, MF-A01).
- MCEER-98-0002 "Methodologies for Evaluating the Importance of Highway Bridges," by A. Thomas, S. Eshenaur and J. Kulicki, 5/29/98, (PB99-118846, A10, MF-A02).
- MCEER-98-0003 "Capacity Design of Bridge Piers and the Analysis of Overstrength," by J.B. Mander, A. Dutta and P. Goel, 6/1/98, (PB99-118853, A09, MF-A02).
- MCEER-98-0004 "Evaluation of Bridge Damage Data from the Loma Prieta and Northridge, California Earthquakes," by N. Basoz and A. Kiremidjian, 6/2/98, (PB99-118861, A15, MF-A03).
- MCEER-98-0005 "Screening Guide for Rapid Assessment of Liquefaction Hazard at Highway Bridge Sites," by T. L. Youd, 6/16/98, (PB99-118879, A06, not available on microfiche).
- MCEER-98-0006 "Structural Steel and Steel/Concrete Interface Details for Bridges," by P. Ritchie, N. Kauh and J. Kulicki, 7/13/98, (PB99-118945, A06, MF-A01).
- MCEER-98-0007 "Capacity Design and Fatigue Analysis of Confined Concrete Columns," by A. Dutta and J.B. Mander, 7/14/98, (PB99-118960, A14, MF-A03).
- MCEER-98-0008 "Proceedings of the Workshop on Performance Criteria for Telecommunication Services Under Earthquake Conditions," edited by A.J. Schiff, 7/15/98, (PB99-118952, A08, MF-A02).
- MCEER-98-0009 "Fatigue Analysis of Unconfined Concrete Columns," by J.B. Mander, A. Dutta and J.H. Kim, 9/12/98, (PB99-123655, A10, MF-A02).
- MCEER-98-0010 "Centrifuge Modeling of Cyclic Lateral Response of Pile-Cap Systems and Seat-Type Abutments in Dry Sands," by A.D. Gadre and R. Dobry, 10/2/98, (PB99-123606, A13, MF-A03).
- MCEER-98-0011 "IDARC-BRIDGE: A Computational Platform for Seismic Damage Assessment of Bridge Structures," by A.M. Reinhorn, V. Simeonov, G. Mylonakis and Y. Reichman, 10/2/98, (PB99-162919, A15, MF-A03).
- MCEER-98-0012 "Experimental Investigation of the Dynamic Response of Two Bridges Before and After Retrofitting with Elastomeric Bearings," by D.A. Wendichansky, S.S. Chen and J.B. Mander, 10/2/98, (PB99-162927, A15, MF-A03).
- MCEER-98-0013 "Design Procedures for Hinge Restrainers and Hinge Sear Width for Multiple-Frame Bridges," by R. Des Roches and G.L. Fenves, 11/3/98, (PB99-140477, A13, MF-A03).
- MCEER-98-0014 "Response Modification Factors for Seismically Isolated Bridges," by M.C. Constantinou and J.K. Quarshie, 11/3/98, (PB99-140485, A14, MF-A03).
- MCEER-98-0015 "Proceedings of the U.S.-Italy Workshop on Seismic Protective Systems for Bridges," edited by I.M. Friedland and M.C. Constantinou, 11/3/98, (PB2000-101711, A22, MF-A04).
- MCEER-98-0016 "Appropriate Seismic Reliability for Critical Equipment Systems: Recommendations Based on Regional Analysis of Financial and Life Loss," by K. Porter, C. Scawthorn, C. Taylor and N. Blais, 11/10/98, (PB99-157265, A08, MF-A02).
- MCEER-98-0017 "Proceedings of the U.S. Japan Joint Seminar on Civil Infrastructure Systems Research," edited by M. Shinozuka and A. Rose, 11/12/98, (PB99-156713, A16, MF-A03).
- MCEER-98-0018 "Modeling of Pile Footings and Drilled Shafts for Seismic Design," by I. PoLam, M. Kapuskar and D. Chaudhuri, 12/21/98, (PB99-157257, A09, MF-A02).

- MCEER-99-0001 "Seismic Evaluation of a Masonry Infilled Reinforced Concrete Frame by Pseudodynamic Testing," by S.G. Buonopane and R.N. White, 2/16/99, (PB99-162851, A09, MF-A02).
- MCEER-99-0002 "Response History Analysis of Structures with Seismic Isolation and Energy Dissipation Systems: Verification Examples for Program SAP2000," by J. Scheller and M.C. Constantinou, 2/22/99, (PB99-162869, A08, MF-A02).
- MCEER-99-0003 "Experimental Study on the Seismic Design and Retrofit of Bridge Columns Including Axial Load Effects," by A. Dutta, T. Kokorina and J.B. Mander, 2/22/99, (PB99-162877, A09, MF-A02).
- MCEER-99-0004 "Experimental Study of Bridge Elastomeric and Other Isolation and Energy Dissipation Systems with Emphasis on Uplift Prevention and High Velocity Near-source Seismic Excitation," by A. Kasalanati and M. C. Constantinou, 2/26/99, (PB99-162885, A12, MF-A03).
- MCEER-99-0005 "Truss Modeling of Reinforced Concrete Shear-flexure Behavior," by J.H. Kim and J.B. Mander, 3/8/99, (PB99-163693, A12, MF-A03).
- MCEER-99-0006 "Experimental Investigation and Computational Modeling of Seismic Response of a 1:4 Scale Model Steel Structure with a Load Balancing Supplemental Damping System," by G. Pekcan, J.B. Mander and S.S. Chen, 4/2/99, (PB99-162893, A11, MF-A03).
- MCEER-99-0007 "Effect of Vertical Ground Motions on the Structural Response of Highway Bridges," by M.R. Button, C.J. Cronin and R.L. Mayes, 4/10/99, (PB2000-101411, A10, MF-A03).
- MCEER-99-0008 "Seismic Reliability Assessment of Critical Facilities: A Handbook, Supporting Documentation, and Model Code Provisions," by G.S. Johnson, R.E. Sheppard, M.D. Quilici, S.J. Eder and C.R. Scawthorn, 4/12/99, (PB2000-101701, A18, MF-A04).
- MCEER-99-0009 "Impact Assessment of Selected MCEER Highway Project Research on the Seismic Design of Highway Structures," by C. Rojahn, R. Mayes, D.G. Anderson, J.H. Clark, D'Appolonia Engineering, S. Gloyd and R.V. Nutt, 4/14/99, (PB99-162901, A10, MF-A02).
- MCEER-99-0010 "Site Factors and Site Categories in Seismic Codes," by R. Dobry, R. Ramos and M.S. Power, 7/19/99, (PB2000-101705, A08, MF-A02).
- MCEER-99-0011 "Restrainer Design Procedures for Multi-Span Simply-Supported Bridges," by M.J. Randall, M. Saiidi, E. Maragakis and T. Isakovic, 7/20/99, (PB2000-101702, A10, MF-A02).
- MCEER-99-0012 "Property Modification Factors for Seismic Isolation Bearings," by M.C. Constantinou, P. Tsopelas, A. Kasalanati and E. Wolff, 7/20/99, (PB2000-103387, A11, MF-A03).
- MCEER-99-0013 "Critical Seismic Issues for Existing Steel Bridges," by P. Ritchie, N. Kauh and J. Kulicki, 7/20/99, (PB2000-101697, A09, MF-A02).
- MCEER-99-0014 "Nonstructural Damage Database," by A. Kao, T.T. Soong and A. Vender, 7/24/99, (PB2000-101407, A06, MF-A01).
- MCEER-99-0015 "Guide to Remedial Measures for Liquefaction Mitigation at Existing Highway Bridge Sites," by H.G. Cooke and J. K. Mitchell, 7/26/99, (PB2000-101703, A11, MF-A03).
- MCEER-99-0016 "Proceedings of the MCEER Workshop on Ground Motion Methodologies for the Eastern United States," edited by N. Abrahamson and A. Becker, 8/11/99, (PB2000-103385, A07, MF-A02).
- MCEER-99-0017 "Quindío, Colombia Earthquake of January 25, 1999: Reconnaissance Report," by A.P. Asfura and P.J. Flores, 10/4/99, (PB2000-106893, A06, MF-A01).
- MCEER-99-0018 "Hysteretic Models for Cyclic Behavior of Deteriorating Inelastic Structures," by M.V. Sivaselvan and A.M. Reinhorn, 11/5/99, (PB2000-103386, A08, MF-A02).

- MCEER-99-0019 "Proceedings of the 7th U.S.- Japan Workshop on Earthquake Resistant Design of Lifeline Facilities and Countermeasures Against Soil Liquefaction," edited by T.D. O'Rourke, J.P. Bardet and M. Hamada, 11/19/99, (PB2000-103354, A99, MF-A06).
- MCEER-99-0020 "Development of Measurement Capability for Micro-Vibration Evaluations with Application to Chip Fabrication Facilities," by G.C. Lee, Z. Liang, J.W. Song, J.D. Shen and W.C. Liu, 12/1/99, (PB2000-105993, A08, MF-A02).
- MCEER-99-0021 "Design and Retrofit Methodology for Building Structures with Supplemental Energy Dissipating Systems," by G. Pekcan, J.B. Mander and S.S. Chen, 12/31/99, (PB2000-105994, A11, MF-A03).
- MCEER-00-0001 "The Marmara, Turkey Earthquake of August 17, 1999: Reconnaissance Report," edited by C. Scawthorn; with major contributions by M. Bruneau, R. Eguchi, T. Holzer, G. Johnson, J. Mander, J. Mitchell, W. Mitchell, A. Papageorgiou, C. Scaethorn, and G. Webb, 3/23/00, (PB2000-106200, A11, MF-A03).
- MCEER-00-0002 "Proceedings of the MCEER Workshop for Seismic Hazard Mitigation of Health Care Facilities," edited by G.C. Lee, M. Ettouney, M. Grigoriu, J. Hauer and J. Nigg, 3/29/00, (PB2000-106892, A08, MF-A02).
- MCEER-00-0003 "The Chi-Chi, Taiwan Earthquake of September 21, 1999: Reconnaissance Report," edited by G.C. Lee and C.H. Loh, with major contributions by G.C. Lee, M. Bruneau, I.G. Buckle, S.E. Chang, P.J. Flores, T.D. O'Rourke, M. Shinozuka, T.T. Soong, C-H. Loh, K-C. Chang, Z-J. Chen, J-S. Hwang, M-L. Lin, G-Y. Liu, K-C. Tsai, G.C. Yao and C-L. Yen, 4/30/00, (PB2001-100980, A10, MF-A02).
- MCEER-00-0004 "Seismic Retrofit of End-Sway Frames of Steel Deck-Truss Bridges with a Supplemental Tendon System: Experimental and Analytical Investigation," by G. Pekcan, J.B. Mander and S.S. Chen, 7/1/00, (PB2001-100982, A10, MF-A02).
- MCEER-00-0005 "Sliding Fragility of Unrestrained Equipment in Critical Facilities," by W.H. Chong and T.T. Soong, 7/5/00, (PB2001-100983, A08, MF-A02).
- MCEER-00-0006 "Seismic Response of Reinforced Concrete Bridge Pier Walls in the Weak Direction," by N. Abo-Shadi, M. Saiidi and D. Sanders, 7/17/00, (PB2001-100981, A17, MF-A03).
- MCEER-00-0007 "Low-Cycle Fatigue Behavior of Longitudinal Reinforcement in Reinforced Concrete Bridge Columns," by J. Brown and S.K. Kunnath, 7/23/00, (PB2001-104392, A08, MF-A02).
- MCEER-00-0008 "Soil Structure Interaction of Bridges for Seismic Analysis," I. PoLam and H. Law, 9/25/00, (PB2001-105397, A08, MF-A02).
- MCEER-00-0009 "Proceedings of the First MCEER Workshop on Mitigation of Earthquake Disaster by Advanced Technologies (MEDAT-1), edited by M. Shinozuka, D.J. Inman and T.D. O'Rourke, 11/10/00, (PB2001-105399, A14, MF-A03).
- MCEER-00-0010 "Development and Evaluation of Simplified Procedures for Analysis and Design of Buildings with Passive Energy Dissipation Systems, Revision 01," by O.M. Ramirez, M.C. Constantinou, C.A. Kircher, A.S. Whittaker, M.W. Johnson, J.D. Gomez and C. Chrysostomou, 11/16/01, (PB2001-105523, A23, MF-A04).
- MCEER-00-0011 "Dynamic Soil-Foundation-Structure Interaction Analyses of Large Caissons," by C-Y. Chang, C-M. Mok, Z-L. Wang, R. Settgast, F. Waggoner, M.A. Ketchum, H.M. Gonnermann and C-C. Chin, 12/30/00, (PB2001-104373, A07, MF-A02).
- MCEER-00-0012 "Experimental Evaluation of Seismic Performance of Bridge Restrainers," by A.G. Vlassis, E.M. Maragakis and M. Saiid Saiidi, 12/30/00, (PB2001-104354, A09, MF-A02).
- MCEER-00-0013 "Effect of Spatial Variation of Ground Motion on Highway Structures," by M. Shinozuka, V. Saxena and G. Deodatis, 12/31/00, (PB2001-108755, A13, MF-A03).
- MCEER-00-0014 "A Risk-Based Methodology for Assessing the Seismic Performance of Highway Systems," by S.D. Werner, C.E. Taylor, J.E. Moore, II, J.S. Walton and S. Cho, 12/31/00, (PB2001-108756, A14, MF-A03).

- MCEER-01-0001 “Experimental Investigation of P-Delta Effects to Collapse During Earthquakes,” by D. Vian and M. Bruneau, 6/25/01, (PB2002-100534, A17, MF-A03).
- MCEER-01-0002 “Proceedings of the Second MCEER Workshop on Mitigation of Earthquake Disaster by Advanced Technologies (MEDAT-2),” edited by M. Bruneau and D.J. Inman, 7/23/01, (PB2002-100434, A16, MF-A03).
- MCEER-01-0003 “Sensitivity Analysis of Dynamic Systems Subjected to Seismic Loads,” by C. Roth and M. Grigoriu, 9/18/01, (PB2003-100884, A12, MF-A03).
- MCEER-01-0004 “Overcoming Obstacles to Implementing Earthquake Hazard Mitigation Policies: Stage 1 Report,” by D.J. Alesch and W.J. Petak, 12/17/01, (PB2002-107949, A07, MF-A02).
- MCEER-01-0005 “Updating Real-Time Earthquake Loss Estimates: Methods, Problems and Insights,” by C.E. Taylor, S.E. Chang and R.T. Eguchi, 12/17/01, (PB2002-107948, A05, MF-A01).
- MCEER-01-0006 “Experimental Investigation and Retrofit of Steel Pile Foundations and Pile Bents Under Cyclic Lateral Loadings,” by A. Shama, J. Mander, B. Blabac and S. Chen, 12/31/01, (PB2002-107950, A13, MF-A03).
- MCEER-02-0001 “Assessment of Performance of Bolu Viaduct in the 1999 Duzce Earthquake in Turkey” by P.C. Roussis, M.C. Constantinou, M. Erdik, E. Durukal and M. Dicleli, 5/8/02, (PB2003-100883, A08, MF-A02).
- MCEER-02-0002 “Seismic Behavior of Rail Counterweight Systems of Elevators in Buildings,” by M.P. Singh, Rildova and L.E. Suarez, 5/27/02. (PB2003-100882, A11, MF-A03).
- MCEER-02-0003 “Development of Analysis and Design Procedures for Spread Footings,” by G. Mylonakis, G. Gazetas, S. Nikolaou and A. Chauncey, 10/02/02, (PB2004-101636, A13, MF-A03, CD-A13).
- MCEER-02-0004 “Bare-Earth Algorithms for Use with SAR and LIDAR Digital Elevation Models,” by C.K. Huyck, R.T. Eguchi and B. Houshmand, 10/16/02, (PB2004-101637, A07, CD-A07).
- MCEER-02-0005 “Review of Energy Dissipation of Compression Members in Concentrically Braced Frames,” by K.Lee and M. Bruneau, 10/18/02, (PB2004-101638, A10, CD-A10).
- MCEER-03-0001 “Experimental Investigation of Light-Gauge Steel Plate Shear Walls for the Seismic Retrofit of Buildings” by J. Berman and M. Bruneau, 5/2/03, (PB2004-101622, A10, MF-A03, CD-A10).
- MCEER-03-0002 “Statistical Analysis of Fragility Curves,” by M. Shinozuka, M.Q. Feng, H. Kim, T. Uzawa and T. Ueda, 6/16/03, (PB2004-101849, A09, CD-A09).
- MCEER-03-0003 “Proceedings of the Eighth U.S.-Japan Workshop on Earthquake Resistant Design of Lifeline Facilities and Countermeasures Against Liquefaction,” edited by M. Hamada, J.P. Bardet and T.D. O’Rourke, 6/30/03, (PB2004-104386, A99, CD-A99).
- MCEER-03-0004 “Proceedings of the PRC-US Workshop on Seismic Analysis and Design of Special Bridges,” edited by L.C. Fan and G.C. Lee, 7/15/03, (PB2004-104387, A14, CD-A14).
- MCEER-03-0005 “Urban Disaster Recovery: A Framework and Simulation Model,” by S.B. Miles and S.E. Chang, 7/25/03, (PB2004-104388, A07, CD-A07).
- MCEER-03-0006 “Behavior of Underground Piping Joints Due to Static and Dynamic Loading,” by R.D. Meis, M. Maragakis and R. Siddharthan, 11/17/03, (PB2005-102194, A13, MF-A03, CD-A00).
- MCEER-04-0001 “Experimental Study of Seismic Isolation Systems with Emphasis on Secondary System Response and Verification of Accuracy of Dynamic Response History Analysis Methods,” by E. Wolff and M. Constantinou, 1/16/04 (PB2005-102195, A99, MF-E08, CD-A00).
- MCEER-04-0002 “Tension, Compression and Cyclic Testing of Engineered Cementitious Composite Materials,” by K. Kesner and S.L. Billington, 3/1/04, (PB2005-102196, A08, CD-A08).


- MCEER-04-0003 “Cyclic Testing of Braces Laterally Restrained by Steel Studs to Enhance Performance During Earthquakes,” by O.C. Celik, J.W. Berman and M. Bruneau, 3/16/04, (PB2005-102197, A13, MF-A03, CD-A00).
- MCEER-04-0004 “Methodologies for Post Earthquake Building Damage Detection Using SAR and Optical Remote Sensing: Application to the August 17, 1999 Marmara, Turkey Earthquake,” by C.K. Huyck, B.J. Adams, S. Cho, R.T. Eguchi, B. Mansouri and B. Houshmand, 6/15/04, (PB2005-104888, A10, CD-A00).
- MCEER-04-0005 “Nonlinear Structural Analysis Towards Collapse Simulation: A Dynamical Systems Approach,” by M.V. Sivaselvan and A.M. Reinhorn, 6/16/04, (PB2005-104889, A11, MF-A03, CD-A00).
- MCEER-04-0006 “Proceedings of the Second PRC-US Workshop on Seismic Analysis and Design of Special Bridges,” edited by G.C. Lee and L.C. Fan, 6/25/04, (PB2005-104890, A16, CD-A00).
- MCEER-04-0007 “Seismic Vulnerability Evaluation of Axially Loaded Steel Built-up Laced Members,” by K. Lee and M. Bruneau, 6/30/04, (PB2005-104891, A16, CD-A00).
- MCEER-04-0008 “Evaluation of Accuracy of Simplified Methods of Analysis and Design of Buildings with Damping Systems for Near-Fault and for Soft-Soil Seismic Motions,” by E.A. Pavlou and M.C. Constantinou, 8/16/04, (PB2005-104892, A08, MF-A02, CD-A00).
- MCEER-04-0009 “Assessment of Geotechnical Issues in Acute Care Facilities in California,” by M. Lew, T.D. O’Rourke, R. Dobry and M. Koch, 9/15/04, (PB2005-104893, A08, CD-A00).
- MCEER-04-0010 “Scissor-Jack-Damper Energy Dissipation System,” by A.N. Sigaher-Boyle and M.C. Constantinou, 12/1/04 (PB2005-108221).
- MCEER-04-0011 “Seismic Retrofit of Bridge Steel Truss Piers Using a Controlled Rocking Approach,” by M. Pollino and M. Bruneau, 12/20/04 (PB2006-105795).
- MCEER-05-0001 “Experimental and Analytical Studies of Structures Seismically Isolated with an Uplift-Restraint Isolation System,” by P.C. Roussis and M.C. Constantinou, 1/10/05 (PB2005-108222).
- MCEER-05-0002 “A Versatile Experimentation Model for Study of Structures Near Collapse Applied to Seismic Evaluation of Irregular Structures,” by D. Kusumastuti, A.M. Reinhorn and A. Rutenberg, 3/31/05 (PB2006-101523).
- MCEER-05-0003 “Proceedings of the Third PRC-US Workshop on Seismic Analysis and Design of Special Bridges,” edited by L.C. Fan and G.C. Lee, 4/20/05, (PB2006-105796).
- MCEER-05-0004 “Approaches for the Seismic Retrofit of Braced Steel Bridge Piers and Proof-of-Concept Testing of an Eccentrically Braced Frame with Tubular Link,” by J.W. Berman and M. Bruneau, 4/21/05 (PB2006-101524).
- MCEER-05-0005 “Simulation of Strong Ground Motions for Seismic Fragility Evaluation of Nonstructural Components in Hospitals,” by A. Wanitkorkul and A. Filiatrault, 5/26/05 (PB2006-500027).
- MCEER-05-0006 “Seismic Safety in California Hospitals: Assessing an Attempt to Accelerate the Replacement or Seismic Retrofit of Older Hospital Facilities,” by D.J. Alesch, L.A. Arendt and W.J. Petak, 6/6/05 (PB2006-105794).
- MCEER-05-0007 “Development of Seismic Strengthening and Retrofit Strategies for Critical Facilities Using Engineered Cementitious Composite Materials,” by K. Kesner and S.L. Billington, 8/29/05 (PB2006-111701).
- MCEER-05-0008 “Experimental and Analytical Studies of Base Isolation Systems for Seismic Protection of Power Transformers,” by N. Murota, M.Q. Feng and G-Y. Liu, 9/30/05 (PB2006-111702).
- MCEER-05-0009 “3D-BASIS-ME-MB: Computer Program for Nonlinear Dynamic Analysis of Seismically Isolated Structures,” by P.C. Tsopelas, P.C. Roussis, M.C. Constantinou, R. Buchanan and A.M. Reinhorn, 10/3/05 (PB2006-111703).
- MCEER-05-0010 “Steel Plate Shear Walls for Seismic Design and Retrofit of Building Structures,” by D. Vian and M. Bruneau, 12/15/05 (PB2006-111704).

- MCEER-05-0011 "The Performance-Based Design Paradigm," by M.J. Astrella and A. Whittaker, 12/15/05 (PB2006-111705).
- MCEER-06-0001 "Seismic Fragility of Suspended Ceiling Systems," H. Badillo-Almaraz, A.S. Whittaker, A.M. Reinhorn and G.P. Cimellaro, 2/4/06 (PB2006-111706).
- MCEER-06-0002 "Multi-Dimensional Fragility of Structures," by G.P. Cimellaro, A.M. Reinhorn and M. Bruneau, 3/1/06 (PB2007-106974, A09, MF-A02, CD A00).
- MCEER-06-0003 "Built-Up Shear Links as Energy Dissipators for Seismic Protection of Bridges," by P. Dusicka, A.M. Itani and I.G. Buckle, 3/15/06 (PB2006-111708).
- MCEER-06-0004 "Analytical Investigation of the Structural Fuse Concept," by R.E. Vargas and M. Bruneau, 3/16/06 (PB2006-111709).
- MCEER-06-0005 "Experimental Investigation of the Structural Fuse Concept," by R.E. Vargas and M. Bruneau, 3/17/06 (PB2006-111710).
- MCEER-06-0006 "Further Development of Tubular Eccentrically Braced Frame Links for the Seismic Retrofit of Braced Steel Truss Bridge Piers," by J.W. Berman and M. Bruneau, 3/27/06 (PB2007-105147).
- MCEER-06-0007 "REDARS Validation Report," by S. Cho, C.K. Huyck, S. Ghosh and R.T. Eguchi, 8/8/06 (PB2007-106983).
- MCEER-06-0008 "Review of Current NDE Technologies for Post-Earthquake Assessment of Retrofitted Bridge Columns," by J.W. Song, Z. Liang and G.C. Lee, 8/21/06 (PB2007-106984).
- MCEER-06-0009 "Liquefaction Remediation in Silty Soils Using Dynamic Compaction and Stone Columns," by S. Thevanayagam, G.R. Martin, R. Nashed, T. Shenthan, T. Kanagalingam and N. Ecemis, 8/28/06 (PB2007-106985).
- MCEER-06-0010 "Conceptual Design and Experimental Investigation of Polymer Matrix Composite Infill Panels for Seismic Retrofitting," by W. Jung, M. Chiewanichakorn and A.J. Aref, 9/21/06 (PB2007-106986).
- MCEER-06-0011 "A Study of the Coupled Horizontal-Vertical Behavior of Elastomeric and Lead-Rubber Seismic Isolation Bearings," by G.P. Warn and A.S. Whittaker, 9/22/06 (PB2007-108679).
- MCEER-06-0012 "Proceedings of the Fourth PRC-US Workshop on Seismic Analysis and Design of Special Bridges: Advancing Bridge Technologies in Research, Design, Construction and Preservation," Edited by L.C. Fan, G.C. Lee and L. Ziang, 10/12/06 (PB2007-109042).
- MCEER-06-0013 "Cyclic Response and Low Cycle Fatigue Characteristics of Plate Steels," by P. Dusicka, A.M. Itani and I.G. Buckle, 11/1/06 06 (PB2007-106987).
- MCEER-06-0014 "Proceedings of the Second US-Taiwan Bridge Engineering Workshop," edited by W.P. Yen, J. Shen, J-Y. Chen and M. Wang, 11/15/06 (PB2008-500041).
- MCEER-06-0015 "User Manual and Technical Documentation for the REDARSTM Import Wizard," by S. Cho, S. Ghosh, C.K. Huyck and S.D. Werner, 11/30/06 (PB2007-114766).
- MCEER-06-0016 "Hazard Mitigation Strategy and Monitoring Technologies for Urban and Infrastructure Public Buildings: Proceedings of the China-US Workshops," edited by X.Y. Zhou, A.L. Zhang, G.C. Lee and M. Tong, 12/12/06 (PB2008-500018).
- MCEER-07-0001 "Static and Kinetic Coefficients of Friction for Rigid Blocks," by C. Kafali, S. Fathali, M. Grigoriu and A.S. Whittaker, 3/20/07 (PB2007-114767).
- MCEER-07-0002 "Hazard Mitigation Investment Decision Making: Organizational Response to Legislative Mandate," by L.A. Arendt, D.J. Alesch and W.J. Petak, 4/9/07 (PB2007-114768).
- MCEER-07-0003 "Seismic Behavior of Bidirectional-Resistant Ductile End Diaphragms with Unbonded Braces in Straight or Skewed Steel Bridges," by O. Celik and M. Bruneau, 4/11/07 (PB2008-105141).

- MCEER-07-0004 “Modeling Pile Behavior in Large Pile Groups Under Lateral Loading,” by A.M. Dodds and G.R. Martin, 4/16/07(PB2008-105142).
- MCEER-07-0005 “Experimental Investigation of Blast Performance of Seismically Resistant Concrete-Filled Steel Tube Bridge Piers,” by S. Fujikura, M. Bruneau and D. Lopez-Garcia, 4/20/07 (PB2008-105143).
- MCEER-07-0006 “Seismic Analysis of Conventional and Isolated Liquefied Natural Gas Tanks Using Mechanical Analogs,” by I.P. Christovasilis and A.S. Whittaker, 5/1/07.
- MCEER-07-0007 “Experimental Seismic Performance Evaluation of Isolation/Restraint Systems for Mechanical Equipment – Part 1: Heavy Equipment Study,” by S. Fathali and A. Filiatrault, 6/6/07 (PB2008-105144).
- MCEER-07-0008 “Seismic Vulnerability of Timber Bridges and Timber Substructures,” by A.A. Sharma, J.B. Mander, I.M. Friedland and D.R. Allicock, 6/7/07 (PB2008-105145).
- MCEER-07-0009 “Experimental and Analytical Study of the XY-Friction Pendulum (XY-FP) Bearing for Bridge Applications,” by C.C. Marin-Artieda, A.S. Whittaker and M.C. Constantinou, 6/7/07 (PB2008-105191).
- MCEER-07-0010 “Proceedings of the PRC-US Earthquake Engineering Forum for Young Researchers,” Edited by G.C. Lee and X.Z. Qi, 6/8/07 (PB2008-500058).
- MCEER-07-0011 “Design Recommendations for Perforated Steel Plate Shear Walls,” by R. Purba and M. Bruneau, 6/18/07, (PB2008-105192).
- MCEER-07-0012 “Performance of Seismic Isolation Hardware Under Service and Seismic Loading,” by M.C. Constantinou, A.S. Whittaker, Y. Kalpakidis, D.M. Fenz and G.P. Warn, 8/27/07, (PB2008-105193).
- MCEER-07-0013 “Experimental Evaluation of the Seismic Performance of Hospital Piping Subassemblies,” by E.R. Goodwin, E. Maragakis and A.M. Itani, 9/4/07, (PB2008-105194).
- MCEER-07-0014 “A Simulation Model of Urban Disaster Recovery and Resilience: Implementation for the 1994 Northridge Earthquake,” by S. Miles and S.E. Chang, 9/7/07, (PB2008-106426).
- MCEER-07-0015 “Statistical and Mechanistic Fragility Analysis of Concrete Bridges,” by M. Shinozuka, S. Banerjee and S-H. Kim, 9/10/07, (PB2008-106427).
- MCEER-07-0016 “Three-Dimensional Modeling of Inelastic Buckling in Frame Structures,” by M. Schachter and AM. Reinhorn, 9/13/07, (PB2008-108125).
- MCEER-07-0017 “Modeling of Seismic Wave Scattering on Pile Groups and Caissons,” by I. Po Lam, H. Law and C.T. Yang, 9/17/07 (PB2008-108150).
- MCEER-07-0018 “Bridge Foundations: Modeling Large Pile Groups and Caissons for Seismic Design,” by I. Po Lam, H. Law and G.R. Martin (Coordinating Author), 12/1/07 (PB2008-111190).
- MCEER-07-0019 “Principles and Performance of Roller Seismic Isolation Bearings for Highway Bridges,” by G.C. Lee, Y.C. Ou, Z. Liang, T.C. Niu and J. Song, 12/10/07 (PB2009-110466).
- MCEER-07-0020 “Centrifuge Modeling of Permeability and Pinning Reinforcement Effects on Pile Response to Lateral Spreading,” by L.L Gonzalez-Lagos, T. Abdoun and R. Dobry, 12/10/07 (PB2008-111191).
- MCEER-07-0021 “Damage to the Highway System from the Pisco, Perú Earthquake of August 15, 2007,” by J.S. O’Connor, L. Mesa and M. Nykamp, 12/10/07, (PB2008-108126).
- MCEER-07-0022 “Experimental Seismic Performance Evaluation of Isolation/Restraint Systems for Mechanical Equipment – Part 2: Light Equipment Study,” by S. Fathali and A. Filiatrault, 12/13/07 (PB2008-111192).
- MCEER-07-0023 “Fragility Considerations in Highway Bridge Design,” by M. Shinozuka, S. Banerjee and S.H. Kim, 12/14/07 (PB2008-111193).


- MCEER-07-0024 “Performance Estimates for Seismically Isolated Bridges,” by G.P. Warn and A.S. Whittaker, 12/30/07 (PB2008-112230).
- MCEER-08-0001 “Seismic Performance of Steel Girder Bridge Superstructures with Conventional Cross Frames,” by L.P. Carden, A.M. Itani and I.G. Buckle, 1/7/08, (PB2008-112231).
- MCEER-08-0002 “Seismic Performance of Steel Girder Bridge Superstructures with Ductile End Cross Frames with Seismic Isolators,” by L.P. Carden, A.M. Itani and I.G. Buckle, 1/7/08 (PB2008-112232).
- MCEER-08-0003 “Analytical and Experimental Investigation of a Controlled Rocking Approach for Seismic Protection of Bridge Steel Truss Piers,” by M. Pollino and M. Bruneau, 1/21/08 (PB2008-112233).
- MCEER-08-0004 “Linking Lifeline Infrastructure Performance and Community Disaster Resilience: Models and Multi-Stakeholder Processes,” by S.E. Chang, C. Pasion, K. Tatebe and R. Ahmad, 3/3/08 (PB2008-112234).
- MCEER-08-0005 “Modal Analysis of Generally Damped Linear Structures Subjected to Seismic Excitations,” by J. Song, Y-L. Chu, Z. Liang and G.C. Lee, 3/4/08 (PB2009-102311).
- MCEER-08-0006 “System Performance Under Multi-Hazard Environments,” by C. Kafali and M. Grigoriu, 3/4/08 (PB2008-112235).
- MCEER-08-0007 “Mechanical Behavior of Multi-Spherical Sliding Bearings,” by D.M. Fenz and M.C. Constantinou, 3/6/08 (PB2008-112236).
- MCEER-08-0008 “Post-Earthquake Restoration of the Los Angeles Water Supply System,” by T.H.P. Tabucchi and R.A. Davidson, 3/7/08 (PB2008-112237).
- MCEER-08-0009 “Fragility Analysis of Water Supply Systems,” by A. Jacobson and M. Grigoriu, 3/10/08 (PB2009-105545).
- MCEER-08-0010 “Experimental Investigation of Full-Scale Two-Story Steel Plate Shear Walls with Reduced Beam Section Connections,” by B. Qu, M. Bruneau, C-H. Lin and K-C. Tsai, 3/17/08 (PB2009-106368).
- MCEER-08-0011 “Seismic Evaluation and Rehabilitation of Critical Components of Electrical Power Systems,” S. Ersoy, B. Feizi, A. Ashrafi and M. Ala Saadeghvaziri, 3/17/08 (PB2009-105546).
- MCEER-08-0012 “Seismic Behavior and Design of Boundary Frame Members of Steel Plate Shear Walls,” by B. Qu and M. Bruneau, 4/26/08 . (PB2009-106744).
- MCEER-08-0013 “Development and Appraisal of a Numerical Cyclic Loading Protocol for Quantifying Building System Performance,” by A. Filiatrault, A. Wanitkorkul and M. Constantinou, 4/27/08 (PB2009-107906).
- MCEER-08-0014 “Structural and Nonstructural Earthquake Design: The Challenge of Integrating Specialty Areas in Designing Complex, Critical Facilities,” by W.J. Petak and D.J. Alesch, 4/30/08 (PB2009-107907).
- MCEER-08-0015 “Seismic Performance Evaluation of Water Systems,” by Y. Wang and T.D. O’Rourke, 5/5/08 (PB2009-107908).
- MCEER-08-0016 “Seismic Response Modeling of Water Supply Systems,” by P. Shi and T.D. O’Rourke, 5/5/08 (PB2009-107910).
- MCEER-08-0017 “Numerical and Experimental Studies of Self-Centering Post-Tensioned Steel Frames,” by D. Wang and A. Filiatrault, 5/12/08 (PB2009-110479).
- MCEER-08-0018 “Development, Implementation and Verification of Dynamic Analysis Models for Multi-Spherical Sliding Bearings,” by D.M. Fenz and M.C. Constantinou, 8/15/08 (PB2009-107911).
- MCEER-08-0019 “Performance Assessment of Conventional and Base Isolated Nuclear Power Plants for Earthquake Blast Loadings,” by Y.N. Huang, A.S. Whittaker and N. Luco, 10/28/08 (PB2009-107912).
- MCEER-08-0020 “Remote Sensing for Resilient Multi-Hazard Disaster Response – Volume I: Introduction to Damage Assessment Methodologies,” by B.J. Adams and R.T. Eguchi, 11/17/08.

- MCEER-08-0021 “Remote Sensing for Resilient Multi-Hazard Disaster Response – Volume II: Counting the Number of Collapsed Buildings Using an Object-Oriented Analysis: Case Study of the 2003 Bam Earthquake,” by L. Gusella, C.K. Huyck and B.J. Adams, 11/17/08.
- MCEER-08-0022 “Remote Sensing for Resilient Multi-Hazard Disaster Response – Volume III: Multi-Sensor Image Fusion Techniques for Robust Neighborhood-Scale Urban Damage Assessment,” by B.J. Adams and A. McMillan, 11/17/08.
- MCEER-08-0023 “Remote Sensing for Resilient Multi-Hazard Disaster Response – Volume IV: A Study of Multi-Temporal and Multi-Resolution SAR Imagery for Post-Katrina Flood Monitoring in New Orleans,” by A. McMillan, J.G. Morley, B.J. Adams and S. Chesworth, 11/17/08.



EARTHQUAKE ENGINEERING TO EXTREME EVENTS

University at Buffalo, The State University of New York
Red Jacket Quadrangle ■ Buffalo, New York 14261
Phone: (716) 645-3391 ■ Fax: (716) 645-3399
E-mail: mceer@buffalo.edu ■ WWW Site <http://mceer.buffalo.edu>



University at Buffalo *The State University of New York*

ISSN 1520-295X